RADIATION DAMAGE

IN

MOLECULAR CRYSTALS

by

HERBERT RINGEL

A dissertation submitted to the Graduate Faculty in Physics in partial fulfillment of the requirements for the degree of Doctor of Philosophy, The City University of New York.

1969

This manuscript has been read and accepted for the Graduate Faculty in Physics in satisfaction of the dissertation requirement for the degree of Doctor of Philosophy.

May 23, 1969 — Arthur C. Damask
Chairman of Examining Committee

May 23, 1969 — Executive Officer

Dr. Richard A. Arndt

Prof. Milton Furst

Prof. Robert D. Hatcher

Prof. Myriam P. Sarachik

Prof. George Skorinko
Supervisory Committee

The City University of New York

To my wife, Ilene,

and my parents, William and Yetta Ringel.

ACKNOWLEDGMENT

Many people have been influential in this endeavor. I wish to express my thanks to Dr. Arthur C. Damask for formulating the problem and for his advice and encouragement throughout the years. I am indebted to Dr. Richard A. Arndt and Dr. William B. Whitten for their valuable advice and many helpful suggestions on all aspects of this work. Gratitude is expressed to Dr. Peter L. Mattern for his helpful discussions concerning electron spin resonance and to Dr. John N. Sherwood for his advice on material purification and crystal growth. Sincere thanks to Mr. Conrad S. Goldberg for his assistance in computer programming. Appreciation is also expressed to Brookhaven National Laboratory for making available many of its research facilities for this investigation.

I wish to thank the National Aeronautics and Space Administration, the City University of New York, and the U. S. Army Research Office-Durham, for their generous financial support.

Table of Contents

List of Tables

List of Illustrations

I. INTRODUCTION

The measurable physical properties of organic semiconductors are known to be sensitive to radiation.[1] Gamma radiation has been shown to affect both the electrical[2] and optical properties of anthracene.[3,4] The properties of naphthalene[5] and phenanthrene[6] are also altered following exposure to gamma irradiation. The results of large doses of radiation ($> 10^5$R) can be noted by the methods of fluorescence[3] and optical absorption.[4] The saliant features of the damage produced by lesser exposures ($< 10^5$R) can be observed by changes in the lifetimes of injected carriers[7] and by steady state space charge limited currents.[2] The purpose of this investigation is to measure the effects of gamma radiation on some of the more important physical properties of anthracene, naphthalene, and phenanthrene.

This chapter summarizes the behavior of organic semiconductors in connection with their electrical and optical properties.

A) Molecular Structure

The group of materials known as aromatic hydrocarbons consists of benzene and higher order benzene based molecules. These molecules are conjugated i.e., they exhibit a repetitious alteration of single and double bonds. The term "aromatic," historically derived from their odor, refers

to the stability exhibited by systems possessing (2+4n) π-electrons, n being the number of benzene rings. The benzene molecule, the prototype structure for these compounds, consists of a rigid skeleton of σ-bonds formed from hybridized or mixed s, p_x, and p_y orbitals and perpendicular to which are directed the delocalized π-electrons in the $2p_z$ atomic orbitals.[8] The σ-electrons give rise to the localized C-C and C-H bonds. The electronic properties of the system, such as conduction, optical absorption, and fluorescence, arise from transitions between electrons in the π-orbitals. Theoretical considerations of the physical and chemical properties exhibited by the molecules are derivable from molecular orbital calculations.[9,10]

The ground state of benzene can be obtained by placing the π-electrons in pairs into the three lowest molecular orbitals, the spins of the electrons in a given orbital being of opposite sign. The resulting spin, S, of the ground state is zero and the groundstate is a singlet. By removing an electron from the uppermost filled orbital of the ground state and placing it into a vacant orbital of higher energy, an excited state is generated. The excited configuration will be either a singlet or a triplet, depending on the spin of the excited electron. If the system is in a triplet state, it possesses paramagnetic

properties. Transitions between triplet and singlet states are "forbidden" and occur only because of the mixing of the singlet and triplet states caused by spin-orbit coupling.

In the solid state the molecular levels are broadened into energy bands. The molecules are bound by weak van der Waals forces and consequently the molecular energy levels are relatively unperturbed in the crystal. Since these crystals exhibit electrical behavior similar to inorganic semiconductors, they are sometimes categorized as large-band semiconductors or organic semiconductors.

The addition of other rings to the basic benzene molecule results in a variety of compounds (as shown in Figure 1) each exhibiting its own characteristic properties (such as a large photoconduction in anthracene) but retaining the basic properties peculiar to organic semiconductors (low mobility of charge carriers, low conductivity). Interest has focused on the aromatic hydrocarbons as organic semiconductors since Szent-Gyorgyi first proposed that a transfer of π-electrons from molecule to molecule played an important role in fundamental processes of biological systems.[11] Many of the benzene derivatives are carcinogenic and it is hoped that an understanding of this property may be facilitated by investigations of the physical properties of the aromatic hydrocarbons.

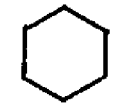

BENZENE

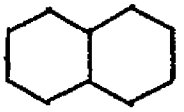

NAPHTHALENE

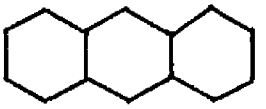

ANTHRACENE

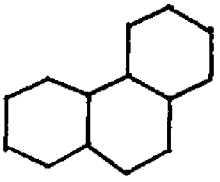

PHENANTHRENE

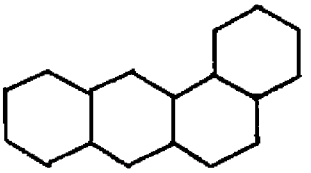

1:2 BENZANTHRACENE

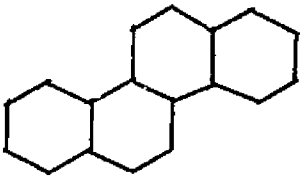

CHRYSENE

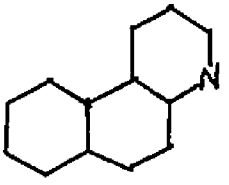

5:6 BENZOQUINOLINE

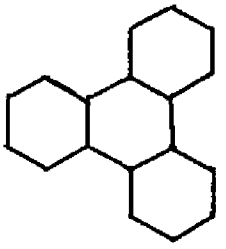

TRIPHENYLENE

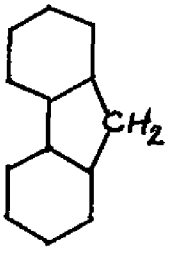

FLUORENE

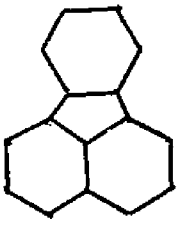

FLUORANTHENE

Figure 1. Aromatic Hydrocarbons

B) Photocarrier Generation

In most inorganic semiconductors photocarrier generation is a direct process: the absorbed photon excites an electron-hole pair. In organic crystals experimental evidence exists showing that conduction involves the singlet and triplet states, both of which are non-conducting states. Hence an additional step is required to produce free carriers in a conduction band. The first step in photocarrier generation involves the creation of nonconducting excitons, an exciton being an excited state of a molecule. An exciton may be considered as a bound electron-hole pair which moves through the crystal transporting excitation energy but not charge. Two limiting approximations are considered for excitons, one due to Mott[12] and Wannier[13] in which the exciton is weakly bound because of a large interparticle distance, and the other due to Frenkel[14] in which the exciton is considered as tightly bound. Molecular crystals furnish examples of the Frenkel exciton. Experimental evidence exists for three processes of photocarrier generation: the single exciton process, double exciton process, and the direct process.

The single exciton or exciton-surface hypothesis is a result of the similarity between the photocurrent spectrum and the optical absorption spectrum in anthracene. The

maxima of the photoresponse coincides with the maxima of the absorption spectrum. The extinction coefficients of the singlet states in many organic crystals are 10^4 - 10^5 cm^{-1} so that photon absorption occurs very near the illuminated surface. Carriers are generated only when the excitons reach the crystal surface.[15]

The double exciton process, whereby the mutual annihilation of two excitons leads to an electron-hole pair, is the dominant mechanism in the interior of the crystal.[16] Silver[17] et al. using weakly absorbed light ($\lambda > 4150$A) found two distinct processes for photocarrier generation: one at the surface and one in the bulk. The bulk generation process followed an I^2 intensity dependence whereas the surface-exciton mechanism was linear in intensity.

The "direct process" involves the creation of free electron-hole pairs by absorbed photons without involving excitons. Castro and Hornig[18] reported a direct photo-generation process using wavelengths of 2500-3000Å.

C) Charge Transport

Three mechanisms have been proposed for the transport of a charge carrier through a molecular crystal: hopping, tunneling and band conduction.[19]

The experimental values of the drift mobility of charge

carriers, together with the temperature variation of this mobility yields information on the type of process involved in charge transport in molecular crystals.

The "hopping" model utilizes the jumping of an electron over a molecular barrier from one excited state to the excited state of an adjacent molecule. This scheme predicts an exponential dependence of the mobility on temperature and a value of mobility of about 1 cm^2/V-sec at room temperature.

A model similar to the hopping mechanism utilizes the tunneling of a π-electron from the excited orbital of one molecule to the equivalent empty level in a neighboring molecule.[19]

In the third model, the band concept, charge transport is described in terms of delocalized wave functions. The band theory employs the "tight binding" approximation whereby the wave function is finite within a unit cell and falls to zero between adjacent cells. Narrow bands of the order of kT, a large effective mass, and low values of mobility are predicted. The predicted values of mobility, determined from quantum mechanical overlap and resonance integrals, are about 1 cm^2/V-sec and decrease with increasing temperature. Kepler[20] and LeBlanc[21] have obtained values of mobility of the order of unity for both electrons and holes in anthracene. The temperature de-

pendence of the mobility, however, appears to be most consistent with the predictions of the band theory. The band theory also predicts the sign and value of the Hall constant and Hall mobility. In particular, crystallographic directions are predicted where the ratio of the Hall mobility to the drift mobility is anomalous, that is, the carriers are deflected in the "wrong" direction in a magnetic field.[19] Measurements, by A. Korn et al.,[22] have shown that the Hall mobility is indeed anomalous in the predicted directions, thus supporting the band scheme of charge transport.

D) Radiation Damage

The effects of high energy radiation on the optical properties of insulating materials were first described by Goldstein[23] and Pohl[24] using alkali halide crystals. Following exposure to radiation the usually translucent materials became colored and prominent absorption bands appeared in the visible region of the spectrum. The color centers are assumed to result from certain lattice imperfections, the most notable of which, the F-center, is the result of an electron trapped at a negative ion vacancy.

Most organic materials become colored when irradiated but the responsible defects are largely unidentified.[25]

Color center absorptions, annealing kinetics and the accompanying ESR signals of alcohols and aromatic solutions have been studied. Compressed powders, liquid solutions, and single crystals of anthracene have been analyzed in relation to fluorescence degradation and reduced scintillation efficiency.[26] Of the aromatic hydrocarbons anthracene, because of its large photo-response and use as a scintillation counter, has been the most widely investigated. However, an understanding of the nature of the radiation damage is at the present time still quite limited. This paper will deal with the effects of gamma radiation on aromatic hydrocarbons. Accordingly, a brief review of the physical and chemical effects of this radiation is in order.

Gamma rays are the highly penetrating electromagnetic radiations accompanying nuclear transitions. The interactions when passing through matter are threefold: (1) photoelectric effect, (2) pair production, (3) Compton scattering.[27]

For low energy gamma rays ($< .5$ Mev) the physical contribution to the absorption is by the photoelectric process whereby the radiation interacts with a bound electron, ejecting it from the atom. This interaction is most efficient for elements with high atomic number Z. At high photon energies (> 1.02 Mev) and large Z the

dominant absorption mechanism is pair production. In this interaction, the photon is completely absorbed and in its place appears a positron-electron pair. For medium energies (~1 Mev), Compton scattering is the dominant dissipative process for all Z. The photon, treated as a particle, interacts elastically with an electron, free or bound. The energy distribution of Compton electrons depends on the energy of the incident photons. For 1 Mev photons, the energy of the electrons varies from 0 to about 0.8 Mev having a mean value of 0.45 Mev.

Cobalt 60 emits two gamma rays of roughly the same intensity and with an average energy of 1.25 Mev (1.17 and 1.33 Mev). In the carbon (organic) system, for incident photons in the energy range 0.1 - 2.0 Mev, Compton scattering is by far the most important interaction mechanism.[28]

The secondary electrons resulting from the Compton interaction are the major source of damage to molecular crystals. The main mode of energy loss of the electrons is by inelastic collisions with atomic electrons whereby the atomic electron is raised (excited) to a higher energy state. If the energy transfer is large enough an unbound state (ionization) results.

Secondary electrons are called "delta rays" if they have sufficient energy to produce further secondaries.[25]

The division between "delta rays" and lower energy secondaries is 75-100 ev. Over one-third of the secondaries have insufficient energy to excite additional molecules and 50-60% of the secondaries are ineffective for ionization (< 10ev). However, despite the preponderance of low energy secondaries, the delta rays, (only ~ 5% of the secondaries),[29] carry enough energy to account for one-third to one-half of the total ionization. Those electrons with energies less than the first electronic excitation potential of the absorber (~3-5 ev) lose their energy by collisions in which the vibration, rotational and translational states of the molecule are excited.[30,31]

Over seventy percent of the radiation products are excited molecules. The major interactions available to these molecules in their pursuit of stability are: radiation emission, radiationless transitions and bond rupture.

In radiation emission, the excited particle reverts to the ground state by giving up a photon of 2-5 ev without undergoing any physical or chemical change. The time requirement in the excited state is of the order of 10^{-8} sec. for an allowed transition (fluorescence). For a forbidden transition, e.g., triplet or singlet state, the time is usually longer than 10^{-6} sec. (phosphorescence).

A radiationless transition is an intramolecular process

whereby a system is transformed from one excited state to another of lower energy and converts the excitation energy into heat. If the two states are of like multiplicity it is called internal conversion. If the states are of different multiplicity (e.g., triplet-singlet), it is called intersystem crossing.[32]

Frequently molecules are produced with sufficient vibrational energy to rupture a bond or produce a rearrangement. Dissociation will result if the molecule is excited to a repulsive state or to a vibrational or rotational level above the dissociation limit. Dissociation may lead to heterocyclic cleavage whereby the excited molecule (M^*) breaks up into a pair of ions ($M^* \rightarrow A^+ + B^-$), it may form two free radicals ($M^* \rightarrow R^\cdot + R^\cdot$), a radical being defined as an atom or a group of atoms with an unpaired electron (the dot representing the unpaired spin), or it may generate two stable molecules ($M^* \rightarrow A + B$). Dissociation is thought to be less likely in solids than in gases,[33] however some fragmentation is required to account for the final radiation products observed.[25] The fragments produced in a solid are not free to escape because of the rigid network of neighboring molecules.[34] Because of this "cage effect," the smaller fragments such as hydrogen gas find it easier to escape and indeed the yield of hydrogen has been noted in radiation experiments.[35]

Free radicals limited by the "cage effect" have little chance of diffusing far from the reaction site before undergoing a subsequent reaction. The most common reaction that radicals undergo is hydrogen abstraction[36] whereby a radical could unite with a hydrogen from an adjoining molecule ($R^{\cdot} + SH \rightarrow H_2 + S^{\cdot}$) where S is an adjoining molecule. A free hydrogen atom, produced during irradiation, could undergo hydrogen abstraction ($H + SH \rightarrow H_2 + S^{\cdot}$). The formation of a cross-link is also a possibility ($R^{\cdot} + R^{\cdot} \rightarrow$ cross-link).

The radiation products can be detected and possibly identified by ESR, optical spectroscopy or gas chromatography. Electron spin resonance is based on the paramagnetism resulting from unpaired electrons. Trapped electrons, radicals, and radical ions are detectable by this technique. If however, more than one type of species is produced by irradiation, overlapping spectra may result, making identification difficult. Examination of radiation products is also possible by studying the reflection, luminescence[25], and optical absorption of the induced color centers.[4] Gas chromatrography could detect the presence of radiation-induced impurities that retain their stability at high temperatures, although radicals have been found to undergo hydrogen addition or abstraction during chromatography.[37]

The overall objective of this work was to compare the effects of gamma radiation on some of the more important properties of the anthracene-type and the phenanthrene-type molecules. An anthracene-type molecule, as is naphthalene, is characterized by a linear alignment of the benzene rings while a non-linearity is exemplified by a phenanthrene-type structure. Phenanthrene has been shown to exhibit both a heat capacity anomaly and an anomaly in its electric resistivity. Therefore, a calorimetric study was made of other phenanthrene-type molecules in the hope of observing similar behavior which would then suggest that an electrical anomaly also exists. Thus, techniques of measurement of radiation effects on the conductivity of the two types of molecules will be entirely different.

The low dose ($< 10^5$R) effects of radiation damage in high purity single crystals of anthracene and naphthalene were examined by measuring changes in carrier lifetime and space charge limited currents. In phenanthrene, the response of the electrical anomaly was examined. At high radiation dose ($> 10^5$R) the electrical signals were too small to be detected and thus high dose effects were studied by measuring the optical absorption of the radiation induced color centers and the response of these defects to thermal annealing. Using electron spin resonance and gas

chromatography, an attempt was made to identify some of the radiation induced defects.

References

1. J. B. Birks, "Scintillators in Organic Solids" in Physics and Chemistry of the Organic Solid State, ed. D. Fox, M. Labes, A. Weissberger, (Interscience Publishers, New York, 1963) Vol. II

2. S. Z. Weisz, A. Cobas, P. E. Richardson, H. H. Szmant and S. Trester, J. Chem. Phys. 44, 1364 (1966)

3. C. F. Sharn, J. Chem. Phys. 34, 240 (1961)

4. H. Blum, P. L. Mattern, R. A. Arndt and A. C. Damask, Mol. Cryst. 3, 269 (1967)

5. T. Okubu, N. Itoh, and T. Suita, J. Phys. Soc. Japan 24, 1179 (1968)

6. R. A. Arndt and A. C. Damask, J. Chem. Phys. 45, 4627 (1966)

7. P. L. Kronick and M. M. Labes, Mol. Cryst. 2, 293 (1967)

8. C. A. Coulson, Valence, (Oxford Univ. Press, London, 1963)

9. A. Liberles, Introduction to Molecular Orbital Theory, (Holt, Rinehard, & Winston, New York, 1966)

10. C. Sandorfy, Electronic Spectra and Quantum Chemistry, (Prentice Hall, New Jersey, 1964)

11. A. Szent-Gyorgyi, Nature 148, 157 (1941), Nature 157, 875 (1946)

12. N. F. Mott, Trans. Far. Soc. 34, 500 (1938)

13. G. H. Wannier, Phys. Rev. 52, 191 (1937)

14. J. Frenkel, Phys. Rev. 37, 17, 1276 (1931)

15. O. H. LeBlanc, "Conductivity" in Physics and Chemistry of the Organic Solid State, ed. D. Fox, M. Labes and A. Weissberger, (Interscience Publishers, New York, 1967) Vol. III

16. D. C. Northrup and O. Simpson, Proc. Roy. Soc. A244, 377 (1958)

17. M. Silver, D. Olness, M. Swicord, and R. C. Jarnagin, Phys. Rev. Letters 10, 12 (1963)

18. G. Castro and J. F. Hornig, J. Chem. Phys. 42, 1459 (1965)

19. F. Guttmann and L. E. Lyons, Organic Semiconductors, (J. Wiley & Sons, New York, 1967) Chapters 4, 7

20. R. G. Kepler, Phys. Rev. 119, 1226 (1960)

21. O. H. LeBlanc, J. Chem. Phys. 33, 626 (1960)

22. A. Korn, R. A. Arndt and A. C. Damask, (to be published)

23. E. Goldstein, Z. Instrumentenk 16, 211 (1896)

24. R. W. Pohl, Physik, Z. 39, 36 (1938)

25. R. S. Alger, "Radiation Ellects in Polymers" in Physics and Chemistry of the Organic Solid State, ed. D. Fox, M. Labes, and A. Weissberger, (Interscience Publishers, New York, 1963) Vol. II

26. J. B. Birks, Proc. Phys. Soc. A63, 1294 (1950)

27. R. D. Evans, The Atomic Nucleus ,, (McGraw Hill, 1955)

28. A. S. Newton, "Interaction of Radiation with Matter" in Radiation Effects on Organic Materials, ed. R. O. Bolt and J. G. Carroll, (Academic Press, New York, 1963)

29. H. A. Bethe, Handbuch der Physik., (Springer-Verlag, Berlin, 1933) Vol. 24, Part I

30. A. S. Newton, "Mechanisms of Chemical Effects of Ionizing Radiation" in Radiation Effects on Organic Materials, ed. R. O. Bolt and J. G. Carroll, (Academic Press, New York, 1963)

31. R. L. Platzman, Radiation Research 2, 1 (1955)

32. M. W. Windsor, "Luminescence and Energy Transfer" in Physics and Chemistry of the Organic Solid State, ed. D. Fox, M. Labes, and A. Weissberger, (Interscience Publishers, New York, 1963) Vol. II

33. W. G. Burns and C. R. V. Reed, Trans. Far. Soc. 59, 101 (1963)

34. J. Franck and E. Rabinowitz, Trans. Far. Soc. 30, 120 (1934)

35. H. A. Schwartz, Ann. Rev. Phys. Chem. 16, 347 (1965)

36. W. A. Pryor, Free Radicals, (McGraw Hill, New York, 1966)

37. L. S. Ettre and A. Zlatkis, ed. The Practice of Gas Chromatography, (Interscience Publishers, New York, 1967)

II. PURIFICATION AND CRYSTAL GROWTH

The electrical and optical properties of aromatic hydrocarbons are quite sensitive to the presence of trace amounts of impurities. The presence of only 0.3 ppm of tetracene completely extinguishes the fluorescence spectrum of anthracene.[1] Anthraquinone, anthrone and tetracene in concentrations of 10 ppm act as traps[2] and affect the drift mobility and lifetimes of electrons and holes in anthracene. Impurities were also found to quench the photoresponse of phenanthrene[3] and anthracene.[4] A study of the effect of radiation on the properties of organic semiconductors must therefore be preceded by an intensive purification scheme.

The basic techniques for the purification of organic solids are chromatography, vacuum sublimation, and zone refining. The latter method is applicable only to those materials which do not decompose upon melting.

A) Chromatography[3-6]

Purification by chromatography is based on the different adsorption characteristics of hydrocarbons on an inorganic oxide such as alumina or silica.

A column (Figure 2) is packed with silica mixed in redistilled n-hexane. The solvent, heated in the lower flask, distills through the system, condenses, and flows

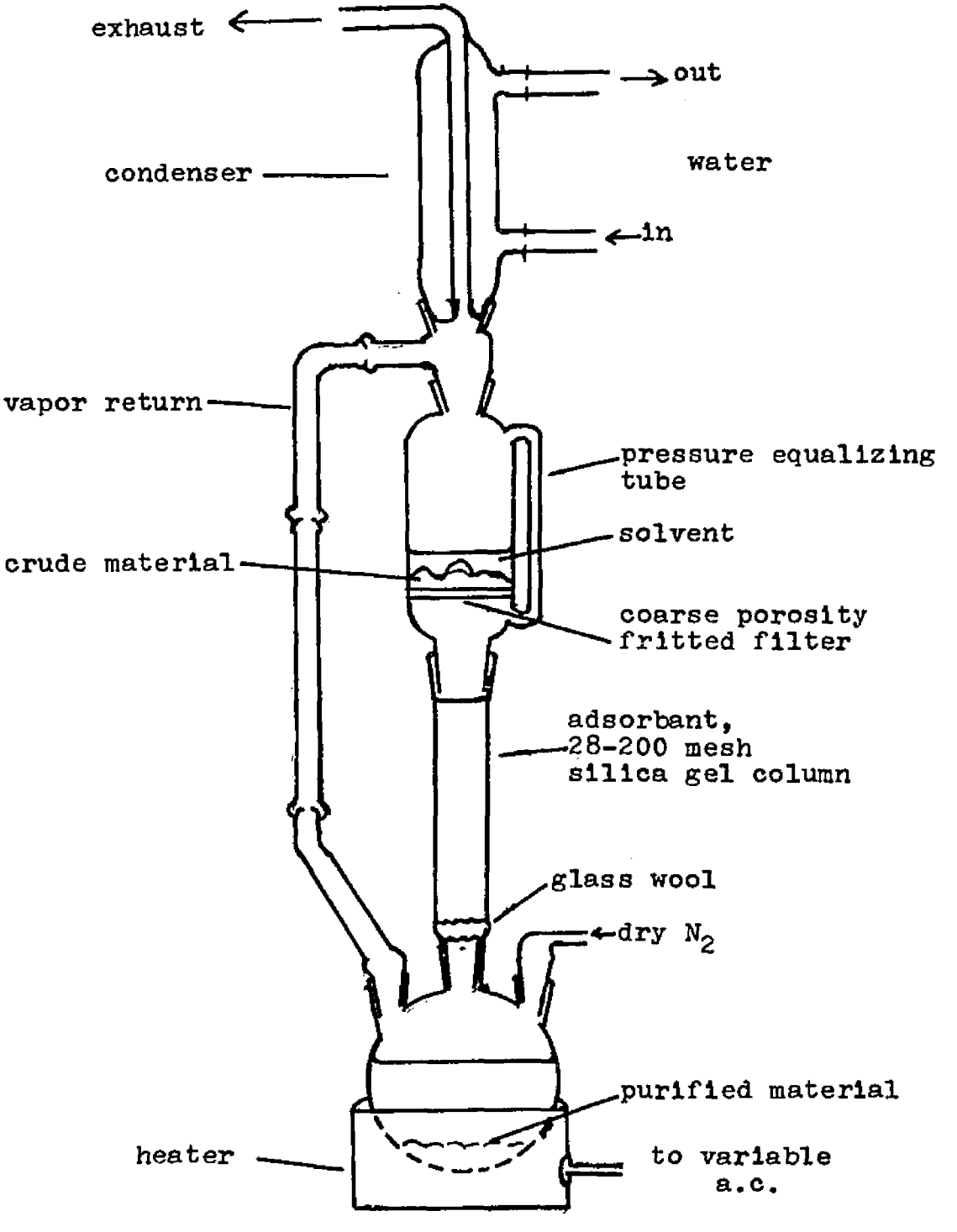

Figure 2. Apparatus for adsorption chromatography

onto the material to be purified. As the organic compound dissolved in the hexane is carried through the column, impurities more polar and less soluble than the host are adsorbed onto the silica. The purified material precipitates in the lower flask. Impurity bands which are formed during the elution are prevented from contaminating the precipitation by a periodic replacement of the silica. A heating tape wrapped around the column prevents the material from precipitating on the silica thereby clogging the column. A continuous slow stream of nitrogen is maintained throughout the system to minimize oxidation. When sufficient material has accumulated in the lower flask, the solution is allowed to cool and the solvent is removed by evaporation.

B) Vacuum Sublimation

The chromatographed material, containing any non-polar impurities which are soluble in hexane, can further be purified by vacuum sublimation.

The material is placed into the first compartment of a combination sublimation-zone refining apparatus (Figure 3). Under an atmosphere of less than 25μ the vessel is raised to a temperature sufficient for sublimation. The first 5% of the sublimate, containing the more volatile impurities is melted into the small chamber and removed. When 90% - 95% of the remaining material has sublimed into

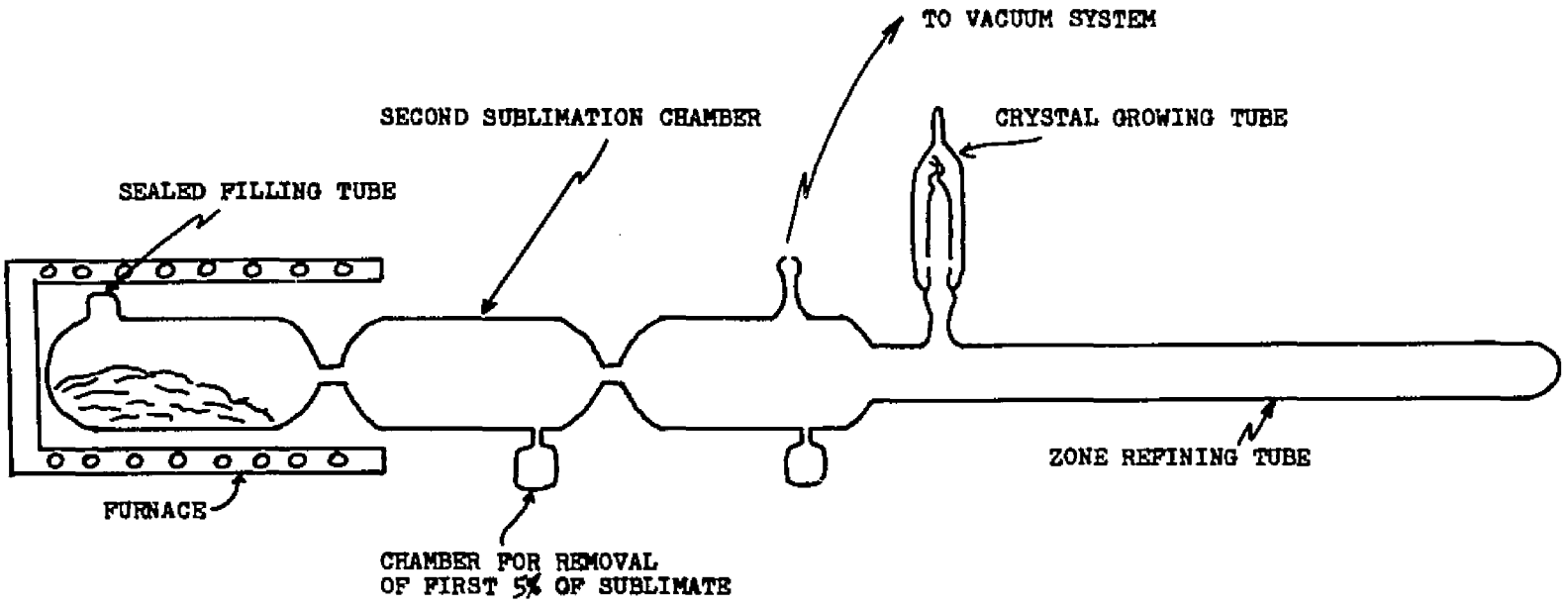

Fig.3. COMBINATION TUBE CONSISTING OF VACUUM SUBLIMATION, ZONE REFINING AND CRYSTAL GROWING VESSELS

the second chamber, heating is stopped and the remaining impure material is sealed in the first chamber by melting the constriction. Following a repetition of this procedure, 1/2 atm. of purified nitrogen is added, and the material is melted into the zone refining tube for further purification.

C) Zone Refining[7,8]

Zone refining is based on the segregation of impurities in the molten material. A narrow molten zone (approximately 3/4 in.) traverses the length of the tube. Trace impurities travel with or opposite to the zone depending on whether the impurity lowers or raises, respectively, the melting point of the material. The impurities become concentrated at the ends of the boule thereby purifying the remainder.

The distribution coefficient k, defined as the ratio of the concentration of impurity (solute) in the solid phase to the concentration in the liquid phase gives an indication of the effectiveness of the zone refining procedure. Impurities for which $k \ll 1$ (those that lower the melting point of the material) move rapidly with the molten zone and thus are easily removed. If $k > 1$ (those impurities that raise the melting point of the material) the impurity is rejected by the melt into its freezing end and eventually is carried to the upper end of the tube.

These impurities move only one zone length per pass and therefore require many passes to travel the length of the tube. Removal of an impurity for which k~1 is virtually impossible by this procedure. (Anthracene impurity in phenanthrene is an example of k~1.)

The degree of purification increases with the number of passes of the molten zone. However, a limiting value is approached as the number of passes becomes infinite.

After 20-30 zone passes, at a rate of 1"/hour, the top and bottom quarters of the tube are discarded and the remaining portion is combined with similarly purified material in a combination sublimation-zone refining tube to which a crystal growing vessel is attached. Prior to its union with the combination tube, the crystal tube is treated with a silicone release agent (Dow Corning #200) to facilitate crystal release. After the subsequent zone refining the top portion of the boule is rejected into the empty portion of the sublimation tube and the central portion of the purified material is melted into the crystal tube and sealed.

D) Crystal Growth[9-11]

The Bridgman method was used to attain single crystals. The vessel is slowly (1/2"/day) lowered through a sharp temperature gradient (Figure 4). The most convenient method is to arrange two isothermal furnaces separated by

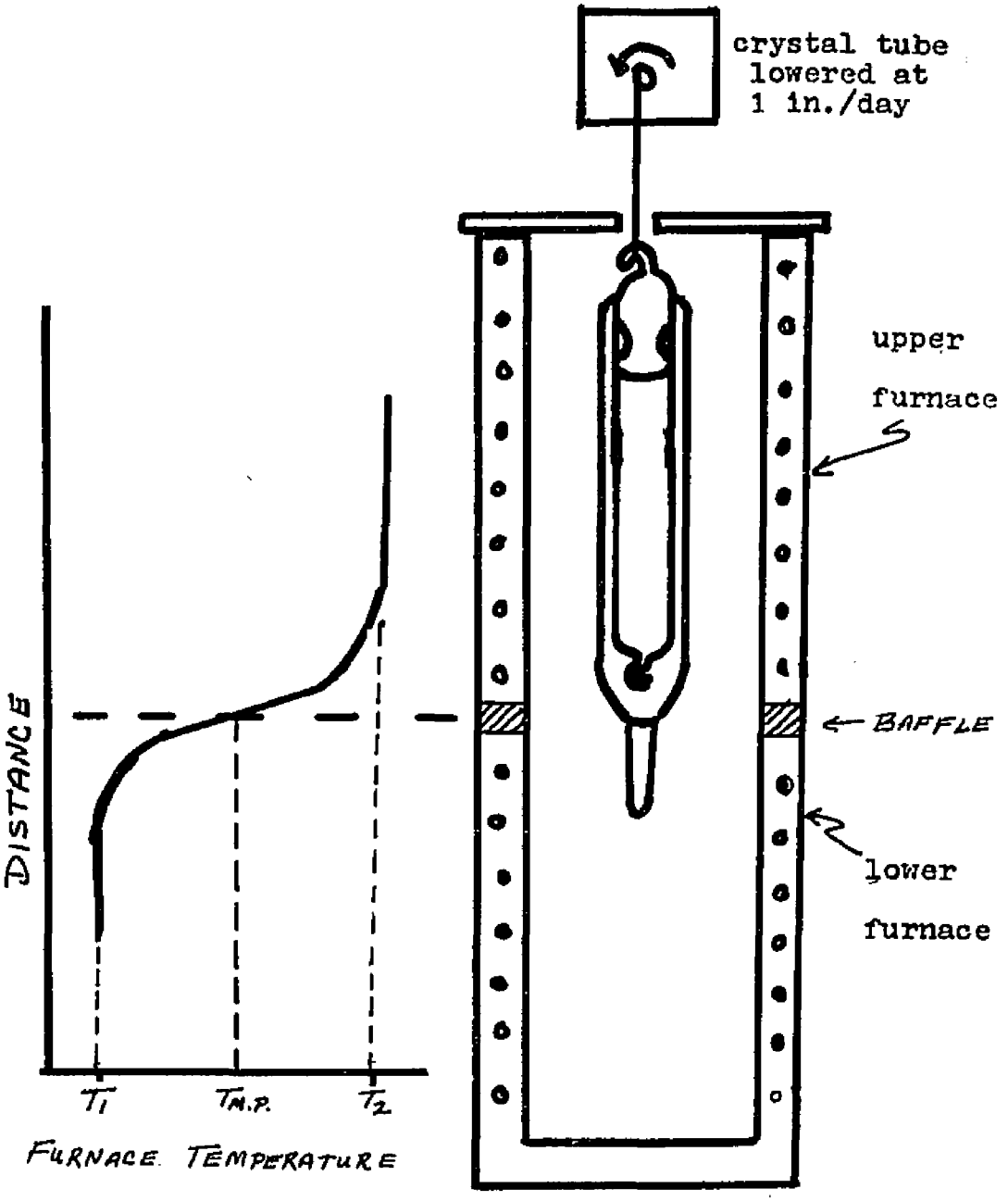

Figure 4. Crystal growing furnace and idealized temperature gradient. T_{mp} is the melting temperature of the material to be grown. The upper furnace is about 10° above the melting temperature (T_2) and the lower furnace is 10° below the melting temperature (T_1).

a non-conducting baffle such that the upper furnace is approximately 10° above and the lower furnace is 10° below the melting temperature.

The crystal tube (Figure 5) is suspended in the oven so that the tip is just below the melting isothermal. This solid portion aids in seed selection for the crystal. If a solid seed is not present before the tube is lowered supercooling with accompanying multiple crystals results. The bent capillary selects one particular seed which then grows into the upper portion of the tube as a large single crystal.

When growth is complete, the crystal is lowered to room temperature in a span of 5-7 days.

E) Crystal Orientation

Inspection of the crystal boule will usually reveal the position of cleavage cracks. Pressure applied to a sharp razor blade in this direction results in cleavage. The cleavage plane for anthracene, naphthalene, and phenanthrene is the (001), ab plane. An optical finish can be obtained by polishing the crystal with an appropriate solvent: xylene for anthracene, ethanol for naphthalene and phenanthrene. The location of the a and b axis in the ab plane can be obtained by using the birefrigence[9,12] of the crystals since the double refraction vanishes along the a-crystallographic axis (Figure 6). With this information and knowing the relative position of the c

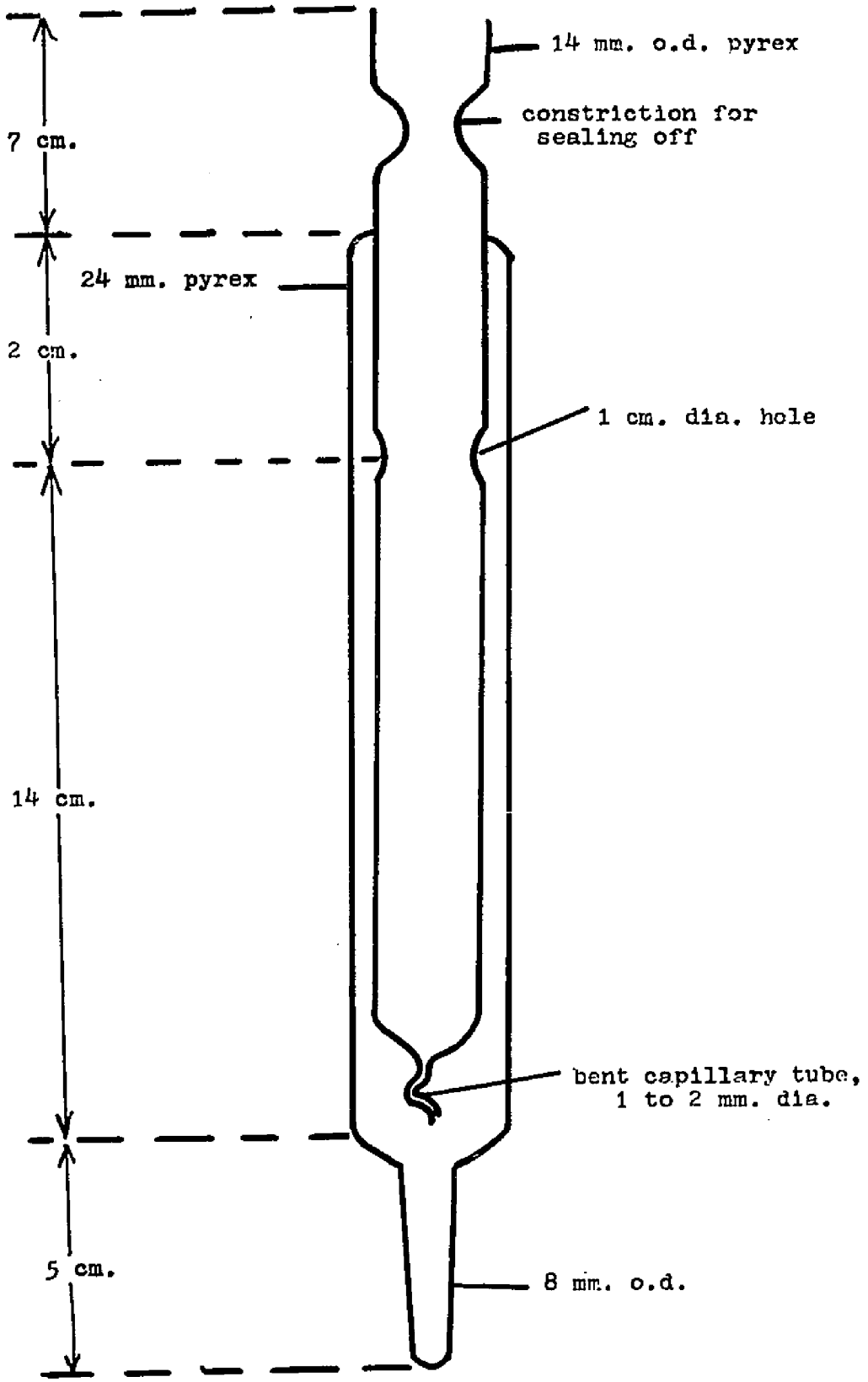

Figure 5. Crystal growing tube.

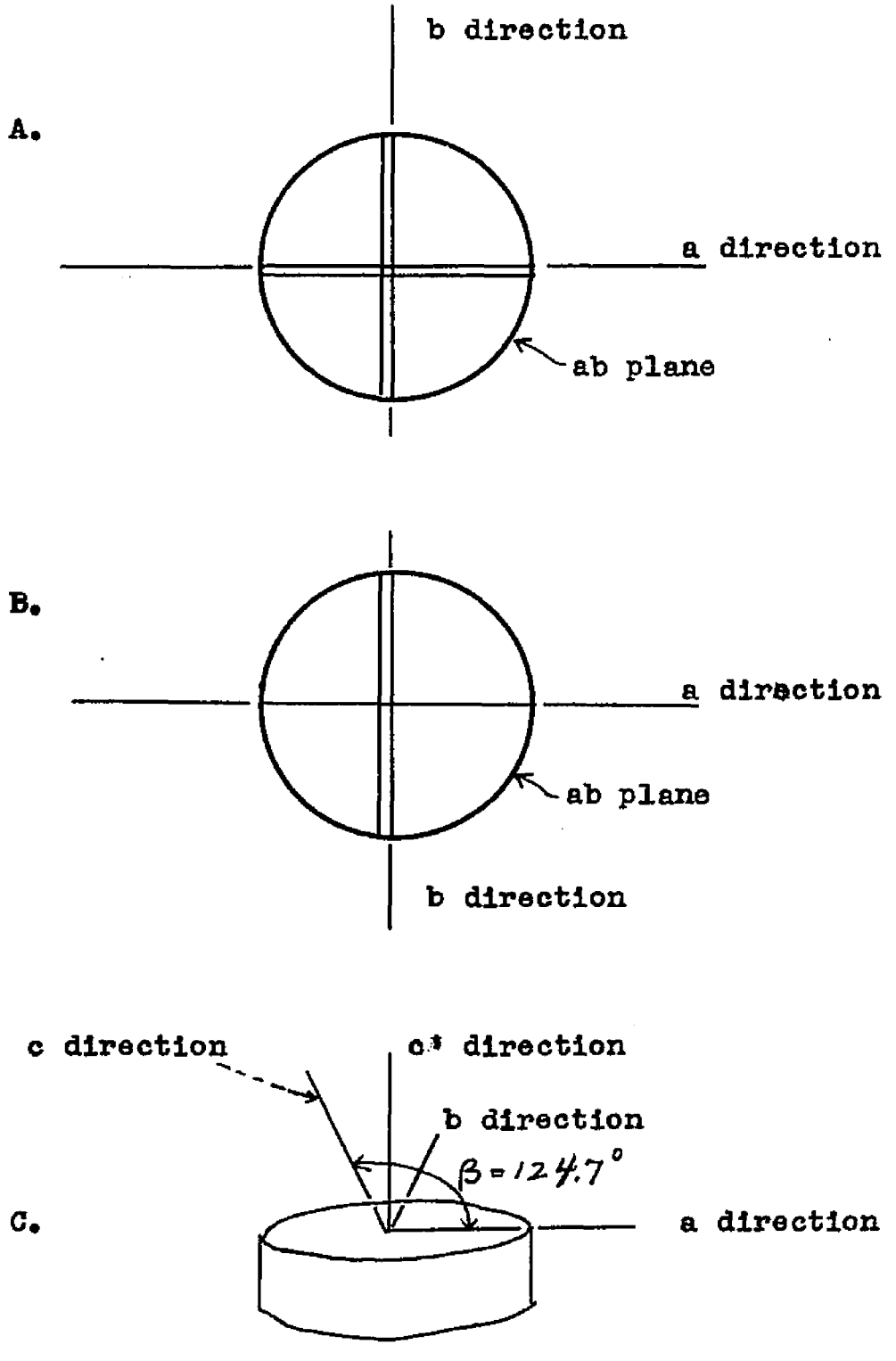

Figure 6. Orienting an anthracene crystal by double refraction. A. non-aligned crystal, top view. B. aligned crystal, top view. C. relative crystallographic axes. The c' direction is normal to the ab-plane.

crystallographic axis,[13] the crystal can be cut in any desired orientation. A string saw using xylene or ethanol as the solvent was used to cut the crystals when directions other than the cleavage plane were needed.

F) Gas Chromatography

Gas chromatography was used to identify, collect, and estimate impurity concentration of our material.

The technique of gas-liquid chromatography is based upon the different adsorptive or solubility characteristics of the components to be analyzed.[14,15] The sample is injected into a moving gas stream and is carried by it through a fractionating column. The column is packed with an inert material that has been pulverized and coated with a non-volatile liquid called a partitioner. This liquid largely determines the performance of the column[16,17] by selectively interfering with the progress of each compound as the carrier gas proceeds through the column. In general, nonpolar substances on a nonpolar column are separated in the order of their boiling points,[18] while polar solutes are eluted in an inverse order of their dipole moments. A detector records the concentrations of the substances and converts the result into an electrical signal which can be recorded. The area under the peaks correspond to the relative amounts of material present.

A Varian Aerograph Model 204B, gas chromatograph was used for the estimation of impurity content. The column consisted of a 1/8" diameter, 5 ft. spiral tube. A solution of 5% Silicone Gum Rubber SE-30 (Methyl) served as the liquid phase and 60/80 mesh Chromosorb W was the inert support. Best results were obtained when the chromatograph was operated in the isothermal mode in the temperature range 100-250°C. The sample was injected as a solid using a Hamilton (SS-60) syringe. Helium served as the carrier gas and detection was via hydrogen flame ionization. The injected material is ionized in the flame and the resulting signal amplified and recorded.

A Varian automatic preparation "Autoprep" A-700 gas chromatograph was used for the collection of impurities. The column 3/8' x 20 ft. consists of 30% SE 30 on 45/60 mesh chromosorb W. Since this unit is used for collection of samples, flame ionization which destroys the material by combustion, was replaced by a thermal conductivity detector. This detector utilizes the relative temperature fluctuations in thermal conductivity between carrier gas alone and a composite of carrier gas and sample. Because of the high thermal conductivity of helium (6-10 times as great as any organic vapor studied), an electrically heated wire in the reference cell is cooled more rapidly than a similar wire in the sample compartment. The accompanying

variation in electrical resistance is converted into an electrical signal and recorded.

The sample (~0.2 gm) was placed directly into the column at room temperature. Prior to this, the helium flow was closed and the column and injector cooled to room temperature. However, the detector and collector were maintained at temperature (200-300°C). Following insertion of the sample, the injector and column temperatures were quickly increased. The impurity is captured by a pyrex vial situated at the exit port.

G) Visible and Ultraviolet Spectroscopy

A Cary Model 14 Spectrophotometer was used to identify impurities that have absorptions at wavelengths greater than the absorption edge of the material. The sample under study was dissolved in a suitable solvent, using ethanol or xylene, to the point of saturation. It was then put into the sample compartment of the instrument. The effect of the solvent is negated by placing a sample of it in the reference chamber. This analysis has the advantage of the possible detection of an impurity possessing the same boiling point as the host, a property which renders gas chromatography ineffective. The relative absorption strengths of the impurity and the host material lead to a determination of the impurity concentration.[19]

The term parts per million (ppm) is used to represent the relative concentration of impurity molecules compared to the number of host molecules.

H) Results

Crystals of synthetic anthracene (Eastman Organic Chem #H480) and naphthalene (Eastman Organic Chem #168) purified and grown by the above procedures were found to be suitable for electrical and optical measurements. Gas chromatography failed to reveal the presence of any impurities. Spectroscopic analysis did not show any absorptions with wavelength greater than the absorption edge of the material.

Phenanthrene, chrysene, triphenylene, 1:2 benzanthracene, and 5:6 benzoquinoline purified by the above processes did not yield high purity material. Additional methods of purification were successful only for phenanthrene.

Prior to the initiation of chemical purification, the crystals of phenanthrene were "milky" in appearance and did not exhibit the phenomenon of "permanent polarization."[20] Spectroscopic analysis revealed 500-5000 ppm of anthracene impurity. In addition, gas chromatography indicated the presence of fluorene, fluoranthene, pyrene, dibenzothiophene and other unidentified agents. To alleviate this situation a supplementary purification scheme was initiated.

The as-received phenanthrene was refluxed for twenty-four hours with excess maleic anhydride in xylene solution.[21] The addition product of anthracene with maleic anhydride

is removed either by adding dilute caustic soda or by chromatography. After evaporation of the xylene approximately 100 gms. of phenanthrene is melted with 20-30 gm KOH pellets and stirred for 2-3 hours. The resulting fluorene-potassium compound is removed by sublimation. Examination of the boule, with ultraviolet light, during zone refining revealed a light blue fluorescent material moving in the direction of the molten zones. This material was identified as fluoranthene. Crystals grown from the central portions of the zone refined boules indicate less than 0.1 ppm anthracene and 10-50 ppm of other impurities.[22]

Gas chromatographic analysis of chrysene revealed the presence of at least three major impurities of the order of 3000 ppm total concentration. Maleic anhydride treatment[23] and reaction with tetrachloroethane and sulfuric acid[24] failed to remove these impurities. Attempts at growing usable single crystals of chrysene were unsuccessful, probably because of the impurities.

References

1. G. J. Sloan, "Definition and Attainment of High Purity of Organic Compounds" in Physics and Chemistry of the Organic Solid State, ed. D. Fox. M. Labes, and A. Weissberger, (Interscience Publishers, New York, 1963) Vol. I

2. D. C. Hoesterey and G. M. Letson, J. Phys. Chem. Solids 24, 1609 (1963)

3. J. N. Sherwood, "The Purification and Growth of Large Anthracene Crystals" in Purification of Inorganic and Organic Materials. Techniques of Fractional Solidification, ed. M. Zeif, (M. Dekker, New York, 1969)

4. J. Kommandeur, "Conductivity" in Physics and Chemistry of the Organic Solid State, ed. D. Fox, M. Labes, and A. Weissberger, (Interscience Publishers, New York, 1963) Vol. II

5. R. G. Sangster and J. W. Irvine, J. Chem. Phys. 24, 670 (1956)

6. G. J. Sloan, Molecular Crystals 1, 161 (1966)

7. W. G. Pfann, Zone Melting, (Wiley & Sons, New York, 1966)

8. A. Matsui and Y. Ishii, Jap. J. of Appl. Phys. 6, 127 (1967)

9. F. R. Lipsett, Can. J. Phys. 35, 284 (1957)

10. J. N. Sherwood and S. J. Thomson, J. Sci. Inst. 37, 242 (1960)

11. G. F. Reynolds, "Crystal Growth" in Physics and Chemistry of Organic Solid State, ed. D. Fox, M. Labes, and A. Weissberger, (Interscience Publishers, New York, 1963) Vol. I

12. I. Nakada, J. Phys. Soc. of Japan 17, 113 (1962)

13. J. M. Robertson, Revs. Mod. Phys. 30, 155 (1958)

14. D. Ambrose and B. A. Ambrose, Gas Chromatography, (G. Newnes Ltd., London, 1963)

15. R. Kaiser, Gas Phase Chromatography, (Butterworths, London, 1963) Vol. I

16. M. H. Abraham and R. E. Marks, J. Chrom. 13, 344 (1964)

17. J. R. Wilmshurst, J. Chrom. 17, 50 (1965)

18. J. F. Palframan and E. A. Walker, The Analyst 92, 71 (1967)

19. P. Bladon and G. Eglinton, "Ultraviolet, Visible and Infrared Spectroscopy" in Physical Methods in Organic Chemistry, ed. J. C. P. Schwarz, (Holden-Day, Inc., San Francisco, 1964)

20. R. A. Arndt and A. C. Damask, J. Chem. Phys. 45, 4627 (1966)

21. E. Clar, Polycyclic Hydrocarbons, (Academic Press, New York, 1964) Vol. II

22. W. B. Whitten et al., (to be published)

23. E. Clar and L. Lombardi, Ber. dtsch. Chem. Ges. 65, 1412 (1932)

24. G. P. Baxter and A. H. Hale, J. Am. Chem. Soc. 58, 510 (1936)

III. CALORIMETRY

Anthracene, of all the aromatic hydrocarbons, has undergone the most intensive study with regard to electrical and optical properties. It has been assumed that the properties of other such molecules would be similar to those of anthracene and that an understanding of the mechanisms of electrical conductivity and optical excitation in this material would lead to an understanding of many other aromatic hydrocarbons. Recently, however, investigations of the electrical properties of phenanthrene, the isomer of anthracene, have led to the discovery of phenomena quite distinct from properties exhibited by anthracene. The non-linear arrangement of the rings in phenanthrene most likely has a bearing upon these phenomena.

Molecules composed of atoms in hybrid sp^2 orbitals, as are anthracene and phenanthrene, are expected to be planar.[1] The fact that a number of aromatic hydrocarbons are found to deviate from planarity is thought to be due to steric effects that may be the result of forces that are either intramolecular or intermolecular in origin. It has been found that nonbonded hydrogen atoms do not approach closer than 2.4 angstroms. The adoption of a planar geometry for phenanthrene would necessitate the compression of the nonbonded hydrogens to within this forbidden range (Figure 7). Relief of the strain produced by the overcrowded

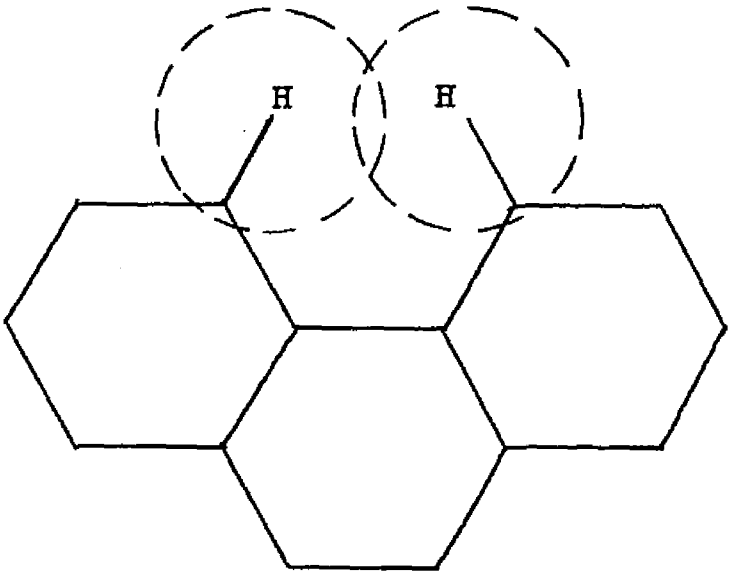

Figure 7. The planar configuration of phenanthrene illustrating the overcrowding of the hydrogen atoms. The figure is drawn to scale using 1.2 Angstroms for the van der Waals radius of hydrogen. (after Ferguson and Robertson[1])

atoms may be brought about either by changes in bond lengths, valence angles and vertical displacements of the overcrowded atoms, or by the deformation of the molecule as a whole.[2] Calculations by Senent and Herraez[3] show that bond angle and vertical deformation are the principal means of relieving steric strain in phenanthrene type molecules. They conclude that phenanthrene is likely to be almost planar but with splayed C-H bonds.

Trotter,[4] using X-ray diffraction, reported that the phenanthrene molecule deviates from planarity, possibly due to the unusual proximity of the overcrowded hydrogen atoms. The outer rings of the molecule deviate from the plane of the central ring and also from the average plane for the entire molecule. One of the rings is bent below the plane of the center ring; the other ring is bent up from the plane of the center ring. Figure 8, taken from Trotter, shows the deviation in Angstroms of each of the carbon atoms from the plane of the central ring.

Phenanthrene was found to exhibit anomalous behavior in its heat capacity[5] and its electrical conductivity.[6,7,8] Matsumoto and Fukada[9] and Andrews et. al.,[8] using polycrystalline material, reported a discontinuous change in the conductivity of phenanthrene at 67°C, presumably the result of a phase transition. Arndt and Damask,[6] using single crystals, observed pyroelectric phenomena in

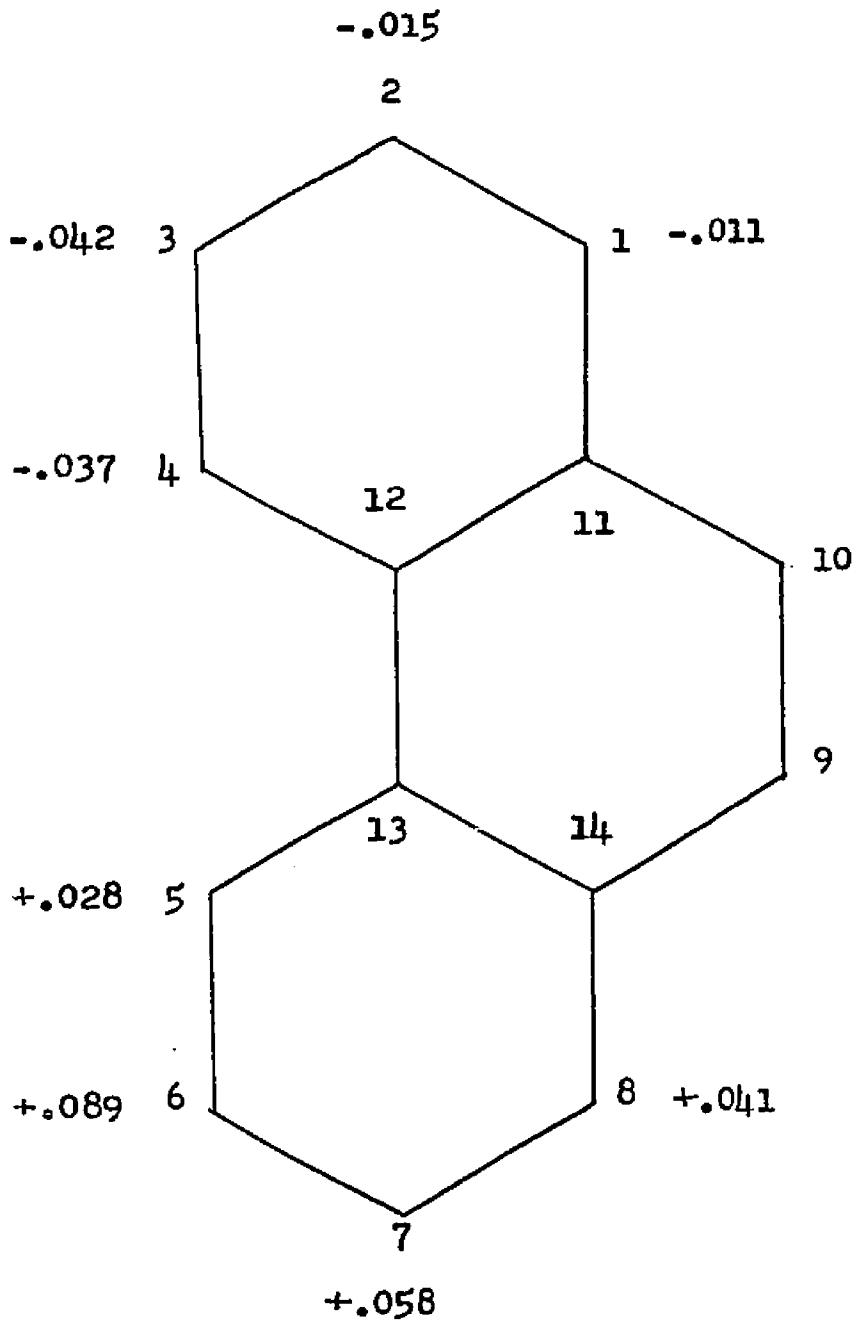

Figure 8 . Deviations in Angstroms of carbon atoms from plane of central ring. (After Trotter[4])

phenanthrene at about 72°C. Cooling a crystal from above this temperature in an electric field produced an electric polarization that persisted after removal of the field. Subsequent heating through this temperature region without an electric field resulted in a charge release. This behavior will be further discussed in a later chapter.

An X-ray study of compressed pellets of phenanthrene by Matsumoto and Fukuda[9] reports that the crystal system, which is monoclinic, and the space group, $P2_1$, may remain unaltered on passing through the transition temperature. They also report that the lattice constants and the axial angle (β) increase with temperature through this region at a rate much larger than can be accounted for by thermal expansion considerations. No anomalous behavior was found in the X-ray measurements by Arndt and Damask.

The conjecture that the dissimilarity in behavior of anthracene and phenanthrene is due to the overcrowded hydrogen atoms suggests a survey of some other aromatic hydrocarbons with crowded hydrogens in the hope of finding materials which exhibit similar behavior.

As will be discussed in section V, the annealing of color centers in irradiated anthracene suggests the possibility of a defect reorientation. A search for a possible heat capacity change associated with this reorientation was also made.

A) Experimental Apparatus and Procedure

An isochronal differential microcalorimeter[10] was used to investigate energy absorptions. The calorimeter (Figure 9) consists of a copper block which serves as a heat reservoir, an evacuated Pyrex tube which contains the copper block, and a heating bath surrounding the tube. Silicone oil served as the bath for measurements above room temperature. From -60°C to 40°C, a mixture of dry ice and methanol was used. Two holes in the copper block house the sample and an inert dummy. A constantan wire is spot welded to each sample and, with an iron support wire (.013" diam.), forms a differential thermocouple. A small thin strip of copper (.040" thick, 200 mg), clamped to the block by screws, holds the iron support wire in place. The thermocouple wires are made of .003" wire to reduce heat losses and are led out of the top of the Pyrex tube through small Kovar tubes. Wax is used to seal these tubes. The Pyrex tube is evacuated to 10^{-5} micron or better. The constantan wires from two copper-constantan thermocouples, one cemented into the block, the other in the oil bath, form a differential thermocouple that provides the signal for the bath temperature controller. This controller is used to keep the temperature difference between the copper block and the oil bath to less than .05°C.

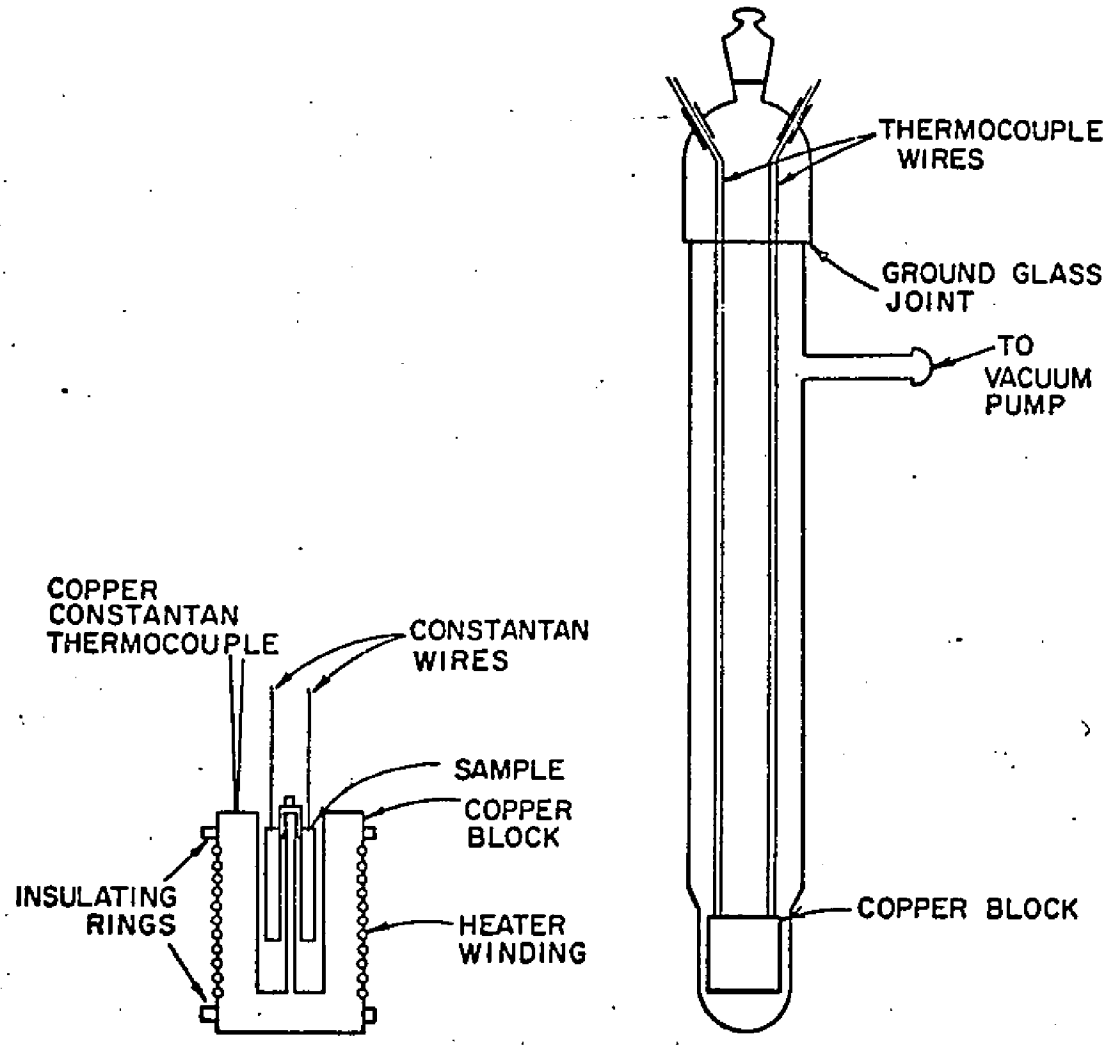

Figure 9. Calorimeter. (a) Cross section of copper heat reservoir showing placement of sample and thermocouples. Electric insulation for the copper-constantan thermocouple is provided by Sauereisen cement. (b) Pyrex tube showing location of reservoir and thermocouple connections.
(from Arndt and Fujita)

The temperature controller controls the power to two knife blade heaters in the oil bath. One of the knife blade heaters is powered by a variable transformer and is the largest source of heat. The second heater is powered from a voltage supply that is modulated by a mercury-wetted relay and is used to keep the temperature difference between the copper block and the oil bath equal to zero. Since there is no heat flow between the copper block and the oil bath, all of the power put into the heater of the copper block goes into raising the temperature of the block. This temperature rise will be linear in time since the power imput is constant. The difference of the voltages of the thermocouples in the bath and the copper block is fed into a modified Brown electronic amplifier. This difference signal is amplified and used to control the mercury-wetted relay.

The energy absorption is determined by measuring the temperature difference between sample and dummy using the iron-constantan differential thermocouple. A Keithley 150AR microvoltmeter amplifies this difference and its output is placed on one point of a multipoint recorder. Figure 10 is illustrative of the energy absorption in chrysene. If the sample undergoes a phase change its temperature rise will be delayed, resulting in a deflection on the microvoltmeter. As the reaction approaches completion

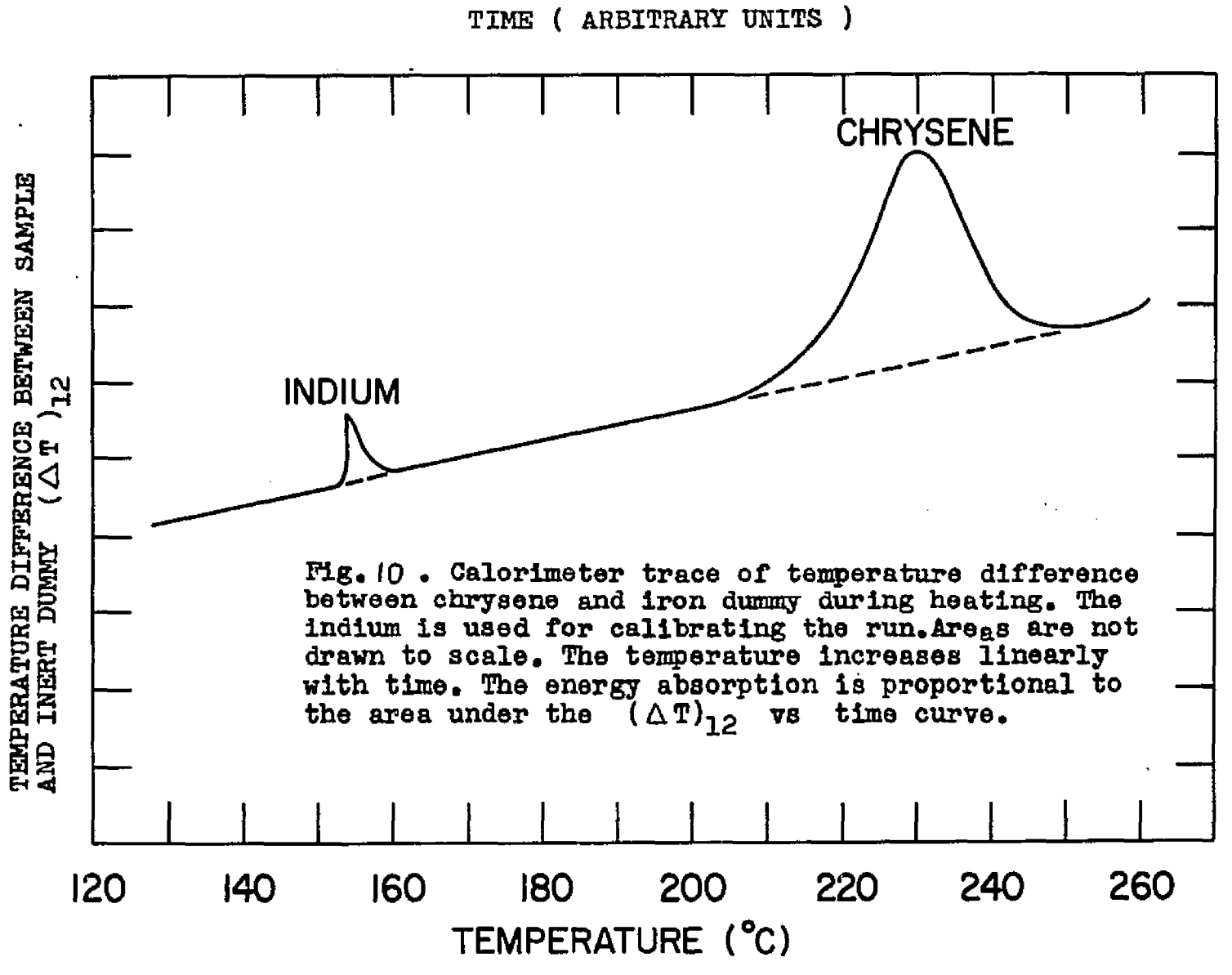

Fig. 10 . Calorimeter trace of temperature difference between chrysene and iron dummy during heating. The indium is used for calibrating the run. Areas are not drawn to scale. The temperature increases linearly with time. The energy absorption is proportional to the area under the $(\Delta T)_{12}$ vs time curve.

the temperature of the sample will increase and a deflection will occur in the opposite direction. The area under this curve is a measure of the quantity of energy absorbed. Each run is calibrated by placing a small piece (~ 5 mg) of metal, whose melting point and heat of fusion are known, on top of the sample. When the temperature of the system reaches this melting point, a deflection is recorded. The area (deflection of recorder) under the peak is measured and a relationship is obtained between area and energy.

The experiment consisted of measuring the difference in the heat absorption between the sample and an inert material, i.e., one that exhibits no peculiar thermal behavior in the temperature range of interest. Approximately 1/2 gm of material was loaded into a thin walled (~.010") stainless steel cylinder under a nitrogen atmosphere. An airtight seal was effected by the use of a copper plug.

The heat conducted to the sample from the reservoir is given by

$$(1) \quad \frac{dQ}{dt} = \frac{KS}{L}\left(T - T_1\right)$$

where K is the thermal conductivity of the support wire, S is the cross section ofthe wire, L is the length of the wire, T is the temperature of the copper block, and T_1 is the temperature of the sample. By melting a small piece

of indium atop the sample, the experimental value of $\frac{KS}{L}$ can be determined since the amount of energy absorbed upon melting is

$$(2)\quad q = \frac{KS}{L} \times \text{Area of } (\Delta T)_{12} \text{ vs. time curve}$$

where $(\Delta T)_{12}$ is the temperature difference between the sample and dummy. Equating this value with the mass and heat of fusion of the indium results in a determination of $\frac{KS}{L}$. Since this value is constant for a particular run:

$$(3)\quad \frac{Q_{SAMPLE}}{q_{INDIUM}} = \frac{(Area)_{SAMPLE}}{(Area)_{INDIUM}}$$

Since the heat absorbed is equal to the mass times the heat absorption (H)

$$(4)\quad H_s = \frac{A_s m_I H_I}{A_I m_s}$$

where H_s represents the heat absorbed by the sample, H_I is the heat of fusion of the indium and m represents mass. Using a heating rate of 1°C/min., the calorimeter is capable of detecting an energy change of 0.005 cal. in a 10 minute interval.[10]

B) Results

The materials surveyed were: anthracene, 1:2 benzanthracene, chrysene, pyrene, triphenylene, 5:6 benzoquinoline, fluorene, and fluoranthene. The latter two materials,

obtained from Eastman Organic Chemicals were purified by zone refining in an atmosphere of purified nitrogen for forty passes. The other chemicals, with the exception of anthracene, were obtained from the K&K Chemical Company and were purified by chromatography, vacuum sublimation and zone refining. Although these purification procedures may not remove all impurities from every material tested, it has been shown that technical grade phenanthrene, as received and with no further purification, still exhibited a substantial anomaly.[11] Anthracene and pyrene do not have overcrowded hydrogens and were run as controls. No heat capacity anomaly was found in these materials from -60°C to their melting points. Of all the others, only chrysene was found to exhibit an anomaly. In the vicinity of 230°C an anomalous absorption of energy of 860 ± 40 cal/mole was noted. An X-ray study of chrysene by Burns and Iball[12] has shown that the atoms at the ends of the molecule are not in the plane of the other atoms, i.e. atoms, D, E, and F are not in the same plane as atoms, A, B, C, G, H, and I (see Figure 11) and are on opposite sides of the mean plane through the other atoms. In addition the hydrogen atoms at C and I' are distorted from their radial positions and are separated by about 2.0Å, a value satisfying the requirement for overcrowding of the hydrogen atoms. Thus chrysene, like phenanthrene,

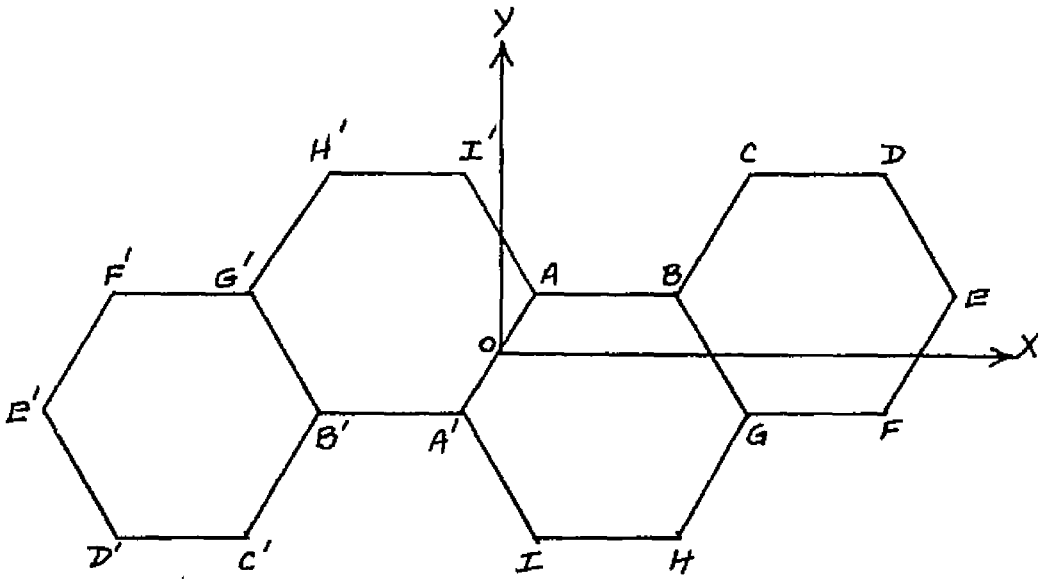

Figure 11. Chrysene molecule. The atoms at the ends of the molecule are not in the plane of the other atoms. Atoms D, E, and F are not in the same plane as atoms A, B, C, G, H, and I and are on opposite sides of the mean plane through the other atoms. (from Burns and Iball)

exhibits a non-planar distortion and an associated specific heat anomaly.

A review of the most recent crystallographic data indicates that a planar structure is warranted for fluorene[13] and, "within experimental error," for 1:2 benzanthracene.[14] Information on the planarity of fluoranthene and 5:6 benzoquinoline is lacking. Tests on the deviations of the carbon atoms from the mean molecular plane of triphenylene show that the molecule is definitely non-planar.[15] Two of the outer rings are displaced below the central plane and the third above this plane. For triphenylene, and in the case of any of the above mentioned materials that may exhibit a non-planar distortion and in which no specific heat anomaly was found, it is possible that either weak intermolecular forces allow the anomaly to occur at temperatures lower than -60°C or strong intermolecular forces force this anomaly to take place above the melting point.

The effect of gamma radiation, using an exposure dose of about 10^8R, on the heat capacity of phenanthrene and anthracene was also studied. No change was found in the heat absorption of phenanthrene nor was an anomaly noted for anthracene.

References

1. G. Ferguson and J. M. Robertson "Planar and Non-planar Aromatic Systems" in Advance in Phys. Chem., ed. V. Gold, (Academic Press, New York, 1963) Vol. I

2. C. A. Coulson and C. W. Haigh, Tetrahedron 19, 527 (1963)

3. S. Senent and M. A. Herraez, Anal. Fiz. Quim. 53B, 257, 325 (1957)

4. J. Trotter, Acta. Cryst. 16, 607 (1963)

5. R. A. Arndt and A. C. Damask, J. Chem. Phys. 45, 755 (1966)

6. R. A. Arndt and A. C. Damask, J. Chem. Phys. 45, 4627 (1966)

7. S. Matsumoto and T. Tsukada, Bull. Chem. Soc. Japan 38, 2023 (1965)

8. P. A. Andrews, A. F. Armington and B. Rubin, Appl. Phys. Letters 7, 86 (1965)

9. S. Matsumoto and T. Fukada, Bull. Chem. Soc. Japan 40, 743 (1967)

10. R. A. Arndt and F. E. Fujita, Rev. Sci. Inst. 34, 868 (1963)

11. H. Ringel, R. A. Arndt and A. C. Damask, Mol. Cryst. 3, 145 (1967)

12. D. M. Burns and T. Iball, Proc. Roy. Soc. A257, 491 (1960)

13. G. M. Brown and M. H. Bortner, Acta Cryst. 7, 139 (1954)

14. P. H. Friedlander and D. Sayre, Nature 178, 999 (1956)

15. F. R. Ahmed and J. Trotter, Acta Cryst. 16, 503 (1963)

IV. LOW DOSE RADIATION DAMAGE

It is well established that, using non-injective electrodes, the photocurrent obtained when the illuminated face of an anthracene crystal is at a positive potential is at least an order of magnitude larger than when the illuminated side is at a negative potential.[1] For this reason, previous works have emphasized the influence of radiation and trapping on the lifetime and trap density of holes whereas little work has been done on electron conduction. Therefore, the primary purpose of this section is a study of the effects of gamma radiation on the lifetime of injected negative charge carriers. Following a calculation of the mobility and lifetime, a study is made of the influence of radiation on the carrier lifetime. The electron trap density can be determined using space charge limited currents and, in conjunction with the values of the lifetime, an estimate is made of the spatial extent of the electron traps in the anthracene crystals. A qualitative discussion is also given on the influence of radiation on the lifetime of the charge carriers in naphthalene.

Phenanthrene, because of its relatively small photoresponse, does not lend itself to the above mentioned measurements. However, a property which is conducive to study is that of a polarization phenomenon in the vicinity

of 72°C. The phenomenon will be discussed in greater detail in a later portion of this section and the effects of gamma radiation on this property noted.

A) Carrier Mobilities

The mobility of charge carriers in organic materials is measured using a pulsed photocurrent technique described by Kepler[2] and LeBlanc[3]. A short duration pulse ($\sim$ 2 microsecond) of highly absorbed light from a Xenon flash tube is used to generate charge carriers at the surface of the crystal. For example, a positive bias applied to the illuminated surface causes holes to traverse the length of the sample. The resulting current pulse is displayed on an oscilloscope and photographed. Figure 12 is a schematic representation of the experimental apparatus and Figure 13 illustrates typical pulses. In the absence of trapping of recombination the current pulse would be of a constant magnitude until the carriers have reached the end of the crystal. The time required for the carriers to traverse the sample is called the transit time t_1. For times greater than the transit time, zero current would result. In actuality, the signal consists of an initial rise due to the circuit response time, a decaying pulse of width equal to the transit time and a second decay for $t > t_1$ indicative of the width of the charge carrier distribution as it hits the back surface of the crystal. The drift mobility is defined as the average velocity achieved by a

carrier per unit electric field in the direction of the carrier motion:

$$(5)\quad \mu = \frac{v}{E}$$

where μ is the mobility in $cm^2/V\text{-}sec$, v is the drift velocity and E is the field. This can be alternately expressed as:

$$(6)\quad \mu = \frac{d^2}{Vt_1}$$

where d is the crystal thickness, V the applied voltage and t_1 the transit time of the carriers across the crystal. In general, the drift mobility is dependent upon the concentration and the depth of the traps in the material. Equation 6 is valid only if ohmic conditions exist across the crystal, i.e. a linear relation between the maximum photocurrent and the applied voltage. For conditions of space charge limited currents whereby a reservoir of carriers is created at the crystal surface, a distortion of the field within the material results and the measured time necessary for the carriers to reach the end of the sample is reduced by twenty percent.

In the measurements to be described, a wavelength of 2600Å was used to generate the charge carriers. The signal was detected by a FET current preamplifier and displayed on a Tektronix 555 oscilloscope. With a 5 megohm input

resistor, the preamplifier had a rise time of 1 microsecond. The crystal holder was of the dry cell variety, one electrode being of transparent SnO_2 coating on quartz, the other of copper. The term dry cell denotes that the sample is sandwiched between two electrodes, neither of which is aqueous. The flash tube (EGG FX-47B-6.5) was energized by a 1 μf, 15 kv capacitor and triggered by a 0.3μ sec., 30 kv pulse (EGG Trigger Module TM-11). A spark gap (EGG Model GP-22) was used to prevent the flash from firing until triggered.[4]

The crystals were cut by a string saw using xylene as the solvent. The sections were then leveled using a razor blade. It was found that the lifetimes of the carriers were sensitive to the surface damage introduced during the cutting and planing procedures. Etching of the crystals in xylene removed this damage. All measurements were made perpendicular to the ab plane.

The mobilities measured perpendicular to the ab cleavage plane for synthetic anthracene and for naphthalene are presented in Table 1. These values are in good agreement with previously published results.[2,3,5] These results indicate a high degree of crystal purity since Hoesterey and Letson[6] have shown that the presence of a few parts per million (ppm) of various impurities substantially affect the mobility.

	Holes	Electrons
Anthracene	.80	.40
Naphthalene	.35	.35

Table 1. Mobility (cm^2/V-sec)

It was found that the mobilities were not affected by the irradiations. This indicates that the radiation induced traps are probably deep in nature and once trapped the carriers are not thermally excited during the time of the measurement.

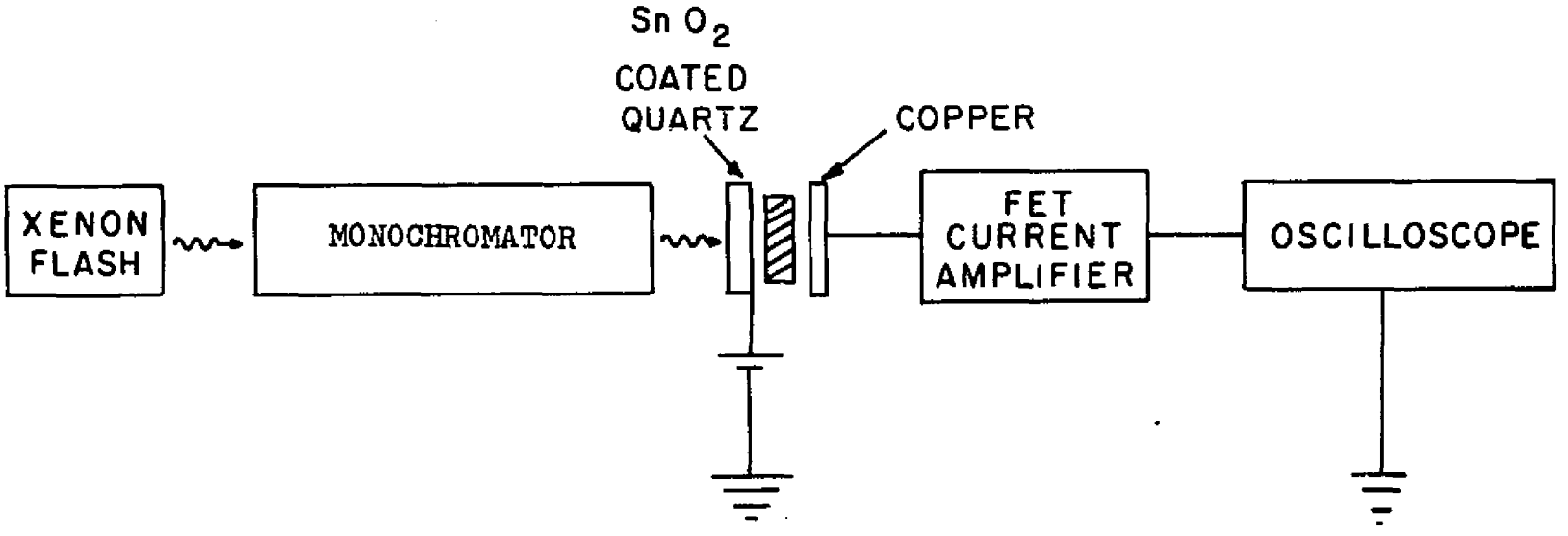

Figure 12. Block diagram of apparatus for measuring the mobilities and lifetimes of carriers.

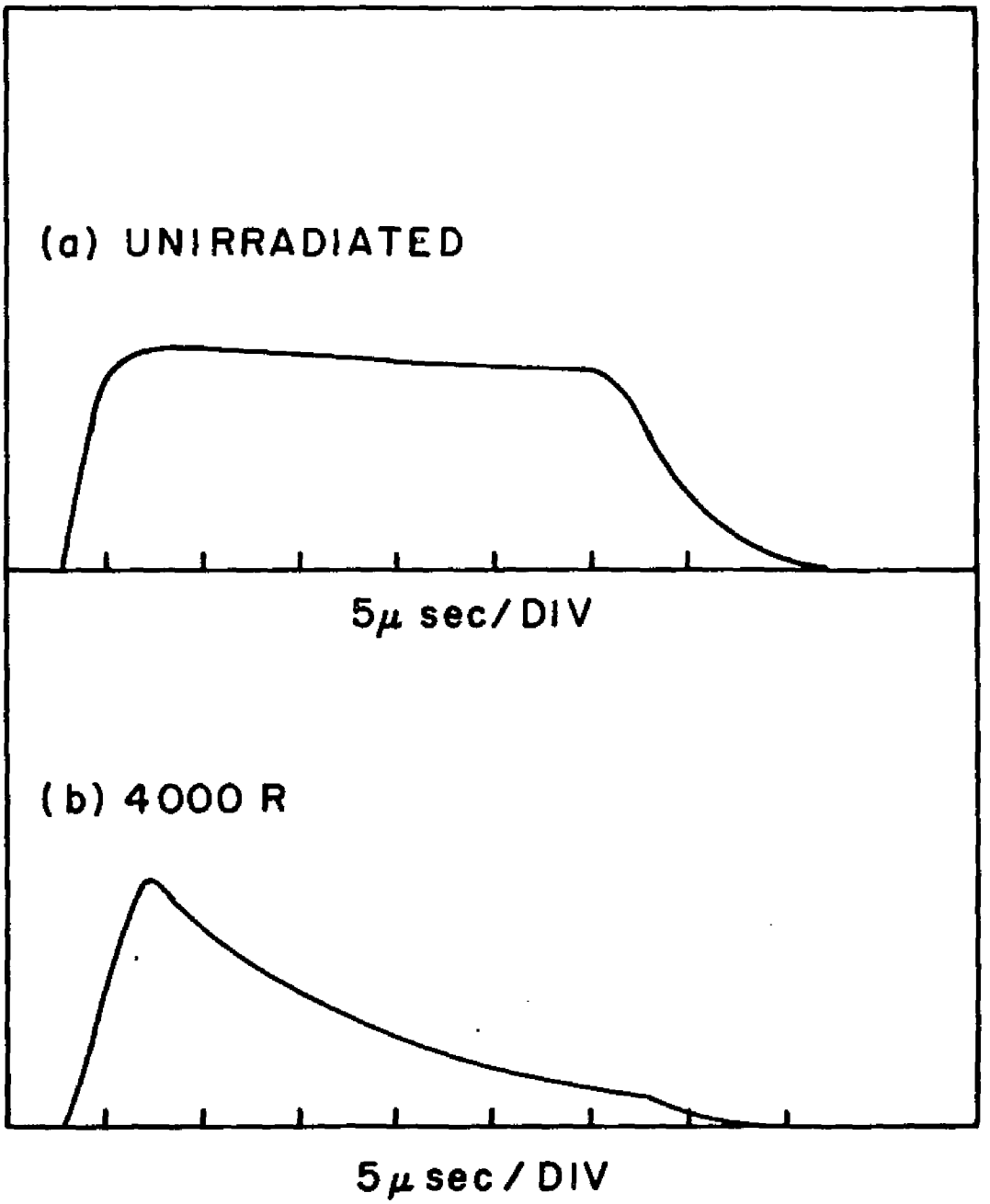

Figure 13. Electron pulses in unirradiated and irradiated anthracene. The radiation causes a decrease in the carrier lifetime.

B) Carrier Lifetimes

Hoesterey and Letson[6] made the first definitive measurements of the lifetimes of electrons and holes in synthetic anthracene. Using the transient photocurrent technique of Kepler,[2] they found that the photocurrents decayed exponentially with time for times less than the transit time of a carrier through the crystal. The decay was attributed to deep traps, implying that, once trapped, a carrier will probably not be thermally excited from the trap to contribute again to the current during the time of the measurement. Doping of the crystals with anthraquinone, anthrone, and tetracene, was found to decrease both the lifetime and mobility of the carriers. Anthraquinone and anthrone were found to be more effective at trapping electrons than holes. Tetracene was found to exhibit substantial trapping properties for both electrons and holes. The cross section of tetracene acting as an electron trap was 3×10^{-17} cm^2. For holes, tetracene was shown to be a trap located 0.43 ev above the hole band and having a capture cross-section greater than 10^{-15} cm^2.

Kronick and Labes,[7] using a similar experimental technique, measured the hole-trapping in anthracene subjected to low dose of soft (7 kev) X-rays. The lifetime decreased with dose and saturated at a value of 20 μ seconds after

1600 rads. Their interpretation considered that the current pulses were due to carriers being released from shallow traps and distributed into deeper-lying traps which were present before the irradiation. The measured lifetime represents the time spent in shallow traps. A second lifetime, representing the release of carriers from the aforementioned deeper traps was also measured. The minimum cross-section for the irradiation induced traps was estimated to be about 10^{-12} cm^2. The traps are considered to arise from spurs, which are mixtures of primary and successive reaction products, which might act as hole-trapping centers. A post-irradiation annealing of the crystal for 7 days at 207°C failed to produce any change in its electrical properties.

The trapping lifetime, i.e. the time before a carrier is trapped, of the photoinjected carrier is obtained from the time constant of the exponential photocurrent decay for times less than the transit time. The equation governing the density of free carriers (holes or electrons) is given by:

$$(7) \quad \frac{dp}{dt} = \frac{-p}{\tau_c} + \frac{p_t}{\tau_r}$$

where τ_c is the trapping lifetime, τ_r is the trap release time, i.e. the average time a carrier resides in a trap,

p is the density of free carriers and p_t is the density of trapped carriers. The pulse of highly absorbed light generates both electrons and holes at the illuminated surface. The density of traps is larger than the density of carriers created, p_o, so that complete trap filling is impossible. The carriers are separated by the applied field thus rendering recombination negligible in the bulk. Setting $p_o = p + p_t$, the solution of (7) is:

$$(8)\quad p = \frac{p_o \tau_c}{\tau_r + \tau_c}\left[1 + \frac{\tau_r}{\tau_c}\exp\left(-\frac{\tau_r + \tau_c}{\tau_r \tau_c}\right)t\right]$$

Using the condition of deep trapping, $\tau_c < \tau_r$, this reduces to

$$(9)\quad p = p_o \frac{\tau_c}{\tau_r}\left[1 + \frac{\tau_r}{\tau_c} e^{-t/\tau_c}\right]$$

Thus, one obtains an exponential decrease of photocurrent, the time constant being the trapping lifetime.

In order to attain a lifetime measurement that is physically significant, the resulting value should be independent of the applied bias. Silver et al.,[8] have shown that if measurements are performed in a space charge limited region, the resulting lifetime is a function of

the applied field. For conditionsof high light intensity and low applied field, the maximum photocurrent varies as V^2, whereas for large voltages and low intensity the behavior is approximately ohmic.[9] Figure 14 illustrates the variation of the photocurrent as a function of applied voltage and light intensity. Neutral density filters were used to reduce the light intensity. The V^2 dependence is characteristic of space charge limited currents. Under space charge conditions, the transit time of the carriers is reduced by twenty-percent and the shape of the current pulse is dependent upon the applied voltage. In order to render the carrier lifetimes independent of external influence, the light intensity and the applied voltage were adjusted to eliminate space charge effects.

C) Results of Lifetime Study

The lifetimes of the photoinjected electrons and holes in our unirradiated anthracene were 240 μ sec. and 160 μ sec. respectively. Following these measurements the samples were irradiated at the BNL gamma facility using a Co^{60} source. The irradiations were done in air at a temperature of 30-40°C and a dose rate of 5977 R/hr. For exposures up to 4800R the reciprocal lifetimes of both electrons and holes were found to increase linearly with dose:

$$(10) \quad \frac{1}{\tau} = \text{Constant} + \alpha D$$

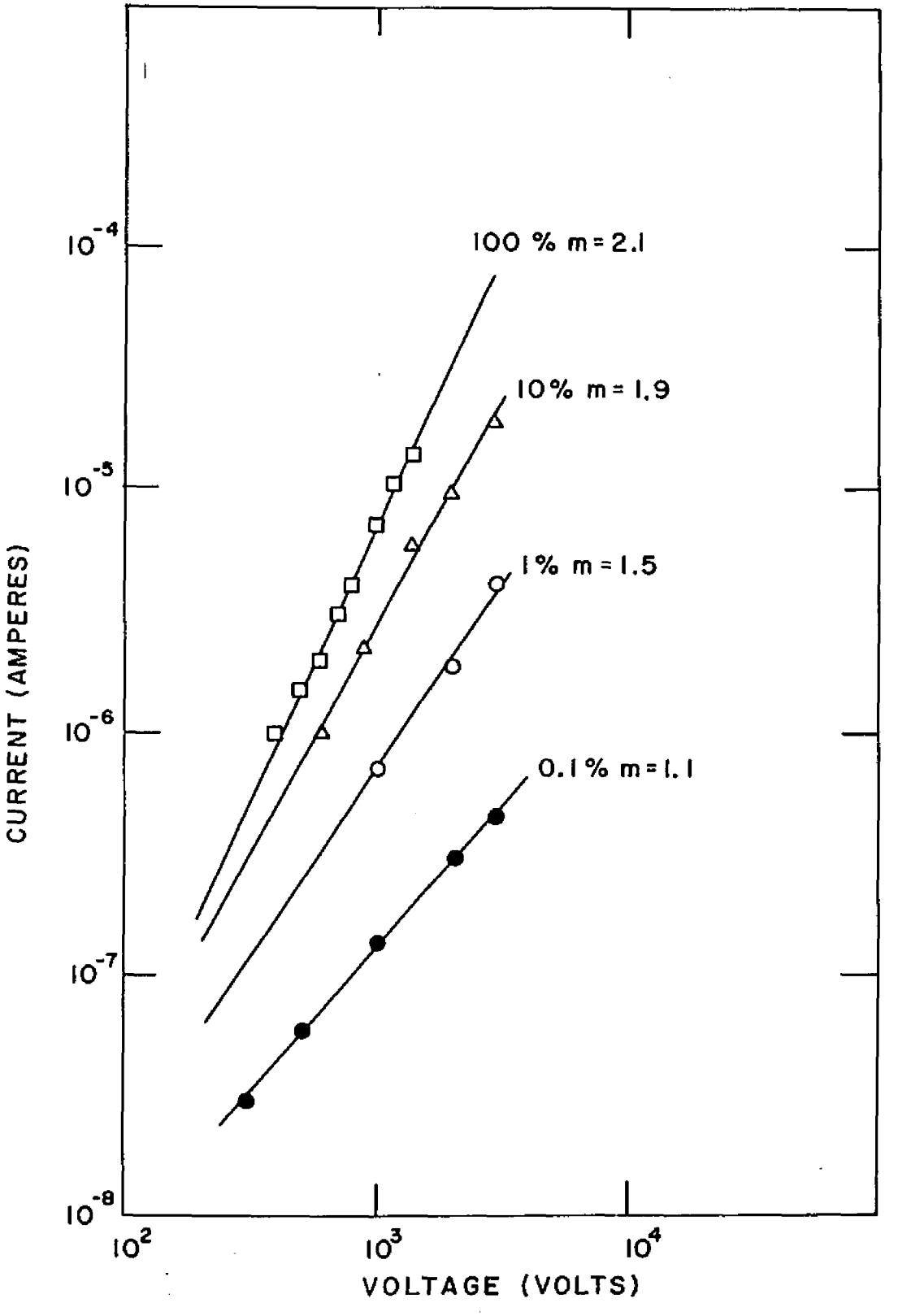

Figure 14. Dependence of peak photocurrent on voltage and light intensity. The slope of the line is represented by the letter m.

where τ is the carrier lifetime, D the exposure dose in Roentgens, and α has the value 18 $sec.^{-1}$ R^{-1} for electrons (Figure 15) and 10 $sec.^{-1}$ R^{-1} for holes (Figure 16). At the maximum dose the lifetimes were an order of magnitude lower than in the unirradiated condition (Table 2). For higher doses of radiation, the current pulses were too small for an accurate determination of lifetime to be made.

The crystals were annealed in order to determine if the radiation-produced defects could be eliminated. The crystals were sealed in a pyrex ampule which had been previously evacuated and filled with nitrogen and the ampule was then placed into a temperature controlled furnace. A West Model TP-22 controller was used to control the temperature. The results, as shown in Table 2, show a slight recovery in carrier lifetime. High doses of gamma radiation are known to produce color centers in anthracene. The defect absorption and thus the number of defects decreases rapidly if the crystal is annealed at temperatures above 140°C. The annealing temperatures shown in Table 2 were therefore chosen above this value.

Using the same light intensity and voltage as in the anthracene measurements, the photoresponse of naphthalene was below the sensitivity of our instrumentation. It was therefore necessary to use higher light intensities thereby entering the space charge realm. Since the lifetimes are

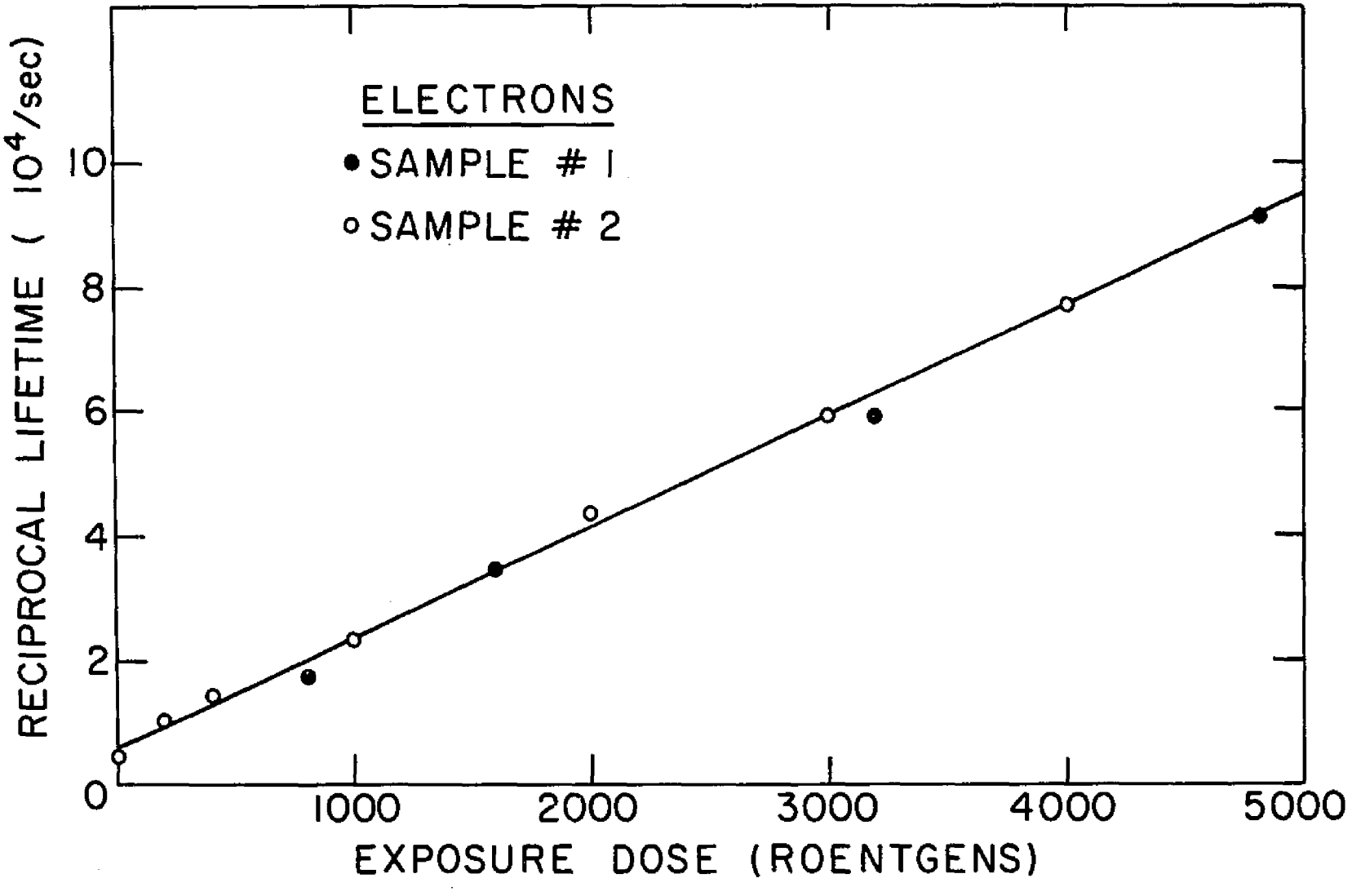

Figure 15. Dosage dependence of electron reciprocal lifetime.

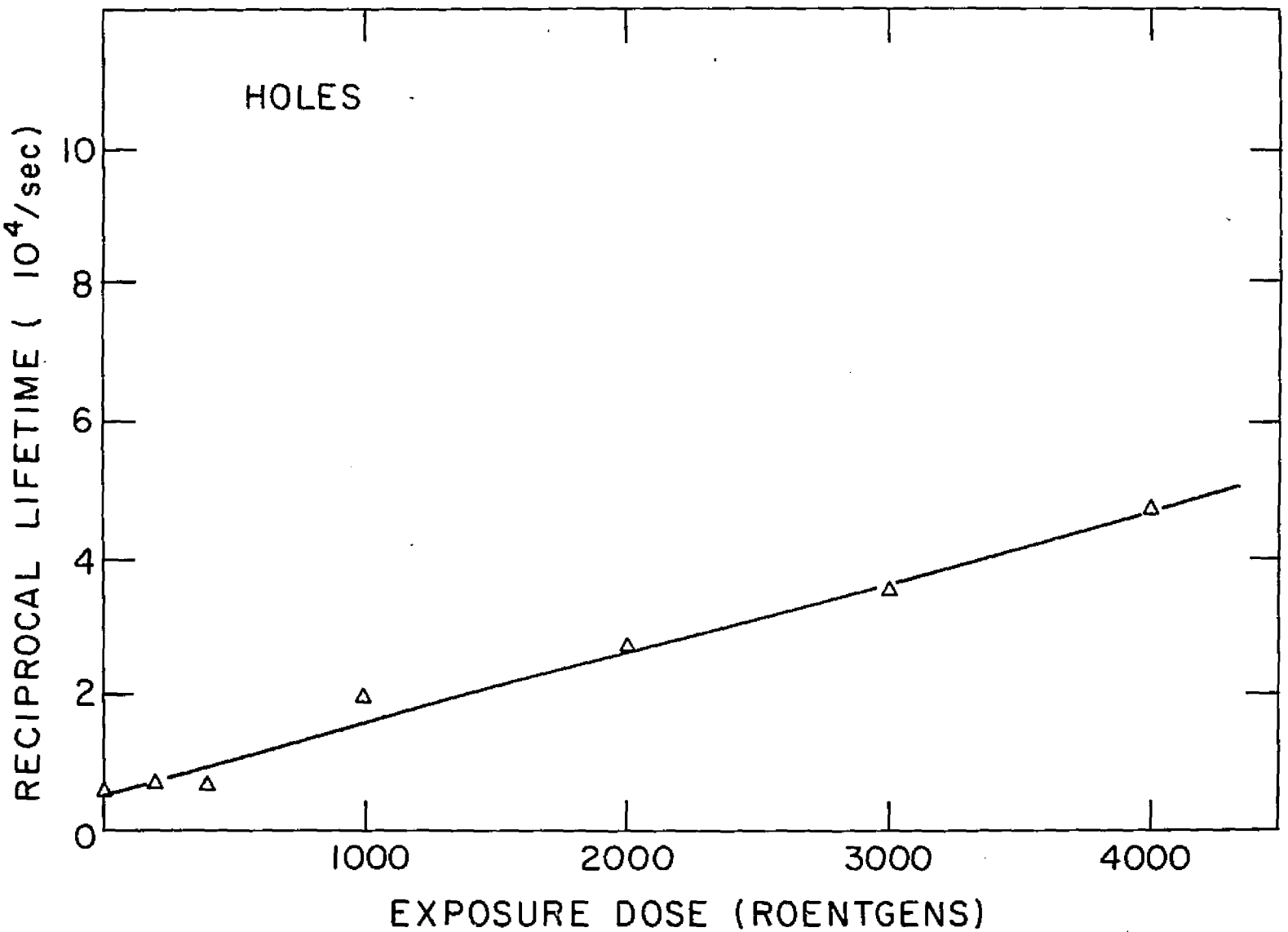

Figure 16. Dosage dependence of hole reciprocal lifetime.

Crystal #1			Crystal #2	
	Electrons	Holes		Electrons
Unirradiated	230	160	Unirradiated	240
4000 R	13	21	4800 R	11
Annealed 1000 minutes @ 145°C	28	33	Annealed 100 minutes @ 145°C	19
Annealed 1300 minutes @ 175°C	29	30	200 minutes @ 145°C	22
			1175 minutes @ 145°C	21

Table 2. Lifetime of Carriers (Microseconds)

now dependent upon voltage, only a qualitative measurement can be made. It was found that for an unchanged value of applied bias the "lifetime" of the carriers after irradiation decreased in a manner similar to anthracene. Annealing for 1000 minutes at 55°C, a temperature at which the optical defects anneal quite readily, showed no significant recovery.

D) Analysis of Results

The lifetime of charge carriers varies inversely with the number of trapping sites[10,11]

$$\tau = \frac{1}{vSN_t} \qquad (11)$$

where v is the thermal velocity of the carrier, S is the capture cross-section of a defect for a particular type of carrier, and N_t is the trap density. A value for the density of traps for electrons can be obtained from space charge limited current measurements using the value for the trap-filled-limit. The density of hole traps vs. energy of the traps follows an exponential distribution, i.e., there is no discreet energy level, so that a value for N_t cannot be obtained.[12] The thermal velocity of electrons has been calculated using the tight-binding[13] approximation and has a value of approximately 10^6 cm/sec. For a thermal velocity of 10^6 cm/sec., a trap density of $50 \times 10^{10}/cm^3$

as determined from steady state space charge limited currents (see page 76), and a lifetime of 240μ sec, one finds the cross section for electron traps in unirradiated anthracene to be about 120 x 10^{-16} cm^2, a value of the order of the geometrical cross sectional area of the anthracene unit cell.

A knowledge of the dosage dependence of the radiation induced trap density, as determined by space charge limited current measurements, in conjunction with Equation 11, can lead to an estimate of the radiation induced trap cross-section for electrons. The induced trap density is found to increase linearly with dose up to 1000 R, the highest dose used. For $\sim$ 1 mm crystals and irradiations $>$ 1000 R, the voltage at which the trap-filled-limit was reached exceeded the available instrumentation.

Using $\frac{1}{\tau} = vSN_t$ and $N_t = N_o + \beta D$ where β, the creation rate of defects as determined by steady state space charge limited measurements (section IV,E) is $\sim 10^9$ cm^{-3} R^{-1}, a value of 180 x 10^{-16} cm^2 is attained for the cross section of the electron traps. This value is of the order of the geometrical cross sectional area of the anthracene unit cell. This is not unreasonable considering that because of the weak intermolecular interactions, the field distortion due to the presence of a defect would probably dissipate within a few lattice constants. The defect is

probably neutral since a charged defect would have a larger cross section, typically $\sim 10^{-11}$ cm^2, due to the long range coulomb interaction.[11]

The absorption coefficient of anthracene[14] for Co^{60} photons is 0.118 cm^{-1}. Since 1 Roentgen[15] of a 1 Mev gamm ray is 1.9×10^9 photons/cm^2 an exposure to 10^3 R presents an energy absorption of 0.2×10^{18} ev/cm^3. Thus, for an induced trap density of 50×10^{10} cm^{-3}, one trap is created for every 400 kev of incident energy absorbed. This represents ~ 0.25 traps per absorbed photon.

An irradiation induced trap filled limit for holes was measured by Weisz and his co-workers[14] for a dose of 50×10^3R. Their results indicate a hole trap density of $\sim 2.5 \times 10^{14}/cm^3$ and a creation rate of 5×10^9 cm^{-3} R^{-1}. Combining this with our value of the rate of change of reciprocal hole lifetime per R, 10 sec^{-1} R^{-1}, and using a thermal velocity of 10^6 cm/sec. a hole trap cross section of 20×10^{-16} cm^2 is obtained. It was found that one deep hole trap was created for every 45 kev of incident energy absorbed.

E) Steady State Space Charge Limited Currents

(1) Theory

Because of the low conductivity of many organic compounds, these materials require either photogeneration

of carriers or injection of carriers for meaningful electrical measurements. The injected current, being independent of the mechanism of carrier generation, gives meaningful information on the transport and trapping properties of the crystal.[11,16]

Given ohmic, i.e. injecting, contacts the current voltage relationship of an organic semiconductor in linear at low fields but becomes nonohmic at higher values of the applied field. At these fields there will be present between the electrodes a relatively large concentration of charge carriers in transit through the crystal. These carriers constitute a space charge in analogy with the space charge encountered in vacuum diodes.

The derivation of the voltage dependence of the space charge limited currents in a trap-free insulator is due to Mott and Gurney.[17] The basic equations are:

the continuity equation

$$(12) \quad J = e n(x) \mu E(x)$$

where x represents the distance from the ohmic electrode

the Poisson equation

$$(13) \quad e n(x) = \epsilon \frac{dE(x)}{dx}$$

and

$$(14) \quad \int_0^L E(x)\, dx = V$$

The boundary conditions are:

$$(15) \quad n(0) = \infty \quad \text{and} \quad E(0) = 0$$

where n(o) is the carrier concentration in the insulator where it is in contact with the injecting electrode and E represents the electric field. Inserting en(x) from equation (13) into (12) gives

$$(16) \quad J = \epsilon \mu E(x) \frac{dE(x)}{dx} = \frac{\epsilon \mu}{2} \frac{d^2E}{dx^2}$$

Integration for E(x) and use of equation (14) leads to:

$$(17) \quad J = \frac{9}{8} \epsilon \mu \frac{V^2}{L^3}$$

The resulting dependence of the current density upon the square of the voltage is known as Child's law for the trap-free insulator. The presence of traps causes the steady-state space charge limited current to be smaller than the Child's law current, often by many orders of magnitude.[18] If θ represents the ratio of free to total carrier concentration, Child's law for an insulator with traps may be written as:

$$(18) \quad J = \frac{9}{8} \theta \epsilon \mu \frac{V^2}{L^3}$$

where θ is a function of the trap distribution.

The current-voltage characteristics for space charge limited currents are shown schematically in Figure 17. At low voltages there is negligible injection of carriers from

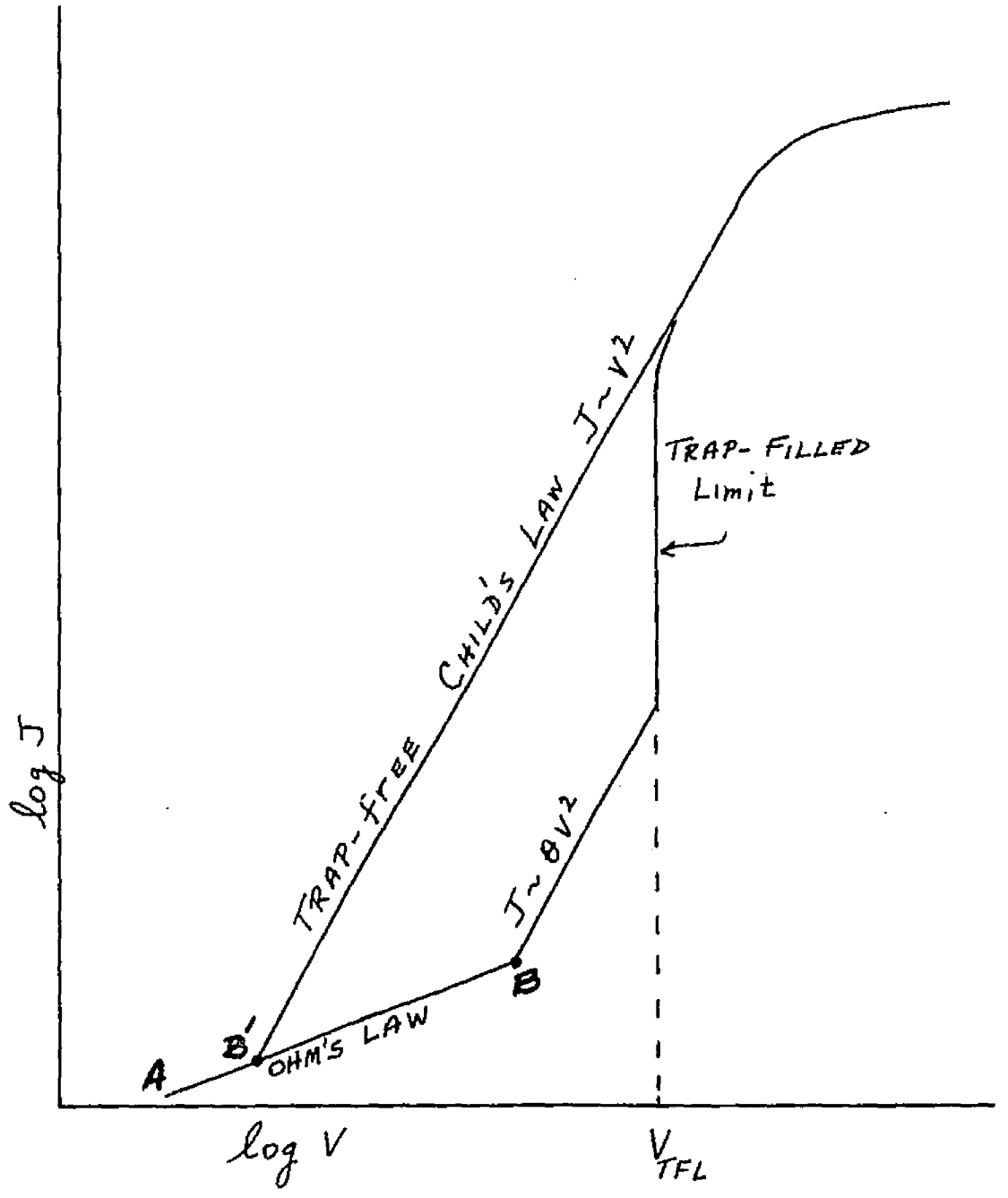

Figure 17. Current-voltage characteristics for space charge limited currents.

the contact and the current obeys Ohm's law. In the absence of traps, space charge limited currents arise at a voltage B'. If traps are present, only a fraction of the injected carriers will be free and the current becomes space charge limited at a higher voltage, point B. Child's law for the insulator with traps is superseded by the law for the trap free case when the injection level becomes so high that the traps are outnumbered by the carriers. The transition from the smaller current to the trap-free current is steep and occurs when the last traps are being filled. The transition voltage V_{TFL} (where TFL stands for trap filled limit) can be used to calculate the concentration of traps N_{TFL} since:[18]

$$(19)\quad N_{TFL} \sim \frac{3}{2}\,\frac{\epsilon}{e}\,\frac{V_{TFL}}{L^2}$$

At sufficiently high voltages the current from the electrode will saturate because the average carrier density in the sample becomes comparable to the concentration of injected carriers and the injecting contact can no longer act as a reservoir.

The existence of a trap-filled limit indicates that the traps are located at a discrete energy level below the conduction band or exist within a discrete energy range. The trap-filled limit for electrons has been shown to exist in very pure crystals. The distribution of hole

traps has been shown to be exponential in character,[20] approaching within kT of the valence band, and therefore not giving rise to a trap-filled limit. The results for a 1mm thick anthracene crystal (crystal number 2 in table 3), shown in Figure 18 illustrates the V^2 dependence of the current and shows that a trap filled limit is attained for electron injection.

(2) Procedure and Results

To investigate the space charge limited characteristics of a material, injecting electrodes must be prepared. A solution of anthracene, lithium, and ethylenediamine was used as the electron injecting electrolyte.[19] A solution of NaCl in water served as the other electrode. The electron injecting electrode was found to oxidize quite readily and therefore the solution was prepared in a flask which was tightly sealed by a rubber stopper. The solution was transferred to the measuring cell with a hypodermic syringe. The sample holder was then placed into a light-tight shielded enclosure. The sample holder consisted of two pieces of teflon rod in which holes were bored to accommodate the electrodes. The crystal was cemented to one portion of the holder with RTV silicone rubber cement and to which, following curing for a few hours in air at

room temperature, the injecting electrode was admitted. The teflon holder is represented schematically below.

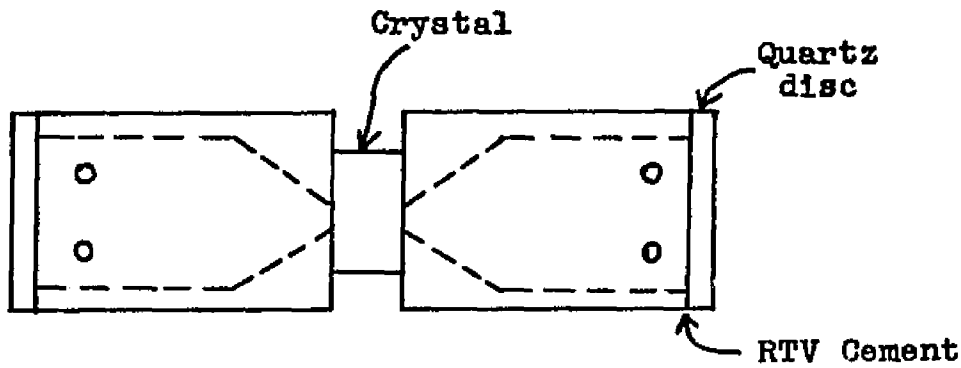

Teflon Sample Holder

Leakage of the NaCl electrolyte was prevented by applying thin layers of vacuum grease around the electrolyte-crystal interface. A negative bias was applied to the injecting solution and the current was measured by either a Cary Model 31 vibrating reed electrometer or a Keithley model 150AR microammeter. The resulting current-time curve was traced on a strip-chart recorder and the equilibrium values of current recorded. The density of electron traps for four unirradiated crystals of the thickness 0.5-1.0 mm is shown

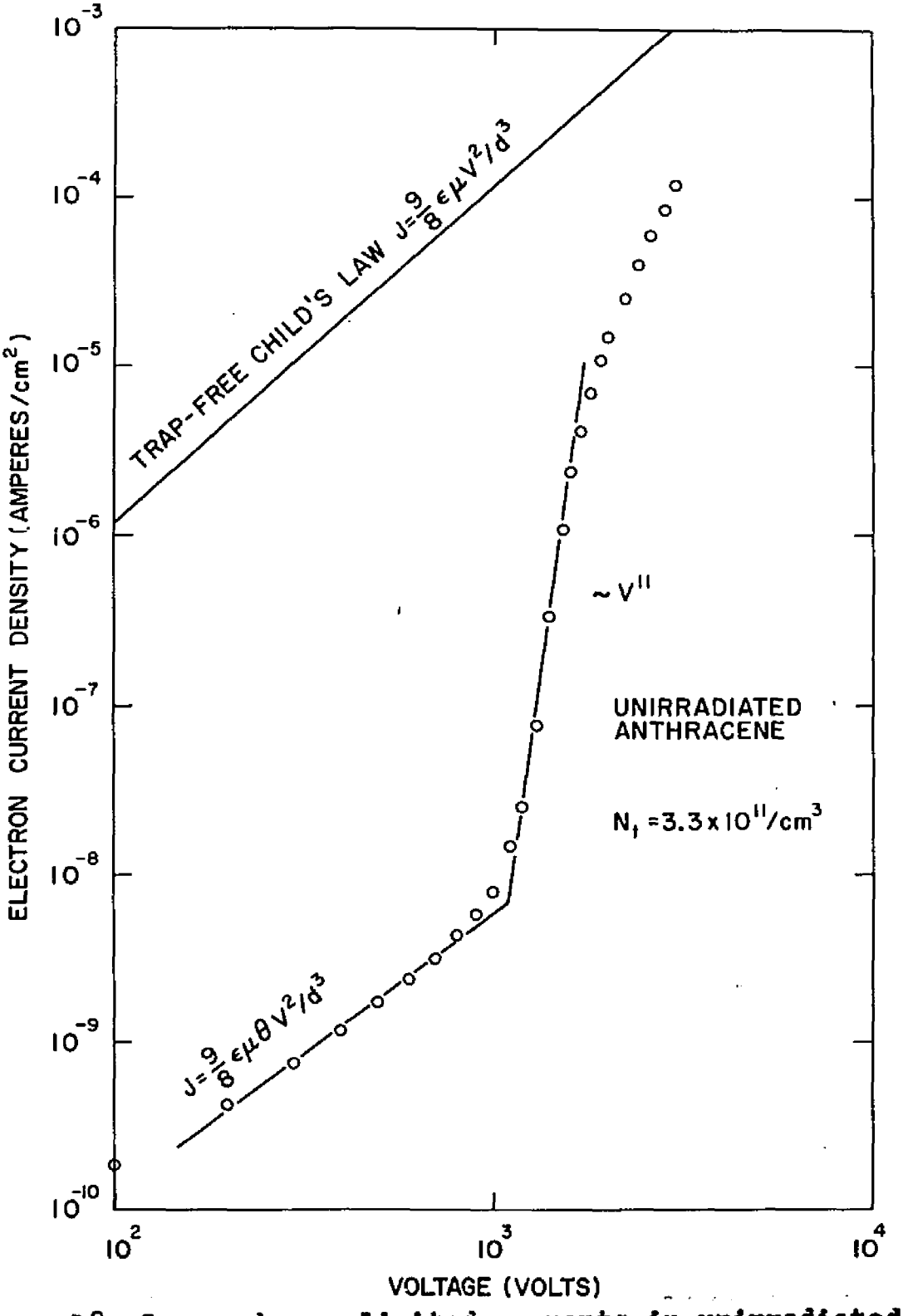

Figure 18. Space charge limited currents in unirradiated anthracene illustrating the steep rise in current at the trap filled limit.

in Table 3:

Crystal Number	Trap Density ($10^{11}/cm^3$)
1	10.5
2	3.3
3	4.0
4	3.3

Table 3. Electron Trap Densities

The increment trap density following radiation at doses of 500 R and 1000 R were found to be $\sim 10^9$ traps/cm^3R. Figure 19, representing crystal #1, shows that the voltage necessary to reach the trap-filled-limit increases as more traps are introduced into the crystal. Also, as the trap density is increased, a smaller fraction of the injected carriers will be free, resulting in a smaller current at a corresponding value of voltage. The voltage threshold is usually less pronounced suggesting a distribution in energy somewhat different from the unirradiated condition.

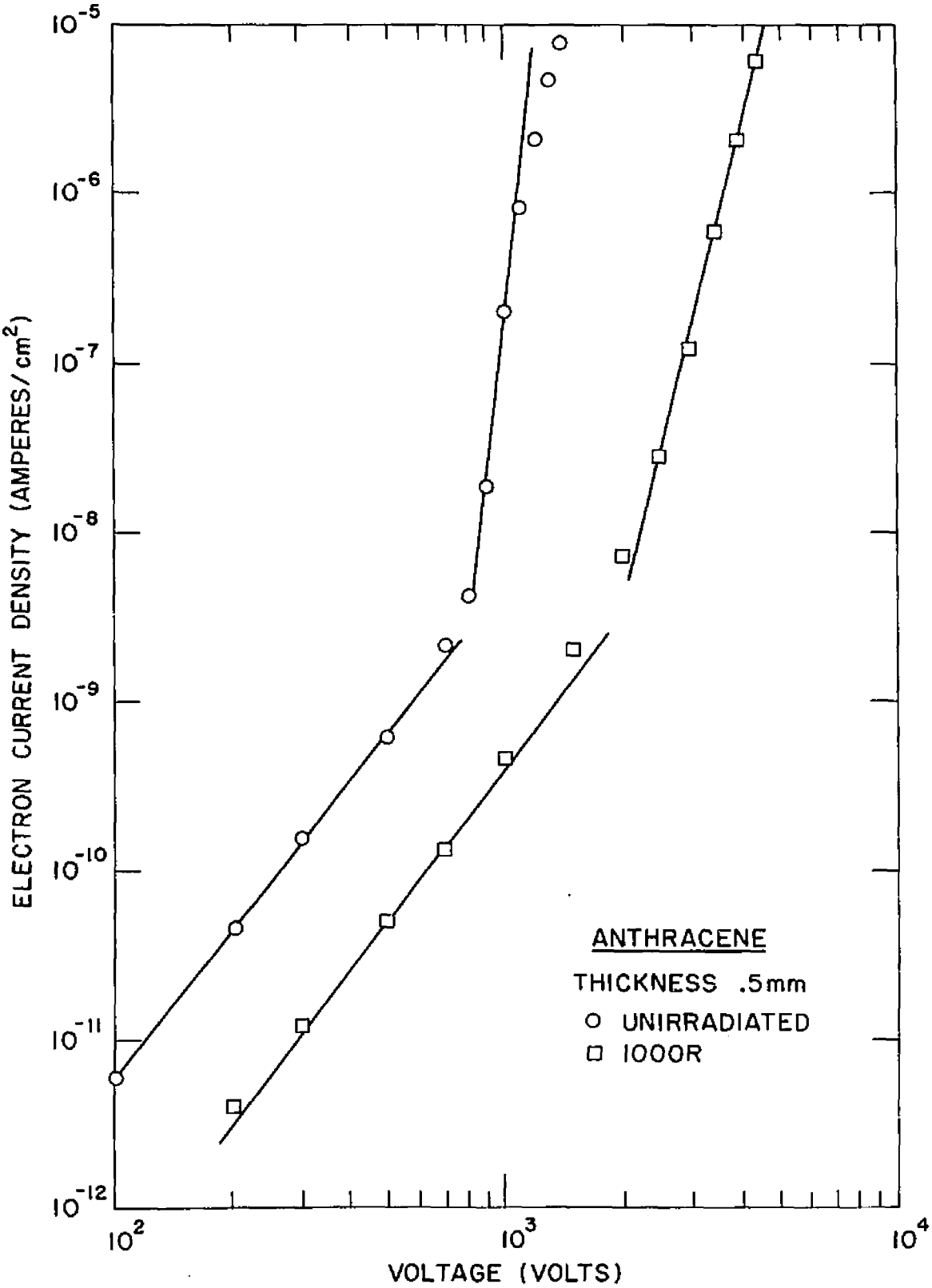

Figure 19. Change in trap filled limit as a result of irradiation.

F) Phenanthrene

The electrical properties of phenanthrene are markedly different from those of anthracene. Whereas the photocurrent of anthracene may be many orders of magnitude above the dark current, no such photocurrent capability has been seen in phenanthrene. Also, as previously noted, anomalous behavior in the electrical conductivity of phenanthrene has been found in the vicinity of 72°C. Peculiarities in the resistivity[21,22,23] of compressed powders of phenanthrene were reported but it was only with the attainment of single crystals[24] that a marked pyroelectric behavior, dependent upon the crystal's history was found.

A phenanthrene crystal is in a "reversibly polarized" state after the material has heated to above 72°C and then cooled in the presence of an electric field. Upon cooling, a pulse of current is detected in the vicinity of 72°C. Upon reheating the crystal a current pulse, opposite in direction to the previous pulse, is obtained. The directions of the pulses are dependent upon the sign of the applied bias. If the crystal is cooled and heated without a bias, no current pulse is observed. The magnitude of the charge release is a function of the applied field and appears to saturate at 10 kv/cm. If the crystal is illuminated in an electric field, with either white or monochromatic light prior to heating, a much larger charge

release is observed. Upon reheating the crystal, this supplementary charge release is not exhibited.

If a crystal has been illuminated and then heated with a biasing field, a new type of polarization appears. This polarization is characterized by the fact that the heating and cooling pulses are independent of any subsequent heating and cooling, direction of bias, or illumination. Crystals which exhibit these current pulses in the absence of an applied field are said to be in the "irreversibly polarized" state. Since neither cleaving nor chemical etching alter this result, the phenomenon is thought to be a volume rather than a surface effect. Occasionally crystals were found to exhibit this irreversible polarization without the necessity of illumination, possibly due to abrasion or the act of cleaving. Because the polarization appeared to be uniform through the crystal, its origin was thought to arise from an ordering effect of the molecules.

The growth of higher purity single crystals of phenanthrene facilitates the examination of certain aspects of the previously published data. Accordingly the dark conductivity and photoresponse at room temperature, and the effect of gamma radiation on the polarization phenomenon were studied.

The phenanthrene crystals used were cleavage plates.

All electrical measurements were made perpendicular to the cleavage plane, the ab plane. For resistivity and space charge measurements a wet cell type[25] of crystal holder, in which the crystal is placed between electrolytic solutions, was used. The contact area was 0.045 cm^2. A dry cell was used for photoconductivity and radiation damage studies. This crystal holder consists of one electrode of transparent SnO_2 conductive coating on quartz and the other of copper with an area of 0.057 cm^2 with a guard ring and thermocouple attached. The dry cell was mounted in an electrically heated oven and continually purged with purified nitrogen.

The conductivity of a phenanthrene crystal in a wet cell using 1 M NaCl electrodes is shown in Figure 20. For applied fields up to 2000 V/cm, the behavior is approximately ohmic and the resistivity of the crystal is $1.4 \times 10^{15}\ \Omega$-cm. At larger values of field, the current increased with the square of the voltage. No trap filled limit was obtained for values of electric fields less than 75,000 V/cm. The dark currents were slightly less than those previously reported but a comparable resistivity was obtained. The added purification procedures appear to have little effect upon these measurements.

The photoresponse of phenanthrene was determined using a dry cell holder. A photocurrent of 10^{-15} amp

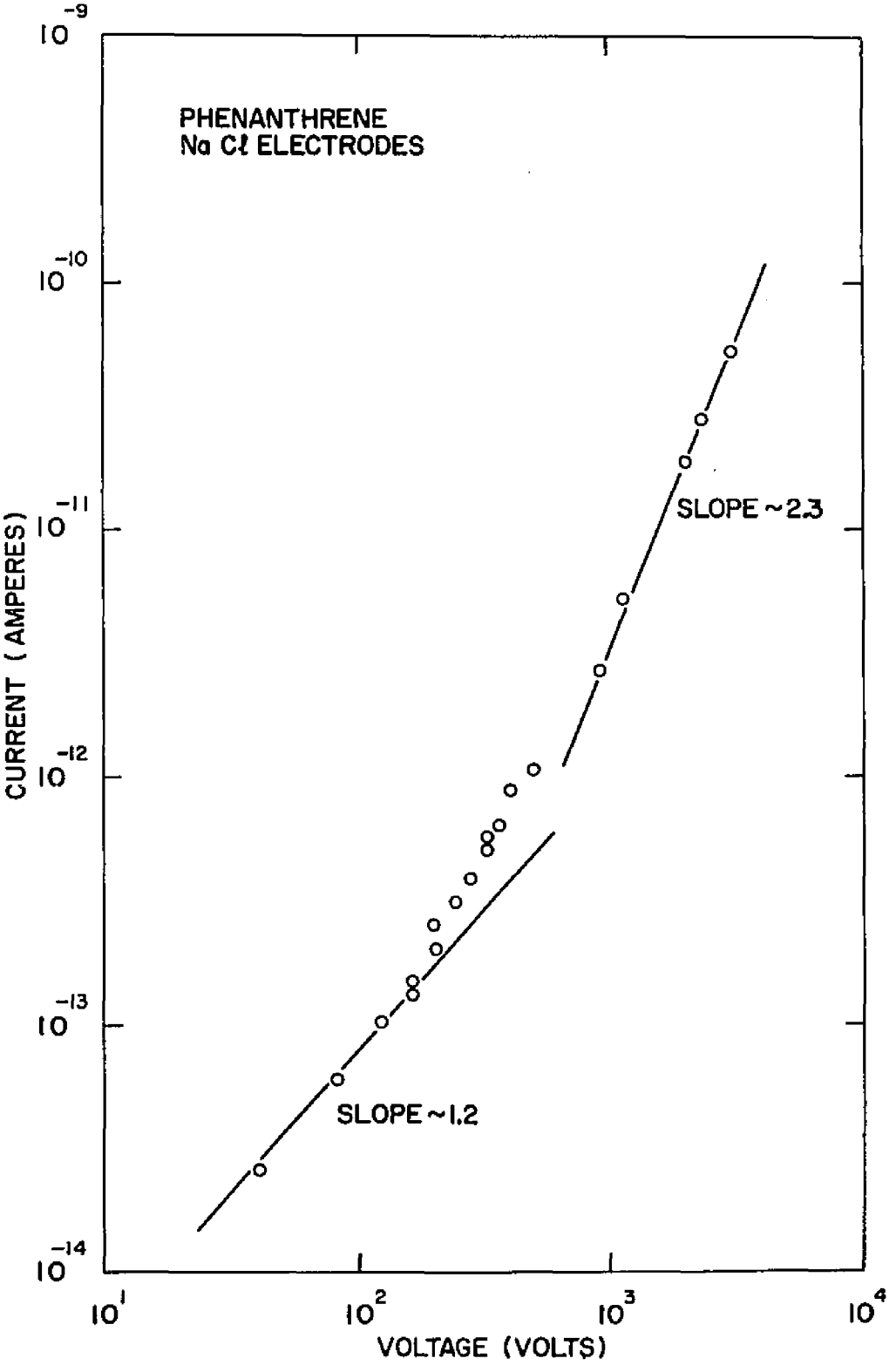

Figure 20. Phenanthrene conductivity using NaCl electrodes showing the transition from ohmic to space charge limited region.

was detected in the region 6000-3000A for a freshly cleaved crystal. Illumination was via an 800 watt Xenon arc lamp. After heating and cooling the illuminated crystal in a field of 10 kv/cm, the photocurrent at 6000A increased to 10^{-12} amps. The wavelength dependence of this photocurrent, uncorrected for lamp output, is shown in Figure 21. An anomalous dip of an order of magnitude in the current at 4200A, present in the previous work[24] is probably due to impurities in the sample, particularly anthracene which has a strong absorption near this wavelength.

To observe the effect of irradiation upon the polarization peaks, the crystal was first put into the "irreversibly polarized" state by illumination for thirty minutes with white light from an 800 watt Xenon source. The current pulse obtained upon heating, in the absence of an applied bias, as shown in Figure 22, can be associated with a charge release of 1.2×10^{-10} coul. Exposure to gamma irradiation led to a decrease of the charge released. As shown in Figure 22, for exposure doses up to 3×10^{3}R, the reciprocal charge decreased linearly with the dose,

$$(20)\quad \frac{1}{Q} = \text{Constant} + \alpha D$$

where Q is the charge released, D the exposure dose in

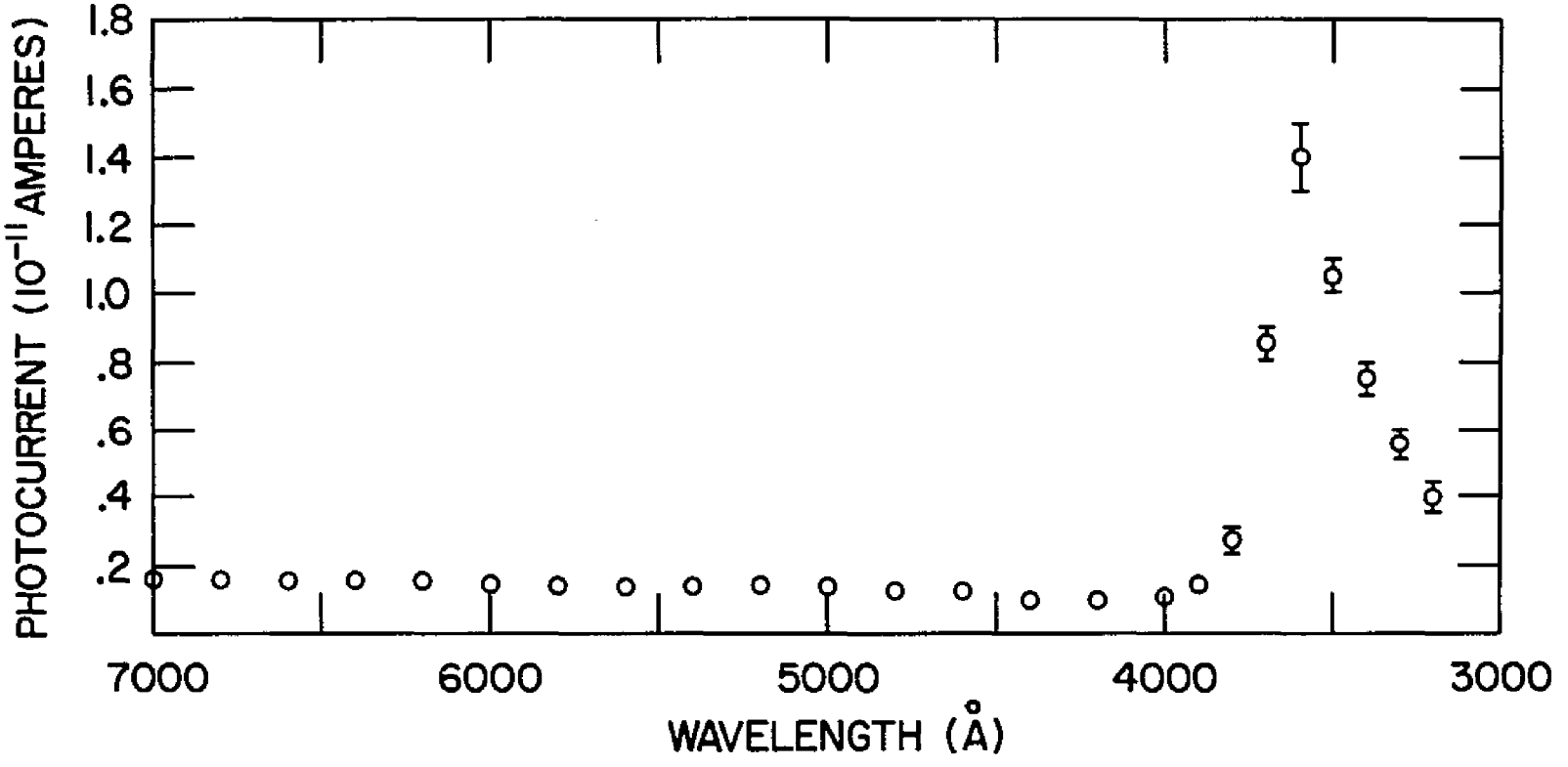

Figure 21. Phenanthrene photocurrent as a function of wavelength.

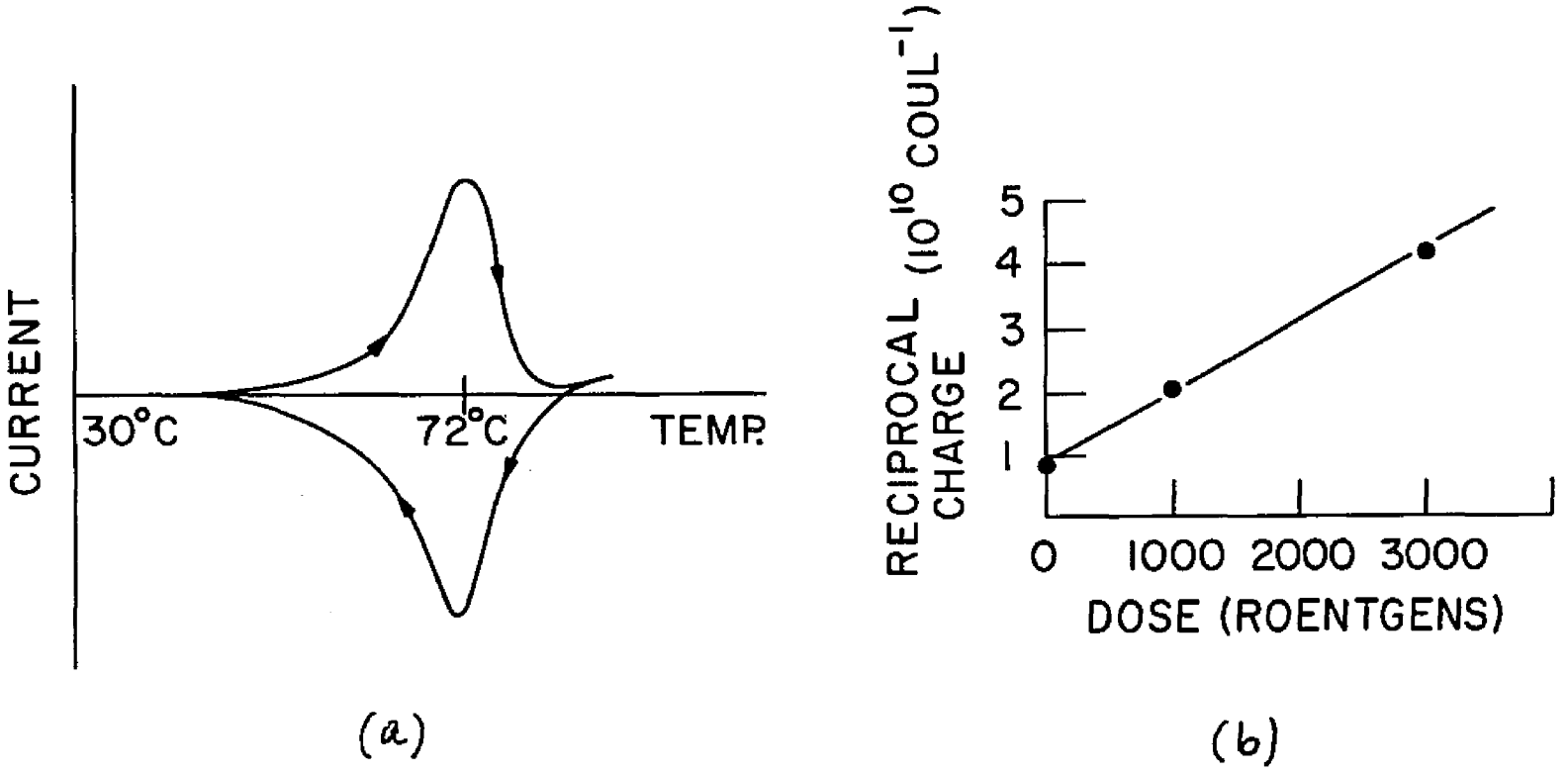

Figure 22. Phenanthrene charge release as a function of temperature and radiation exposure. (a) Charge pulse as a function of heating and cooling (not to scale). (b) Reciprocal charge release as a function of exposure dose.

Roentgens, and α has the value of 1.1×10^{7} coul^{-1} R^{-1}. A dose of 3×10^{3}R reduced the magnitude of the charge release by eighty percent. Annealing of the crystal at 85°C for 1100 minutes, in an atmosphere of nitrogen, did not result in recovery of the damage. The polarization believed arise from an ordering effect of the molecules. If every phenanthrene molecule contributes to the charge release, the pulse would be due to 4×10^{21} molecules/cm^{3}. From Figure 22, an exposure of 1000 R decreased the charge release by 50%, thus preventing 2×10^{21} molecules/cm^{3} from contributing to the pulse. This radiation produced 10^{12} traps/cm^{3} in anthracene and it is reasonable to assume that an equivalent number of phenanthrene molecules will be damaged by this dose. This strongly suggests that the polarization, which is the origin of the charge release in phenanthrene, is a cooperative phenomenon because the damage of one molecule hinders the molecular alignment within a distance of 10^{3} molecular centers from the damage site.

References

1. M. Pope and H. Kallman, "A-C and D-C Photoconductivity in Anthracene Single Crystals" in Symposium on Electrical Conductivity in Organic Solids, ed. H. Kallmann and M. Silver, (Interscience Publishers, New York, 1961)

2. R. G. Kepler, Phys. Rev. 119, 1226 (1960) and "Charge Carrier Mobility and Production in Anthracene" in Organic Semiconductors, ed. J. J. Brophy and J. W. Buttrey, (MacMillan Co., New York, 1962)

3. O. H. LeBlanc Jr., J. Chem. Phys. 33, 626 (1960), J. Chem. Phys. 30, 1443 (1959)

4. D. N. Bailey and D. M. Hercules, J. Chem. Educ. 42, A83 (1965)

5. M. Silver, J. R. Rho, D. Olness, and R. C. Jarnagin, J. Chem. Phys. 38, 3030 (1963)

6. D. C. Hoesterey and G. M. Letson, J. Phys. Chem. Solids, 24, 1609 (1963)

7. P. L. Kronick and M. M. Labes, Mol. Cryst. 2, 293 (1967)

8. M. Silver, M. Swicord, R. C. Jarnagin, A. Many, S. Z. Weisz and M. Simhony, J. Phys. Chem. Solids 23, 419 (1962)

9. A. Many, M. Simhony, S. Z. Weisz, and J. Chem. Phys. Solids 22, 285 (1961)

10. R. A. Smith, Semiconductors, (Cambridge U. Press, London, 1959)

11. R. H. Bube, Photoconductivity in Solids, (J. Wiley, New York, 1960)

12. P. Mark and W. Helfrich, J. Appl. Phys. 33, 205 (1962)

13. O. H. LeBlanc Jr., J. Chem. Phys. 35, 1275 (1961), J. Chem. Phys. 36, 1082 (1962), J. L. Katz, S. A. Rice, S. I. Choi and J. Jortner, J. Chem. Phys. 39, 1683 (1963), R. Silbey, J. Jortner, S. A. Rice, and M. T. Vala Jr., J. Chem. Phys. 42, 733 (1965), J. Chem. Phys. 43, 2925 (1965)

14. S. Z. Weisz, A. Cobas, P. E. Richardson, H. H. Szmant and S. Trester, J. Chem. Phys. 44, 1364 (1966)

15. G. J. Dienes and G. H. Vineyard, Radiation Effects in Solids, (Interscience Publishers, New York, 1957)

16. W. Helfrich, "Space-charge-limited and volume-controlled currents in organic solids" in Physics and Chemistry of the Organic Solid State, ed. D. Fox, M. M. Labes, and A. Weissberger, (Interscience Publishers, New York, 1967), Vol. III, R. H. Tredgold, Space Charge Conduction in Solids (Elsevier Pub. Co., New York, 1966)

17. N. F. Mott and R. W. Gurney, Electronic Processes in Ionic Crystals, (Clarendon Press, Oxford, England, 1940)

18. A. Rose, Phys. Rev., 97, 1538 (1955), M. Lampert, Phys. Rev., 103, 1648 (1956)

19. W. Buchner and W. Mehl, Z. Physik, Chem. N. F. 44, 376 (1965), W. Mehl and W. Buchner, Z. Physik Chem. N. F. 47, 76 (1965), I. Granacher, Solid State Comm. 3, 331 (1965)

20. P. Mark and W. Helfrich, J. Appl. Phys. 33, 205 (1962)

21. P. A. Andrews, A. F. Armington and B. Rubin, Appl. Phys. Letters 7, 86 (1965)

22. S. Matsumoto, Bull. Chem. Soc. Japan 40, 2749 (1967)

23. S. Matsumoto & T. Tsukada, Bull. Chem. Soc. Japan 38, 2023 (1965)

24. R. A. Arndt and A. C. Damask, J. Chem. Phys. 45, 4627 (1966)

25. H. Kallman and M. Pope, Rev. Sci. Intr. 29, 993 (1958), Rev. Sci. Inst. 30, 44 (1959)

V. HIGH DOSE RADIATION DAMAGE

The relationship between radiation damage and fluorescence changes in anthracene and related organic solids has been studied by several investigators under a variety of experimental conditions.[1] From the irradiation of aromatic hydrocarbons with either alpha rays, gamma rays, or electrons, a quantitative relation between fluorescence degradation and exposure dose was determined. Sharn[2] also observed an increase in optical absorption of an anthracene flake in the region of 4000Å for an exposure of $\sim 10^7$R.

Blum et al.,[3] were the first to investigate color center absorption in anthracene single crystals. Following a Co^{60} gamma irradiation of $\sim 10^8$R, the crystals became brownish-yellow in color. Optical absorption peaks, situated on a broad background absorption, were prominant at 6060A and 5350A. Samples irradiated in vacuum and in air gave identical results. Figure 23 illustrates the absorption peaks in irradiated anthracene. The peak height of the absorptions were found to increase linearly with dose for doses of $10^7 - 10^9$R. To study the kinetics of the absorption, the crystals were annealed isochronally for 45 minutes in the temperature range 40-200°C. At the lower temperatures the annealing resulted in the reduction of the

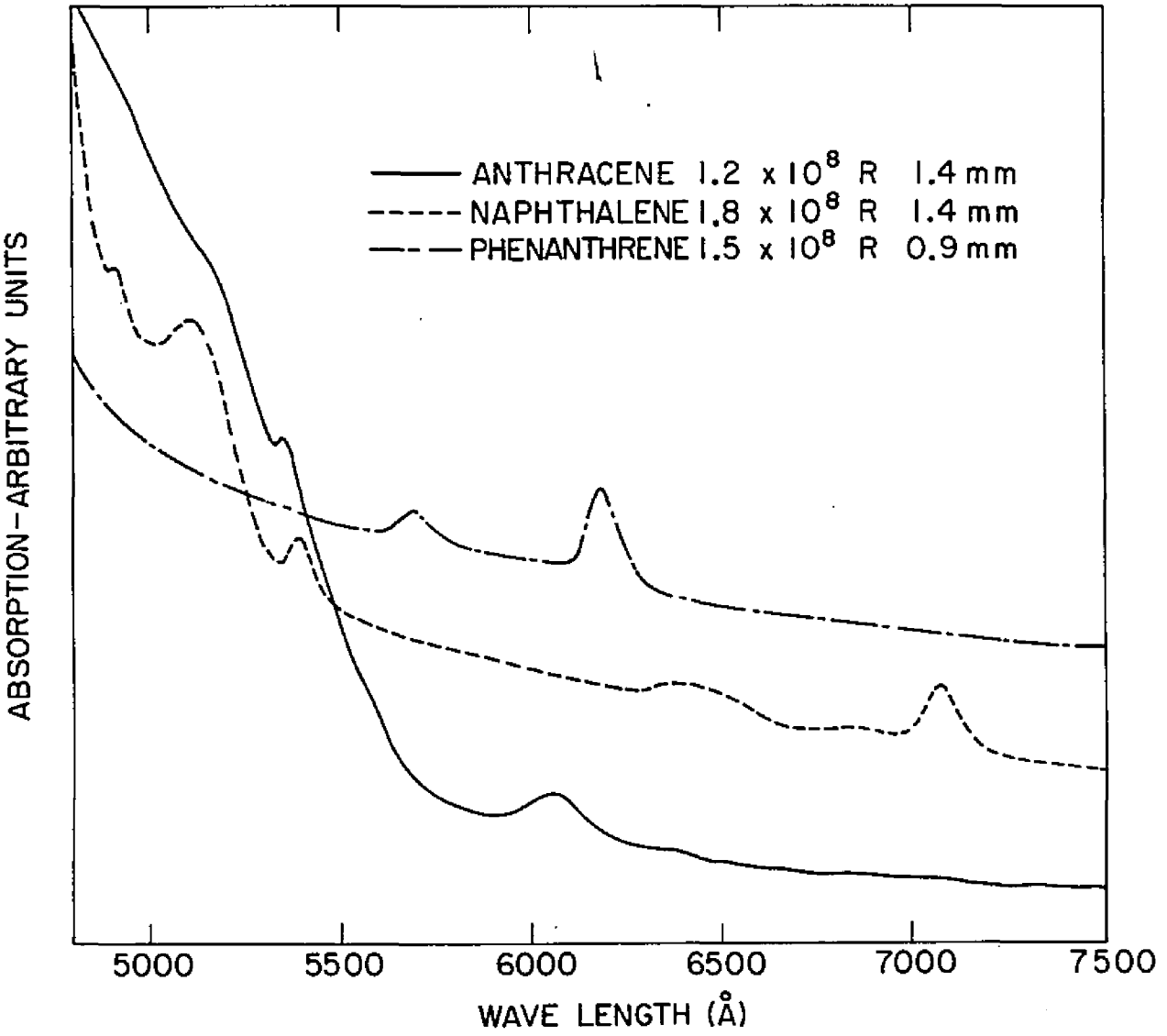

Figure 23. Color centers in irradiated anthracene, naphthalene, and phenanthrene. Crystal thickness is designated in millimeters(mm).

radiation induced background and in the growth of the absorption peaks. At 140°C these peaks reached a maximum in intensity and further annealing reduced the magnitude of the absorptions. Figure 24 illustrates the relative changes in the color center absorptions as a function of wavelength and annealing temperature. Figure 25 shows the optical density of the 5350Å and 6060Å absorption peaks as a result of 45 minute isochronal annealing. As a result of the annealing, the crystal changes color from brown-yellow (at 30°C) to bright orange (at 170°C). Absorption peaks at 4950Å and 4530Å become apparent at these higher temperatures.

In addition to optical absorption, electron paramagnetic resonance measurements revealed the presence of an absorbing defect which was attributed to the formation of a cross-linked polymer. The signal strength increased linearly with dose up to 10^9R and consisted of four equally spaced Gaussian lines with an intensity ratio of 1:3:3:1. Annealing of the crystal resulted in a decrease in signal strength (Figure 25). A comparable spectrum was reported by Harrah and Hughes[4] and by Inoue.[5] These investigators attributed the signal to the addition of a hydrogen atom to the 9 position in anthracene.

Thermal bleaching of radiation produced defects in organic materials is not considered unusual.[6] However, the

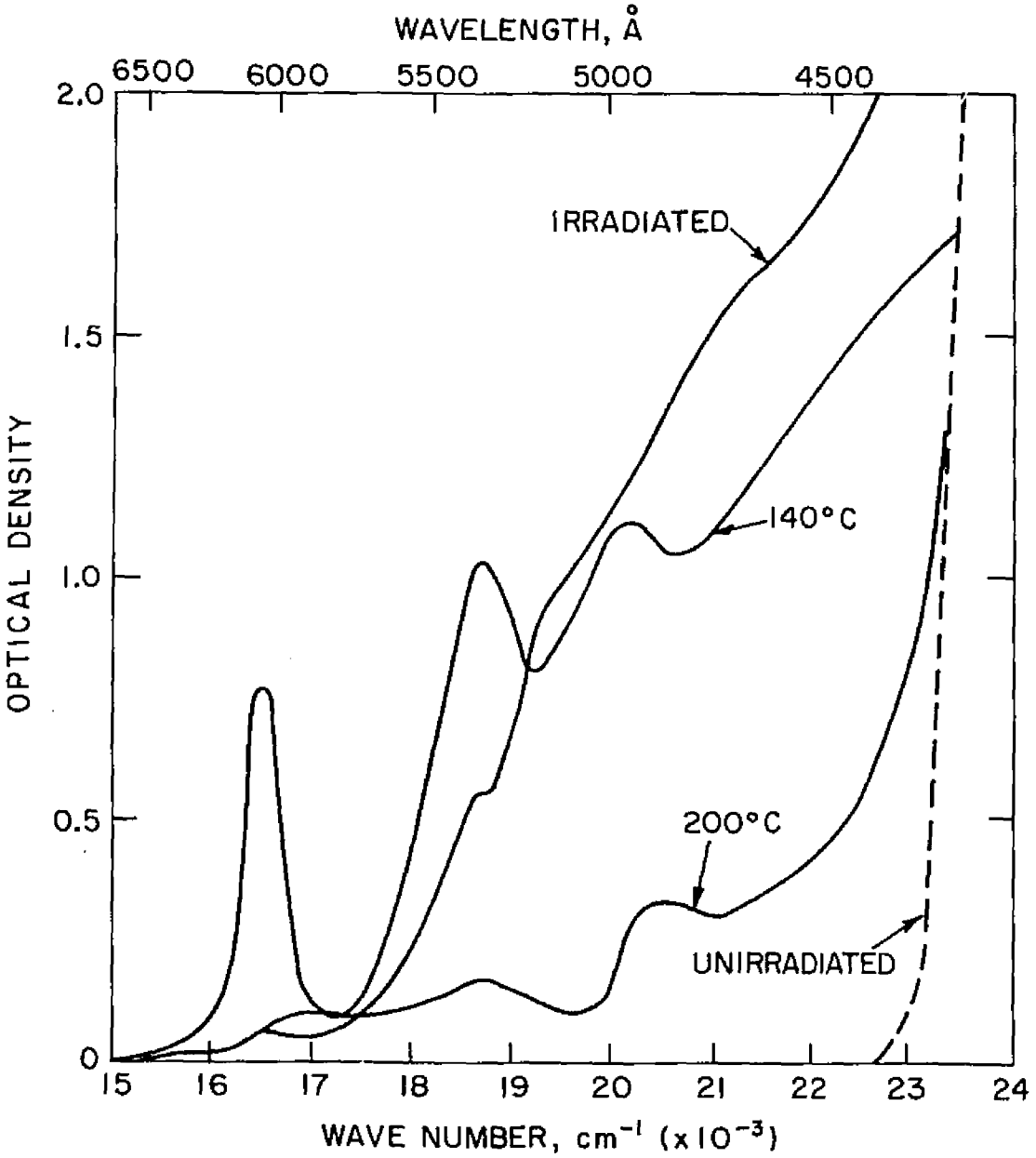

Figure 24. Optical density of anthracene crystals as a function of wavelength. The 140°C and 200°C indicate annealing temperature following gamma irradiation.
(from Blum et al.)

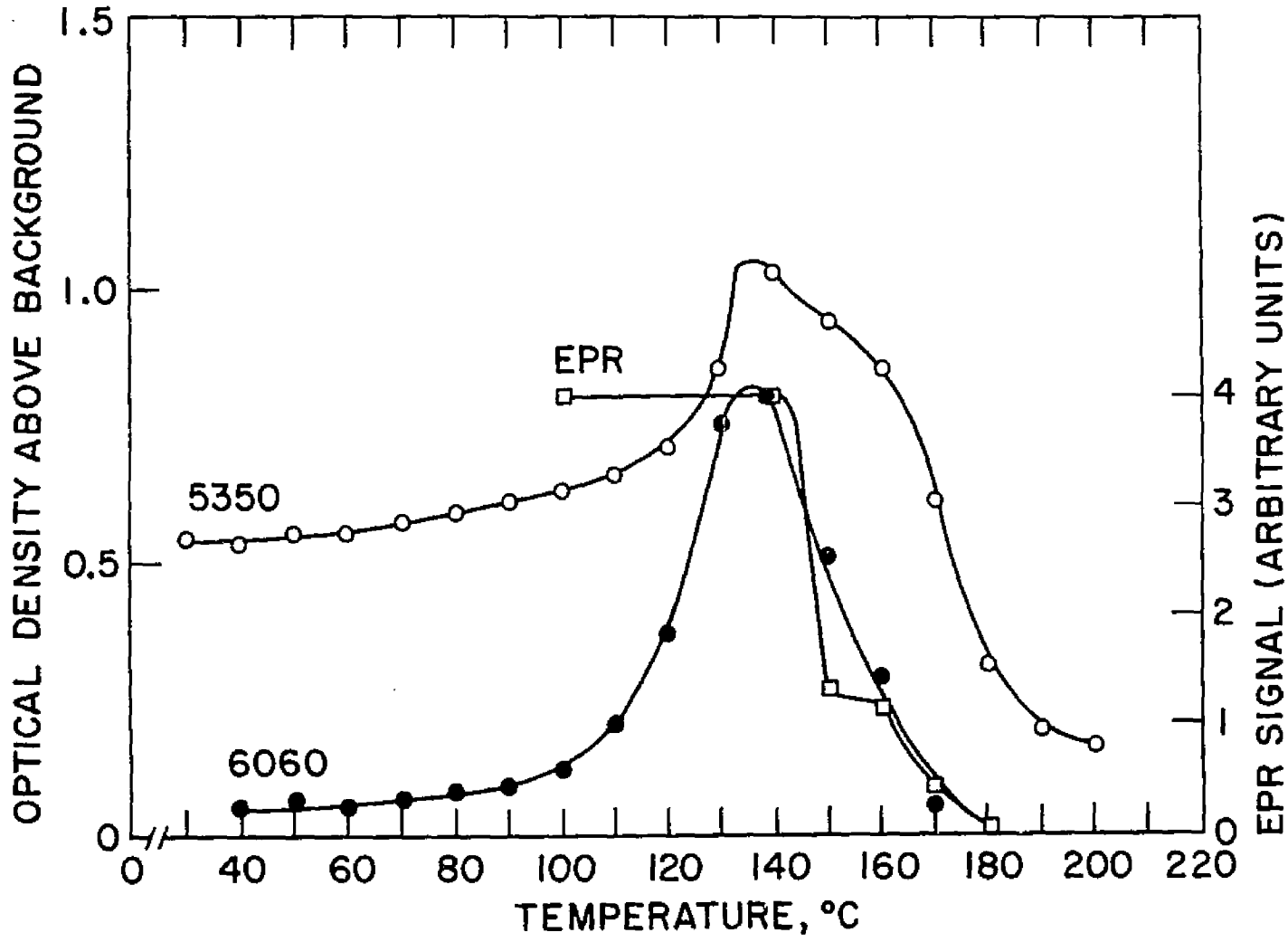

Figure 25. Optical density of 5350Å and 6060Å absorption peaks (left scale) and ESR signal (right scale) during 45 minute isochronal annealing. (from Blum et al.)

report by Blum et al.,[3] that the concentration of the optical absorbing species increased with annealing indicates a behavior pattern not previously reported for these materials.

The primary objective of this part of the investigation is an analysis of the annealing kinetics of color centers in irradiated anthracene, naphthalene, and phenanthrene. Because of the similarity in structure of naphthalene and anthracene, a similarity in reaction kinetics and thermal stability of the radiation induced defect would not be surprising. No color center formation in phenanthrene has been previously reported. In anthracene crystals, the 5350A peak is obscured to some extent by the background at the lower annealing temperatures. For this reason, and because of the steep rise in background in this region, the 6060Å absorption was used for the kinetic analysis. In naphthalene the 7070Å absorption and in phenanthrene the 6150Å absorption are analyzed. Attempts at identification of the defects using the techniques of EPR and gas chromatography will also be described.

A) Experimental Techniques

Using the technique of isothermal annealing of a set of identically irradiated samples, one may obtain both the activation energy and the rate constants governing the reaction.[7]

The crystals to be studied were irradiated at the Brookhaven gamma facility for doses of 10^8R. The surfaces of the material were polished using an appropriate solvent, usually either xylene of alcohol, and the crystal was then placed into the sample compartment of a Cary 14 spectrophotometer.

The Cary 14 is a dual beam spectrometer employing automatic compensation for the reference signal. Automatic scanning from 26,000-1800Å at a variety of speeds is provided. A scanning rate of 10Å/sec was used for all measurements. The instrument is capable of measuring optical densities of 0.01-2.00. For absorptions greater than 2.00 neutral density filters are necessary. The optical density is obtained from Beer's Law and is defined as:[8]

$$(21) \quad O.D. = \log_{10} \frac{I_o}{I}$$

where I_o and I represent respectively the intensities of the incident and transmitted radiation. The crystals were oriented by noting the double refraction along the b-axis.[9] Fiducial marks were scribed onto the crystal to indicate orientation. A polaroid filter, inserted between the light source and the crystal, served to polarize the beam. Unless otherwise stated, all absorption measurements are made with the incident light beam perpendicular to the ab cleavage plane.

For annealing, the crystals were placed in a pyrex vial and packed in a powder of the same material to reduce surface sublimation. A copper-constantan thermocouple, situated near the crystal, monitored the temperature. The annealing was in air in a furnace regulated by a West Model JP-S 22 temperature controller. Samples annealed in vacuum gave results identical to those annealed in air.

B) Anthracene - Unpolarized Light

Isothermal annealing curves for the 6060Å absorption of 1 mm thick anthracene crystals are shown in Figure 26. The incident light is normal to the ab plane and no polarizer has been inserted between the light and the crystal. The curves are characterized by an increase, followed by a decrease, in optical absorption. The data has been normalized with respect to the absorption maximum of each curve. A physical property characterized by the behavior of these curves can arise from consecutive first-order reactions of the type[10]

$$(22) \qquad N \longrightarrow n \longrightarrow N'$$

where N and n are the concentrations of a non-absorbing (at 6060Å) and an optically absorbing defect respectively

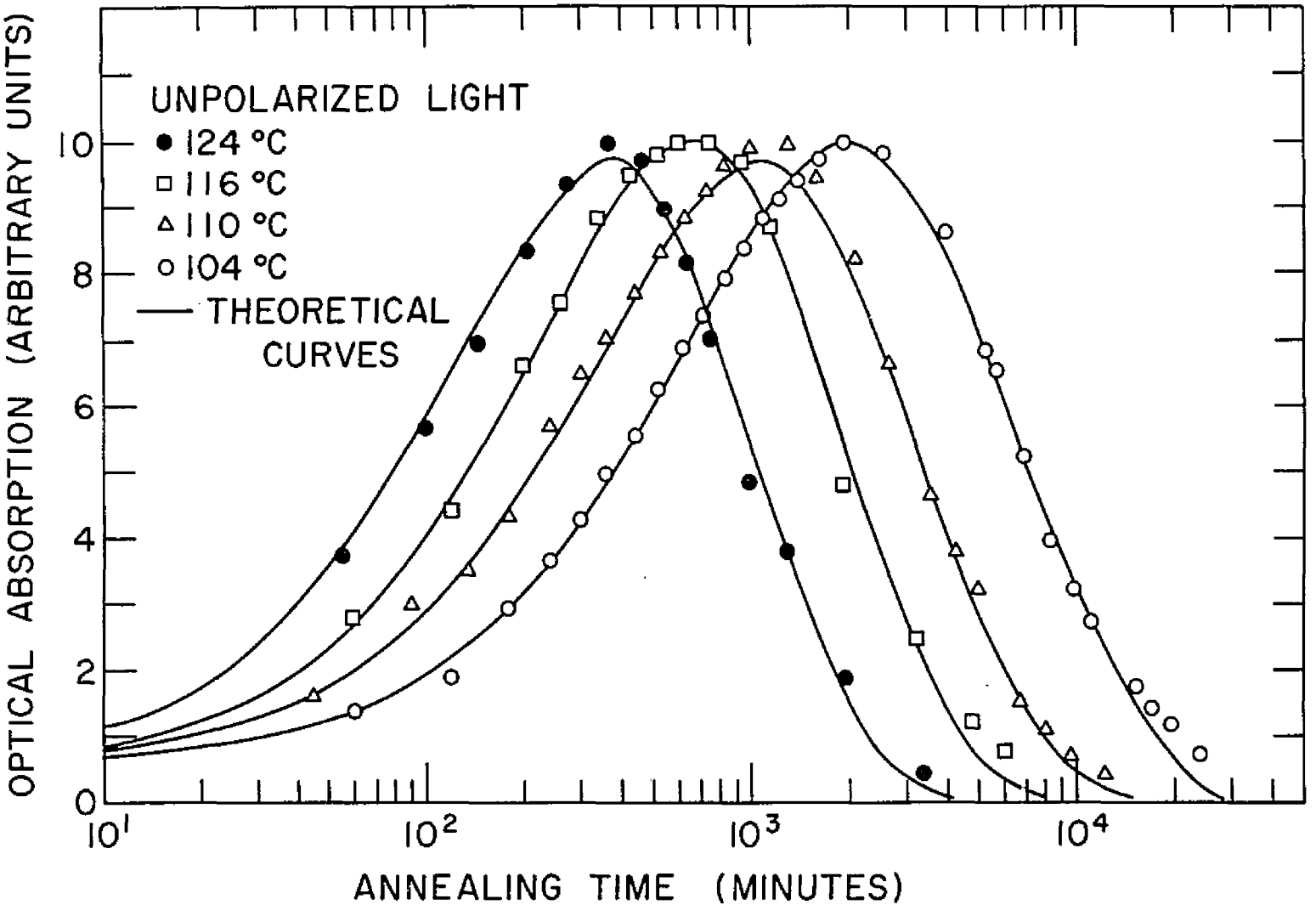

Figure 26. Isothermal annealing of irradiated anthracene: unpolarized light.

and N' represents the concentrations of a second non-absorber (at 6060Å) or the elimination of n from the crystal by diffusion. The rate constants for growth and decay are represented by k_1 and k_2.

For a first-order reaction, the rate of disappearance of N is given by:

$$(23) \quad \frac{dN}{dt} = -k_1 N$$

and the rate of change of n by:

$$(24) \quad \frac{dn}{dt} = k_1 N - k_2 n$$

Insertion of (23) into (24) and integration yields:

$$(25) \quad n = n_0 e^{-k_2 t} + \frac{k_1 N_0}{k_2 - k_1} \left[e^{-k_1 t} - e^{-k_2 t} \right]$$

where n_o and N_o are the defect concentrations prior to annealing. Approximate values of the rate constants and the activation energies of the growth and decay processes are obtained using the data points at short and long times, i.e. where the curves are governed by either growth or decay. Since $k_1 > k_2$ for the region following the maximum, equation (25) leads to:

$$(26) \quad n = (N_o + n_o) e^{-k_2 t}$$

whereby the decay constant and the value for N_o can be obtained graphically. For small values of time, k_1 can be obtained from the expansion of the exponentials in (25) to give:

$$(27)\quad n = n_o + bt \quad \text{where} \quad b = k_1 N_o - k_2 n_o$$

Using the assumption that a rate constant can be expressed in the Arrhenius form[11] $k = A e^{-E/KT}$ a value for the activation energy E is obtained. The largest source of error in the above analysis is the fact that the growth process is the resultant of two reactions, one, a decrease in the concentration of n and the other, an increase in n due to a decrease of N. A computer fit, utilizing the three parameters k_1, k_2, and N_o, of the experimental data to equation (25) results in a more accurate determination of the rate constants and energies. The solid lines in Figure 23 represent the computer curves. The rate constants are given in Table 4. The activation energies for growth and decay are 1.0 ± 0.2 eV and 1.5 ± 0.1 eV respectively.

C) Anthracene - Polarized Light

If the light which is incident perpendicular to the ab crystallographic plane is polarized parallel to either the a-axis or the b-axis, the intensity of the absorption is altered. In the as-irradiated condition, the b-axis

Temperature	k_1 (10^{-3})	k_2 (10^{-3})
104°C	1.14	.16
110°C	1.90	.36
116°C	2.82	.68
124°C	4.60	1.40
	1.0 ± 0.2 eV	1.5 ± 0.1 eV

Table 4. Rate Constants and Activation Energies. Unpolarized Light.

absorption exceeds that of the a-axis. The b-axis absorption remains dominant in the early stages of annealing and reaches a maximum value while the a-axis absorption is still increasing. As the b-absorption diminishes, the a-absorption reaches a maximum and becomes the major absorption constituent. A curve of this behavior is shown in Figure 27. These curves indicate that the absorptions are controlled by different rate mechanisms and that the absorption maxima for the orientations mentioned do not coincide. The growth of the a-absorption is probably a response to the decay of the b-absorption i.e., a process converting a defect from a b-dominant to an a-dominant absorption is involved. A simple rotation of the absorbing defect may give rise to the above conditions.

One possible kinetic scheme which may be responsible for the observed annealing of the absorptions may be written as:

(28)

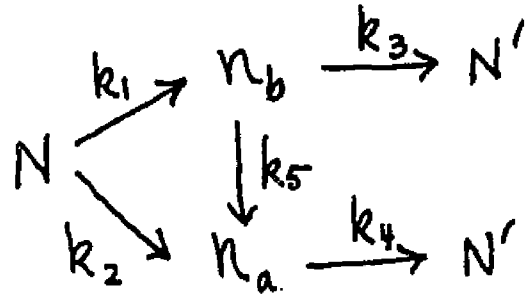

where N and N' are non-absorbers at 6060Å and n_b and n_a are the optical absorptions for the incident light parallel to the b and a-axes respectively. The rate constant k_1 is

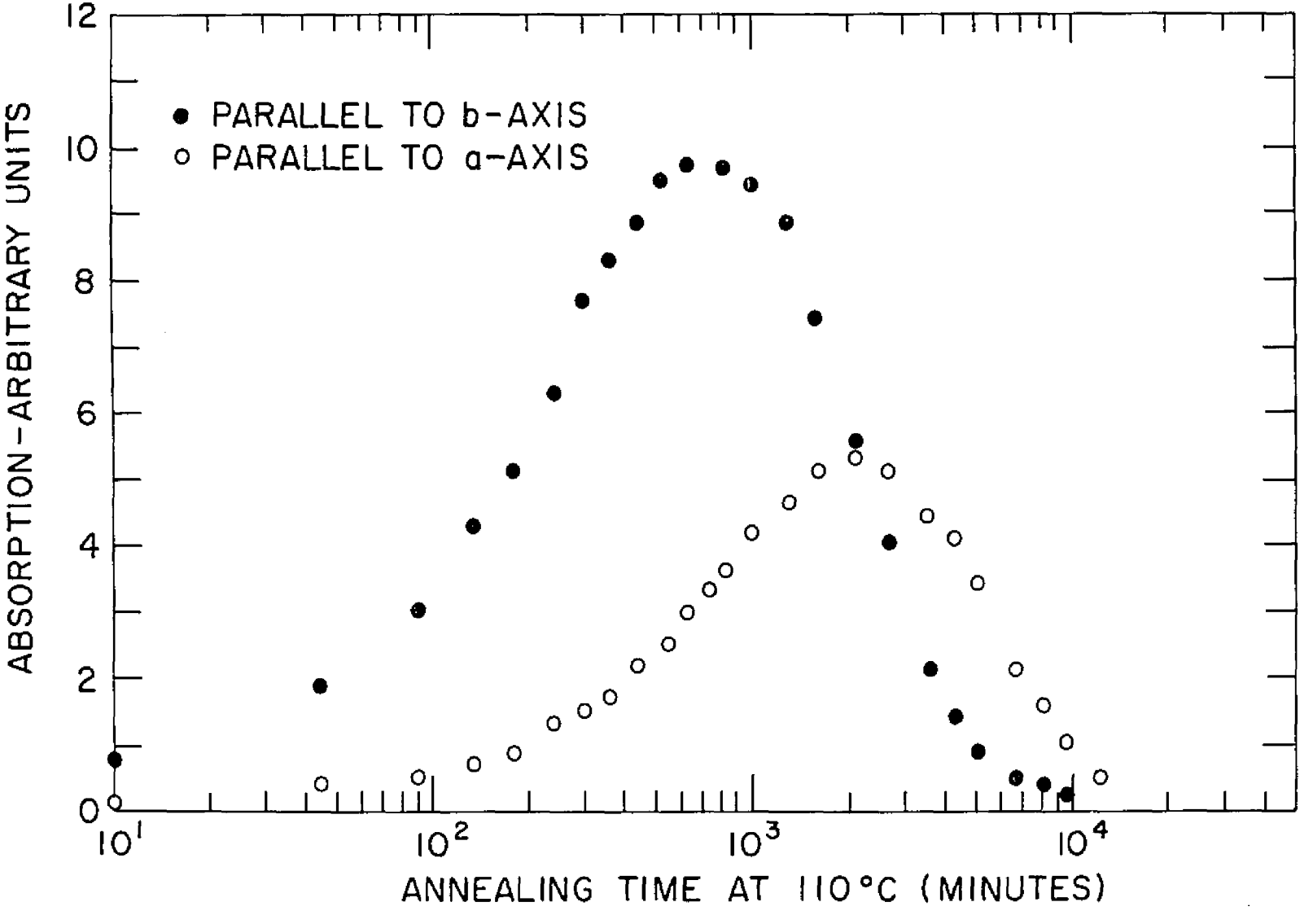

Figure 27. Splitting of absorption maxima using polarized light.

responsible for the growth and the constants k_3 and k_5 are responsible for the decay of the b absorption. In a similar fashion, k_2 and k_5 govern growth and k_4 governs decay of the a-absorption. The equations governing these reactions are:

$$(29)\quad \frac{dn_b}{dt} = k_1 N - (k_3 + k_5) n_b$$

$$(30)\quad \frac{dn_a}{dt} = k_2 N + k_5 n_b - k_4 n_a$$

$$(31)\quad \frac{dN}{dt} = -(k_1 + k_2) N$$

The solution of these equations gives rise to:

$$(32)\quad n_b = n_{bo} e^{-kt} + \frac{k_1 N_0}{k - K}\left[e^{-Kt} - e^{-kt}\right]$$

and

$$(33)\quad n_a = e^{-kt}\left[\frac{k_5 n_{bo}}{k_4 - k} - \frac{k_5 k_1 N_0}{(k-K)(k_4-k)}\right]$$

$$+ e^{-Kt}\left[\frac{k_2 N_0}{k_4 - K} + \frac{k_5 k_1 N_0}{(k-K)(k_4-K)}\right]$$

$$+ e^{-k_4 t}\left[n_{a_0} - \frac{k_5 n_{bo}}{k_4 - k} + \frac{k_5 k_1 N_0}{(k_4-k)(k_4-K)} - \frac{k_1 N_0}{k_4 - K}\right]$$

where n_{bo} and n_{ao} are the values of n_b and n_a prior to annealing, $k = k_3 + k_5$, and $K = k_1 + k_2$. All five rate constants can be determined by the procedure used to solve the equation for the unpolarized light absorptions, i.e. a linear approximation of the growth at short annealing times and a semi-log plot of the decay at long annealing times. As with the unpolarized light absorptions, computer processed solutions justify this procedure. Curves for a variety of annealing temperatures, using the b-absorption maximum as the normalization constant are shown in Figures 28 - 31. Values of the rate constants and activation energies are given in Table 5. The energies are determined from a semi-log plot of the rate constants.

It was of interest to investigate the splitting of the annealing maxima for light incident in directions other than perpendicular to the ab plane. Accordingly, a cube of anthracene of length 0.62 cm was irradiated to a dose of 10^8R. Light was incident perpendicular to the ab, bc, and ac' planes. Measurements were made with the light polarized parallel to the a, b, and c' directions, the c' direction being perpendicular to the ab plane. The cube was annealed isochronally for 45 minute intervals. A separation of the absorption maxima occurred only for light incident normal to the ab plane, as is shown in Figures 32 and 33. The magnitudes of the absorptions in the directions measured were: $c' > a$, $c' > b$, and $b > a$, indicating that the

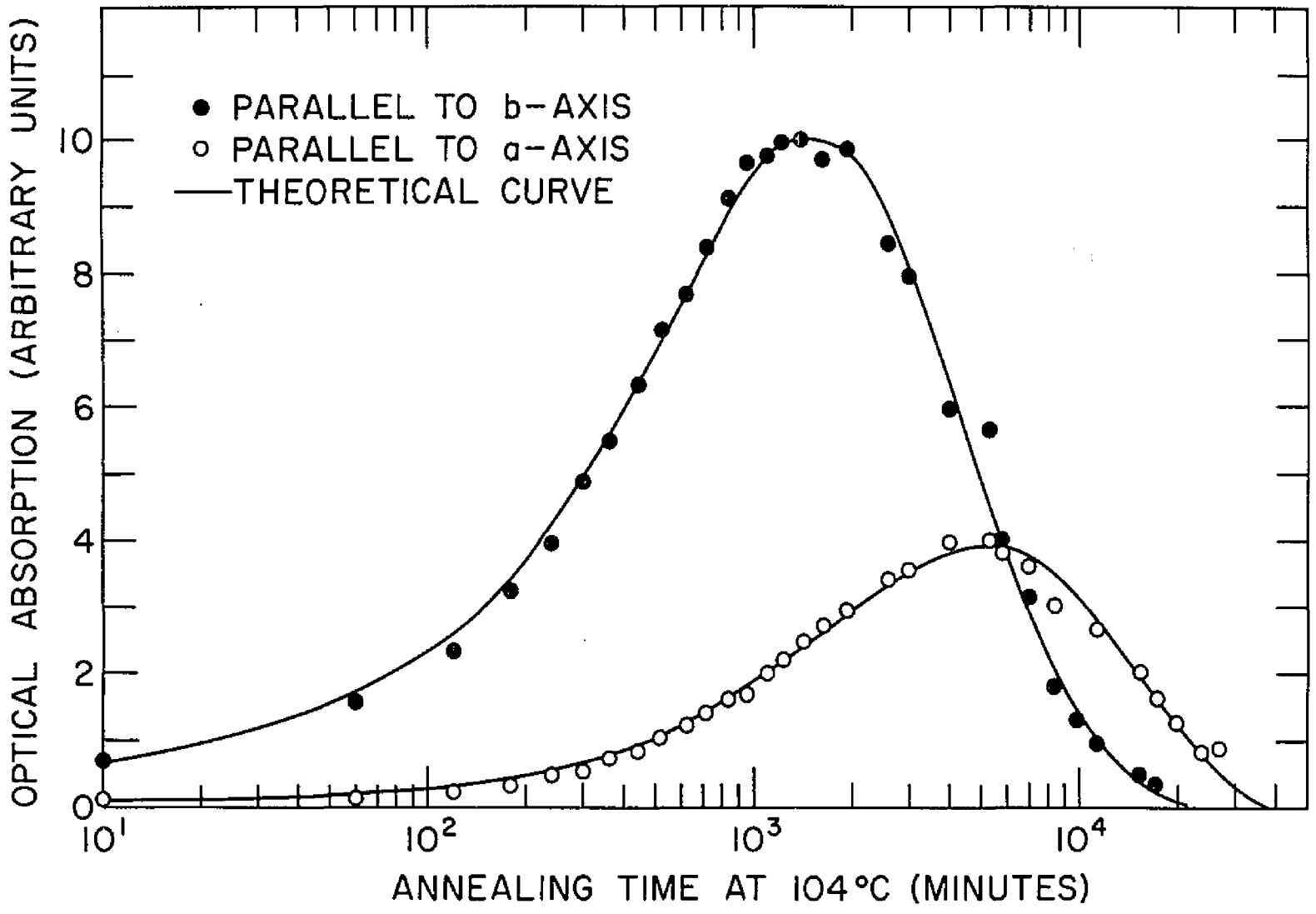

Figure 28. Isothermal annealing at 104°C: polarized light.

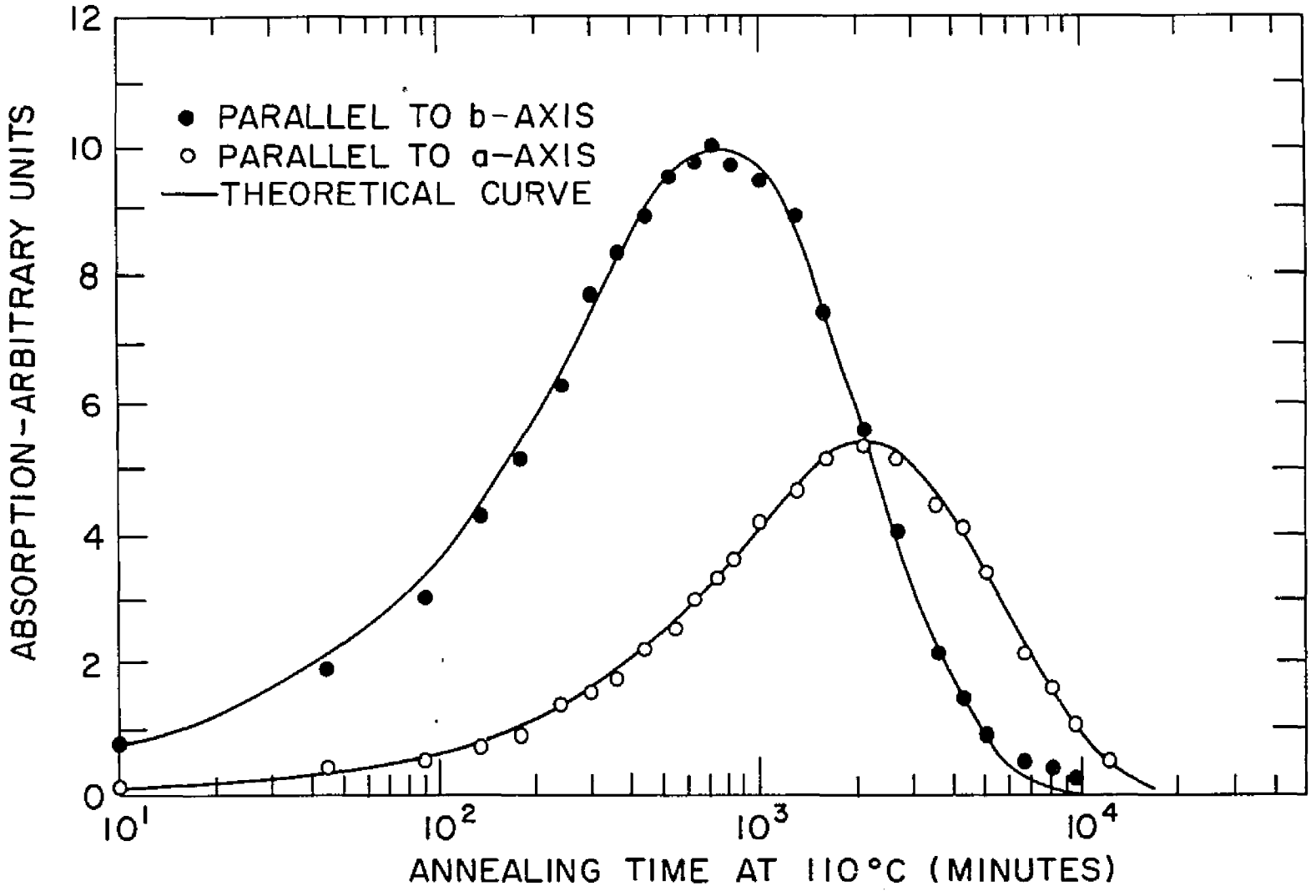

Figure 29. Isothermal annealing at 110°C: polarized light.

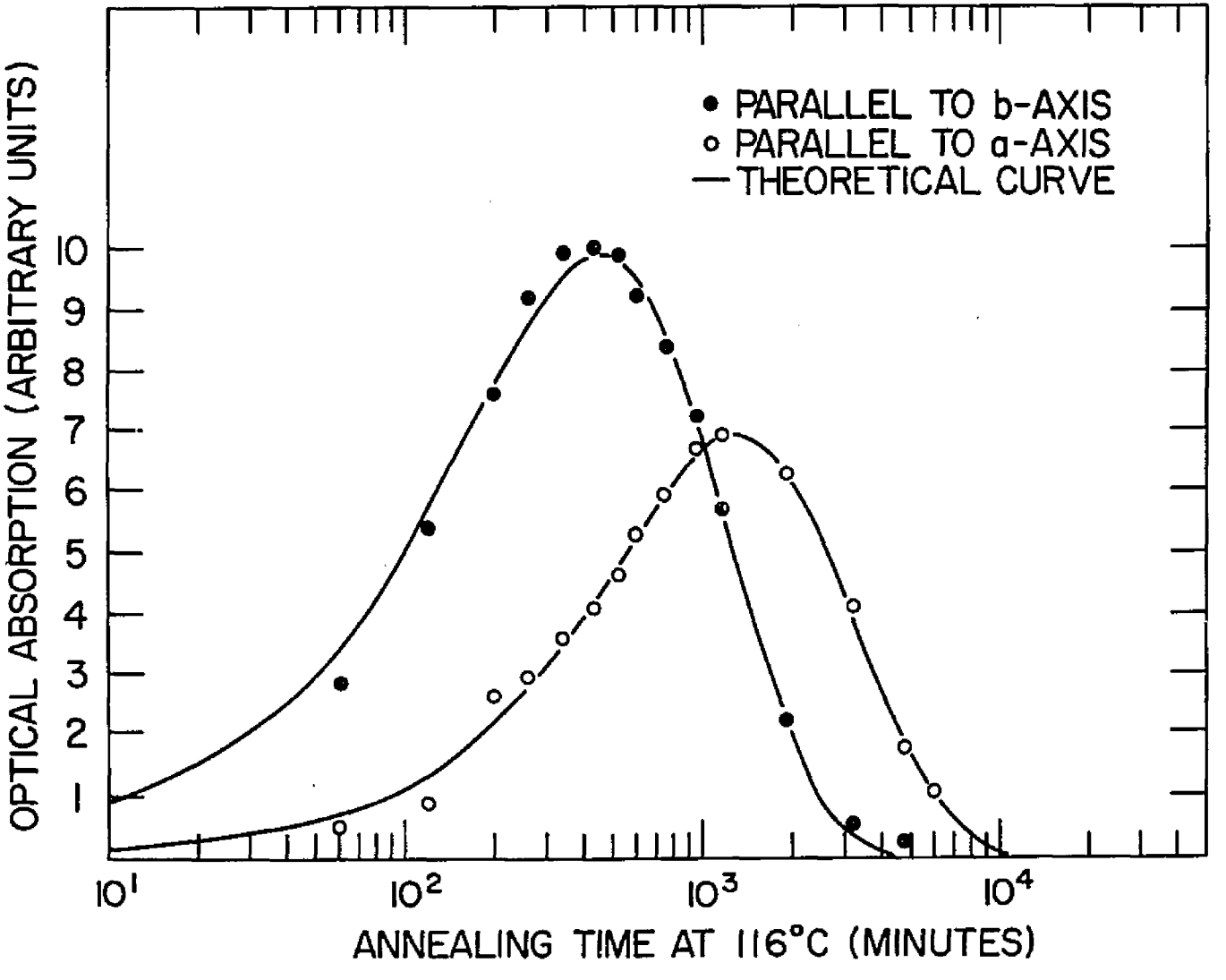

Figure 30. Isothermal annealing at 116°C: polarized light.

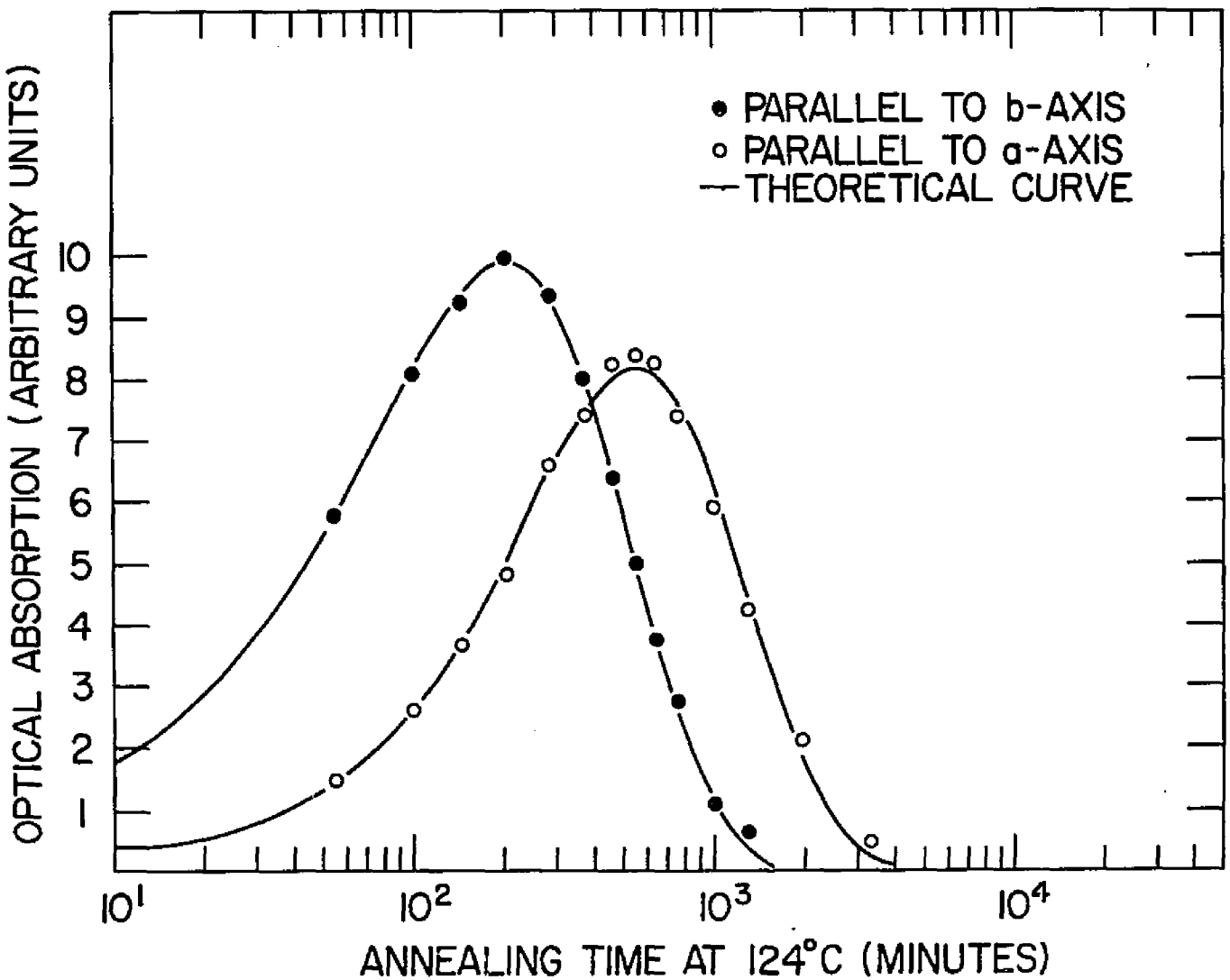

Figure 31. Isothermal annealing at 124°C: polarized light.

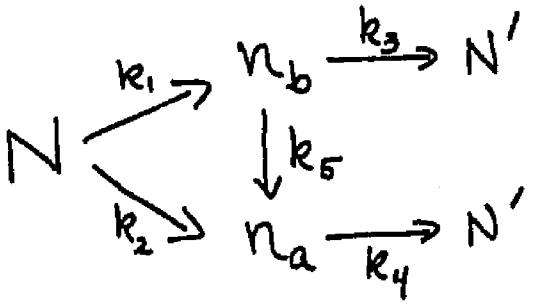

Temperature (°C)	$k_1(10^{-3})$	$k_2(10^{-3})$	$k_3(10^{-3})$	$k_4(10^{-3})$	$k_5(10^{-3})$
104	1.21	0.14	0.16	0.12	0.10
110	1.83	0.28	0.38	0.32	0.30
116	2.72	0.50	0.72	0.50	0.68
124	5.00	0.80	1.68	1.46	2.20
(eV)	1.2± 0.2	1.2± 0.2	1.6± 0.1	1.6± 0.1	2.0± 0.1

Table 5. Rate Constants and Activation Energies. Polarized Light.

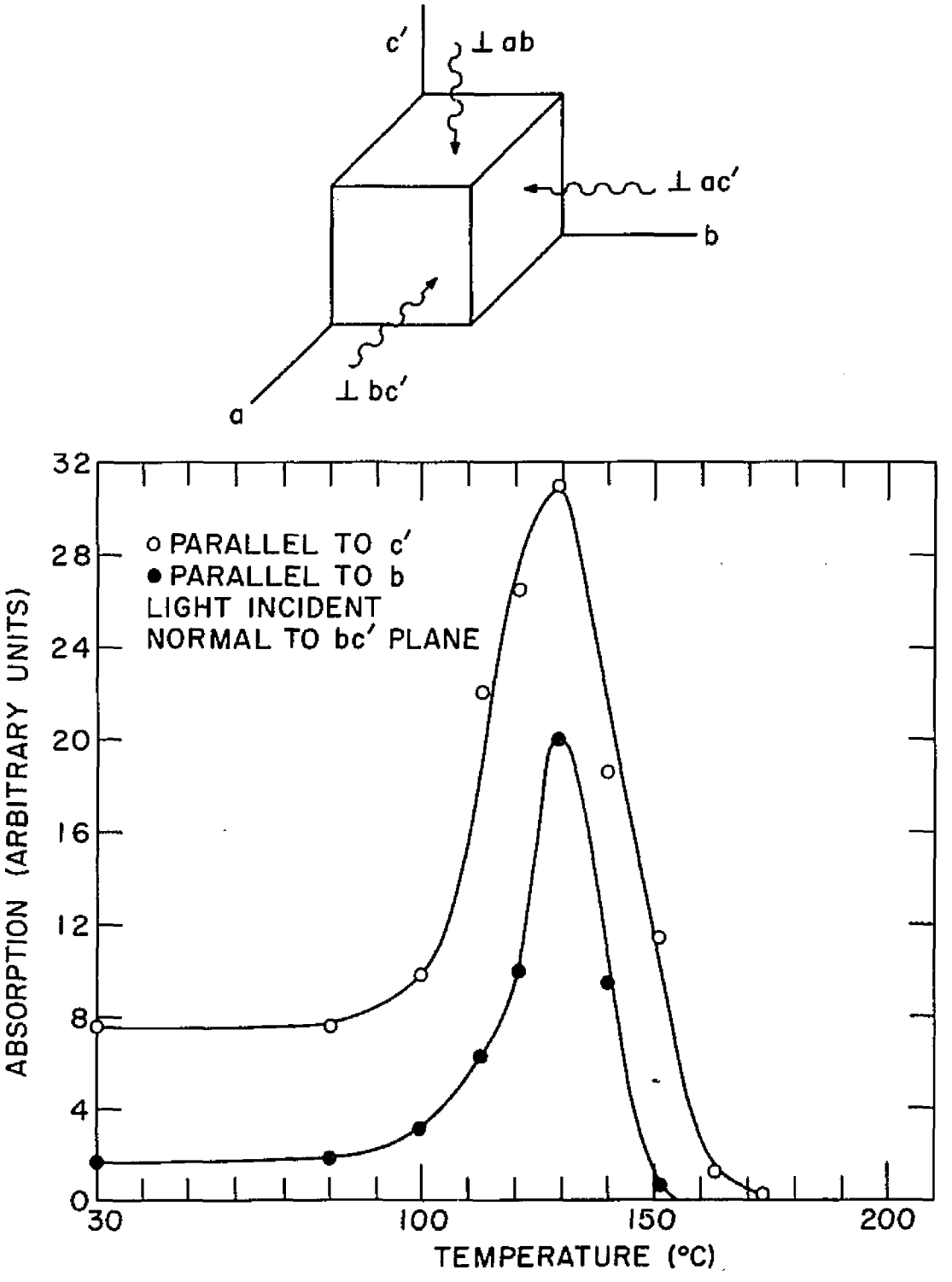

Figure 32. (a) Anthracene cube and directions of incident light. (b) 45 minute isochronal annealing curves for light incident normal to the bc′ plane.

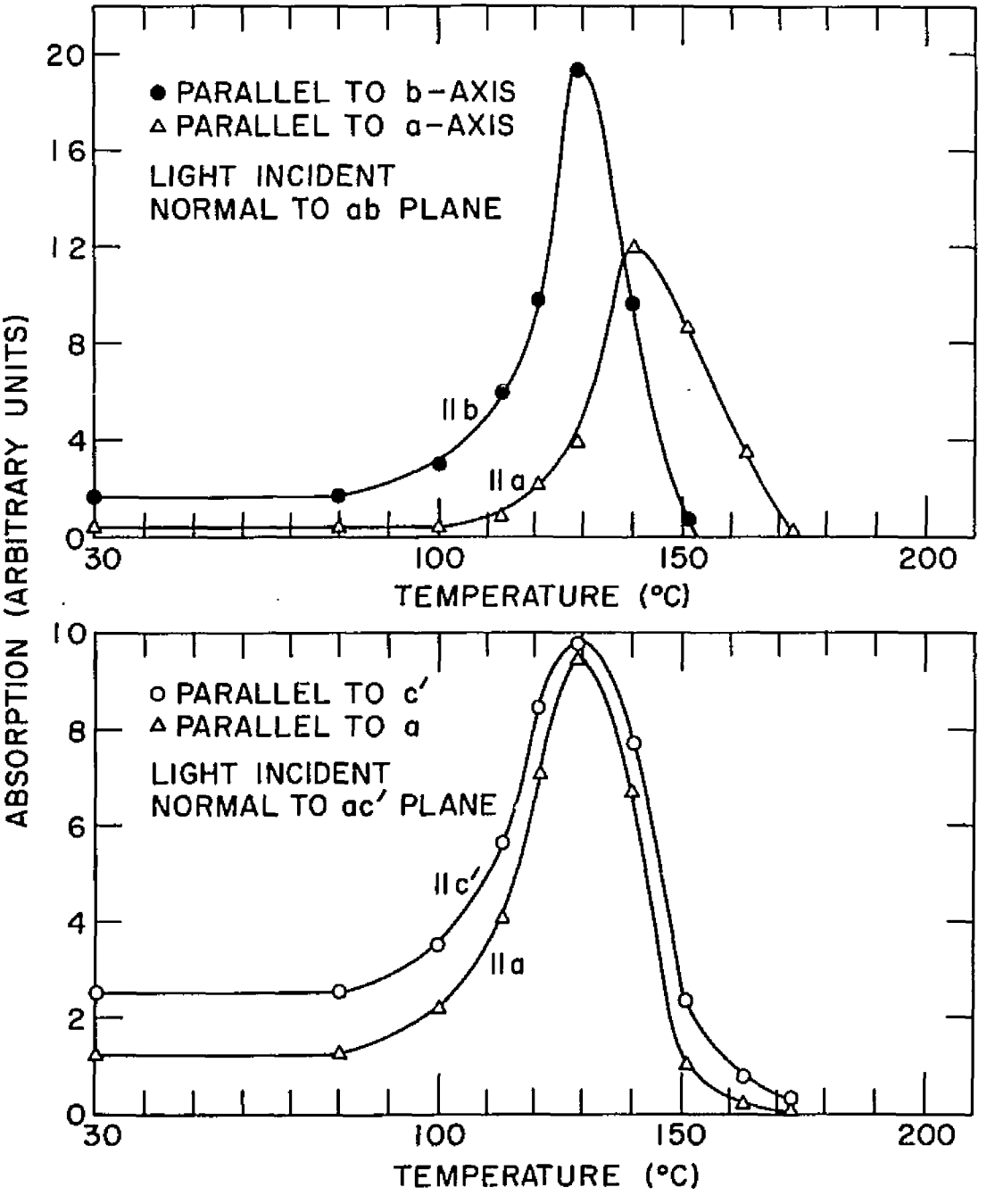

Figure 33. Isochronal annealing curves. (a) light incident normal to ab plane. (b) light incident normal to ac' plane.

defect is probably aligned along the length of the molecule. At the conclusion of the annealings, the absorptions were: $c' > a$, $c' > b$, and $a > b$, possibly indicating a rotation of the absorbing species in the ab plane. Figure 34 shows the orientation of the anthracene molecule in the unit cell and indicates that the molecule is aligned along the c-crystallographic axis.

If a plane polarized electromagnetic wave with electric vector E enters a crystal, the absorption will depend on the orientation of E with respect to the molecular transition moments. If the vector E is incident normal to the crystal surface, and the vibration direction of E does not coincide with one of the principal axes of the optical indicatrix, the vector E will undergo a change in direction in passing the air-crystal interface.[12] The optical indicatrix, in general elliptical in shape, is a device by which the optical phenonema associated with transparent crystals may be interpreted and predicted. The properties of the indicatrix are governed by three mutually perpendicular axes, called the principal axes, whose lengths, expressed as vectors, are proportional to the crystals refractive index for light vibrating parallel to that vector direction. In a monoclinic material such as anthracene, one of the principal axes coincides for all wavelengths of light with the crystallographic b-axis.

MONOCLINIC

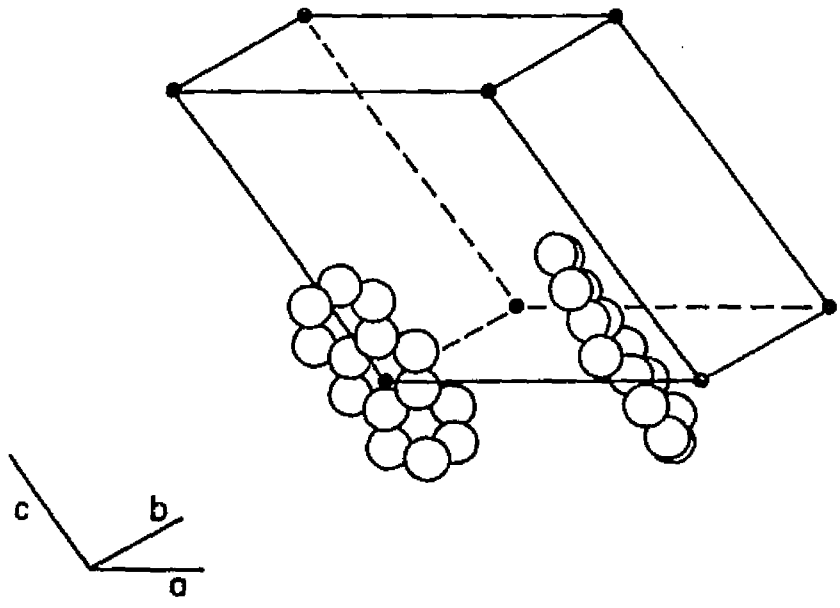

a = 8.56 Å
b = 6.04
c = 11.16
∢a,c = 124.7°

Figure 34. Anthracene molecule: orientation in unit cell.

Figure 35 shows the directions of the principal axes of anthracene referred to the crystal axes. Anthracene is biaxial and has two optic axes in the ac plane. A beam of polarized light with vibration direction E along the b-axis does not suffer any change in its direction as it enters the material. The absorption intensity is dependent only on the geometrical arrangement of the absorbing oscillators.[13] For any direction other than the three principal directions X, Y, and Z, the beam divides into two rays, both extraordinary in character and each is absorbed differently when travelling through the crystal. The optical path in the material is generally longer than the thickness of the sample. Also, one can expect different values of absorption for light polarized along the, say a axis, and whose propagation direction is normal to the ac' and ab planes. This is illustrated in Figure 33 where the values of the optical density of the a-polarized vibration at 30°C were 0.30 and 1.40 for light entering normal to the ab and ac' planes respectively. No such discrepancy is apparent for E vector along the b axis since the b axis is also one of the principal directions. The results of experiments performed on this sample are sufficient to give qualitative information concerning the orientation of the absorber. The above results indicate that the primary absorption direction has approximately a

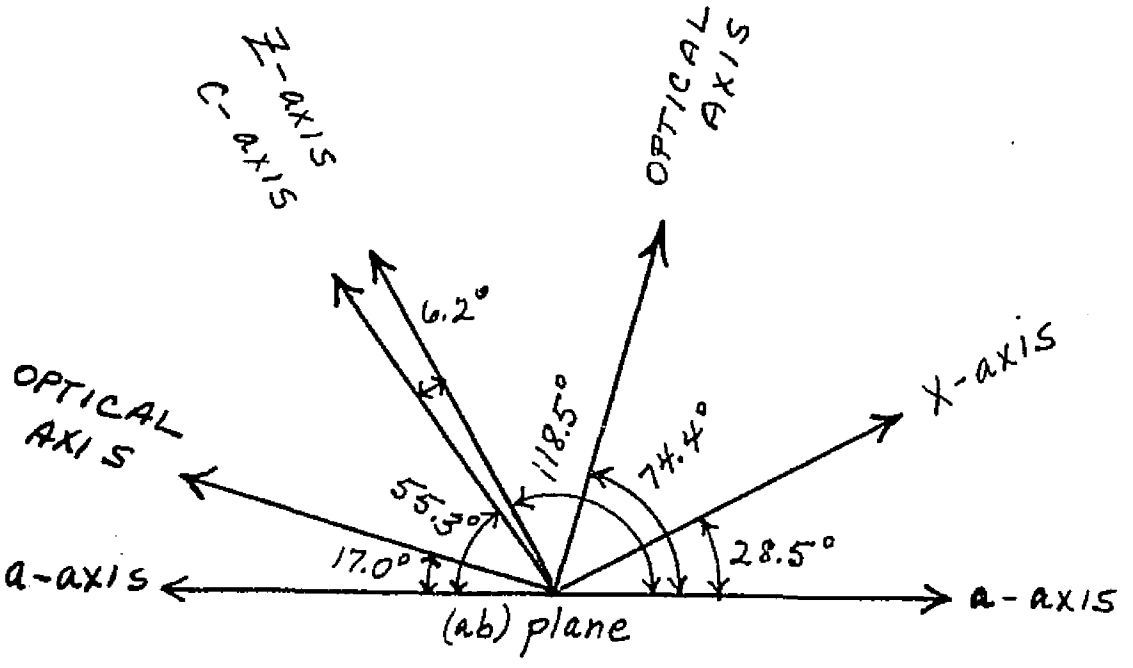

Figure 35. Directions of principal axes of anthracene referred to crystallographic axes. (after Nakada)
The Y and b axes are coincident and normal to the plane of the diagram, the ac plane.

c-axis alignment. They also indicate a thermal reorientation of the defect in the ab plane. This apparent reorientation could also be accomplished by the migration of the absorbing species from one position to another on the anthracene molecule. The migrating defect may be hydrogen since hydrogen has been found to be present in irradiated organic molecules. It will be shown later that dihydroanthracene is a radiation induced product in anthracene.

A quantitative determination of the orientation of the absorbing defect requires a crystal cut along the principal axes (X,Y,Z) not along the crystallographic axes (a,b,c). The c-axis is situated at an angle of 124.7° with the a-axis (Figure 35). A determination of the c-axis requires an X-ray analysis of the crystal. The apparatus for the study was not available.

D) Naphthalene

The absorption spectrum for gamma irradiated naphthalene is shown in Figure 23 for incident light perpendicular to the ab plane. The 7070Å absorption was studied as a function of isothermal annealing and the magnitude of the absorption was found to give rise to only a first-order reaction with an activation energy of 1.0 ± 0.2 eV. A first-order decay is represented by an equation of the form:

$$(34) \quad \frac{dn}{dt} = -kn$$

where k is the rate constant. Isothermal annealing curves, normalized with respect to the unannealed absorptions, are shown in Figure 36. The similarity in structure of naphthalene and anthracene suggests that the radiation defects in both of these materials should exhibit similar behavior. If the light incident upon naphthalene is polarized, it is found that the defect absorption is greater along the a-axis than along the b-axis, as is shown in Figure 37. The a-axis absorption in anthracene was dominant only at the latter stages of annealing, i.e. along the decay portion of the annealing curve. This suggests that, in naphthalene, annealing may have occurred during the irradiation and that a low temperature irradiation is necessary to produce all of the annealing and polarization behavior exhibited by anthracene. However, the orientation of the absorbing defect can be obtained in a qualitative manner by irradiating a cube of naphthalene and measuring the absorptions along the various axes. The limitations of this method have already been mentioned in connection with anthracene. The result for naphthalene indicates the major absorption is close to the c direction, with relative values: $c' > b$, $c' > a$, $a > b$. The results are the same as those in anthracene after the annealing maximum.

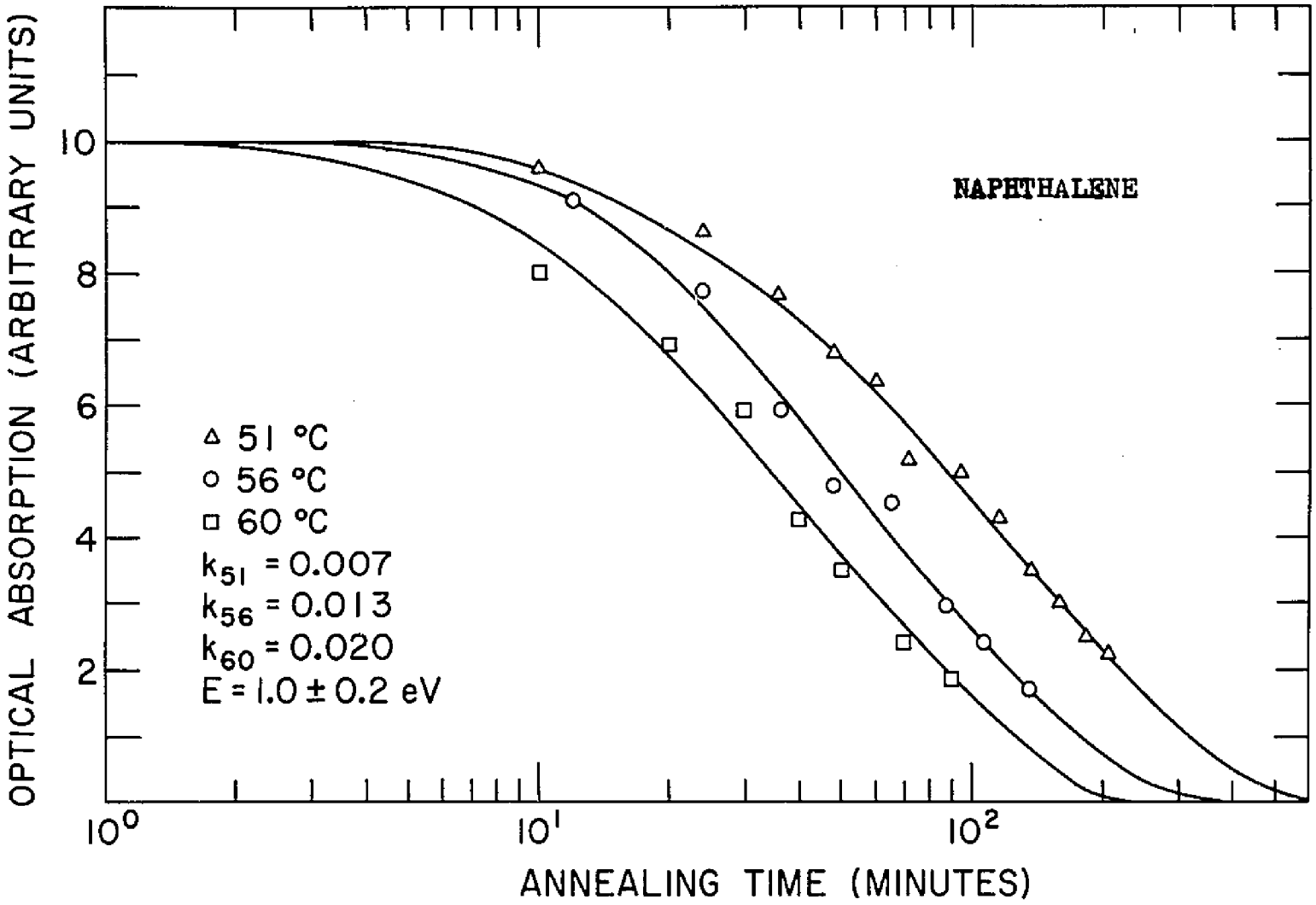

Figure 36. Naphthalene: isothermal anneals.

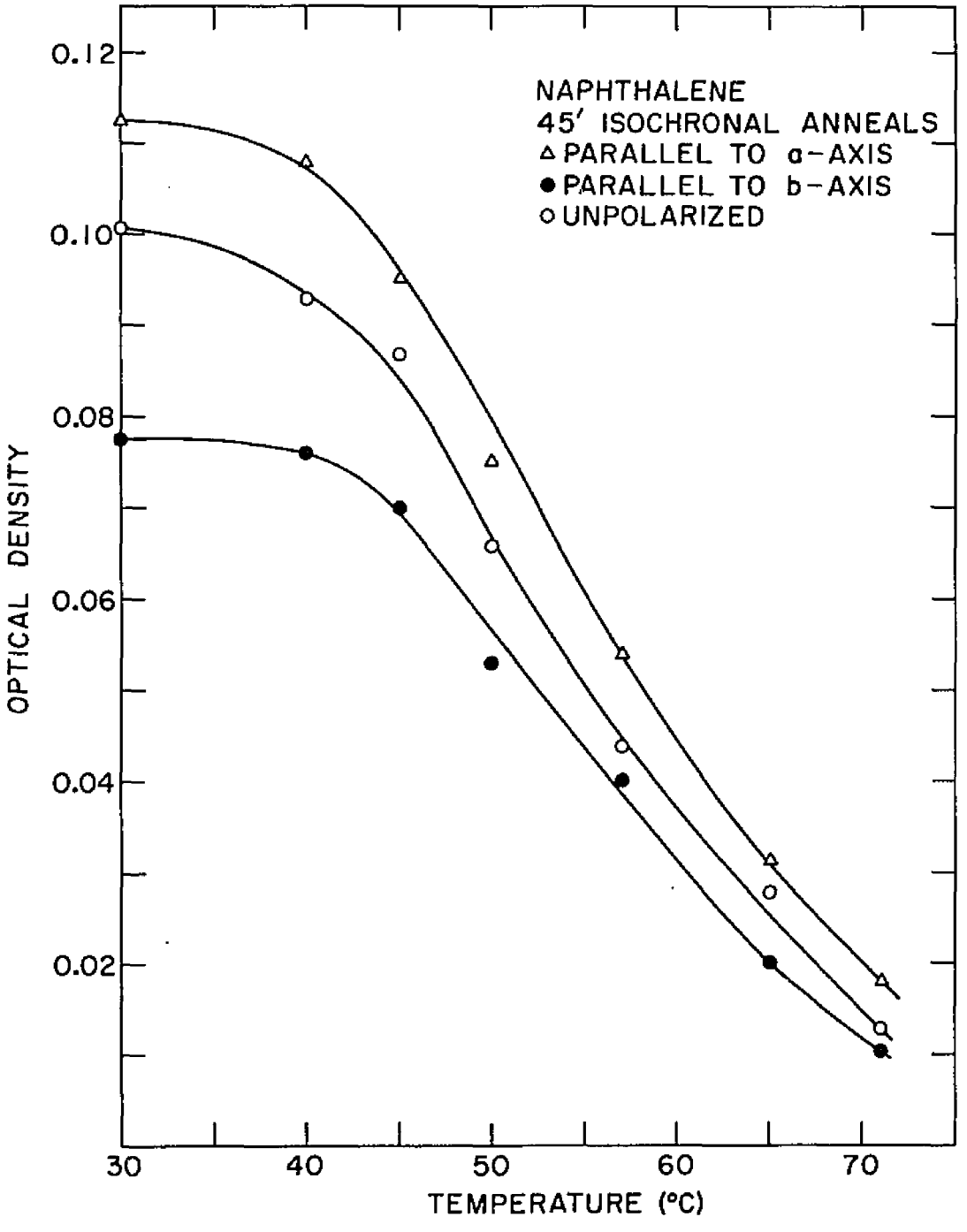

Figure 37. Naphthalene: Isochronal anneals.

E) Phenanthrene

The color center absorption spectrum of phenanthrene is shown in Figure 23. The 6150Å absorption exhibits only a decay which is first-order with an activation energy of 2.7 ± 0.2 eV. The magnitude of the absorption is greatest for light incident parallel to the b axis of the ab plane (Figure 38). Isothermal annealing curves, normalized with respect to the unannealed absorption, are shown in Figure 39. Irradiation of a cube of phenanthrene indicates that the relative values of the absorptions are: $c' > a$, $c' > b$, and $b > a$. These results differ from those of anthracene and naphthalene.

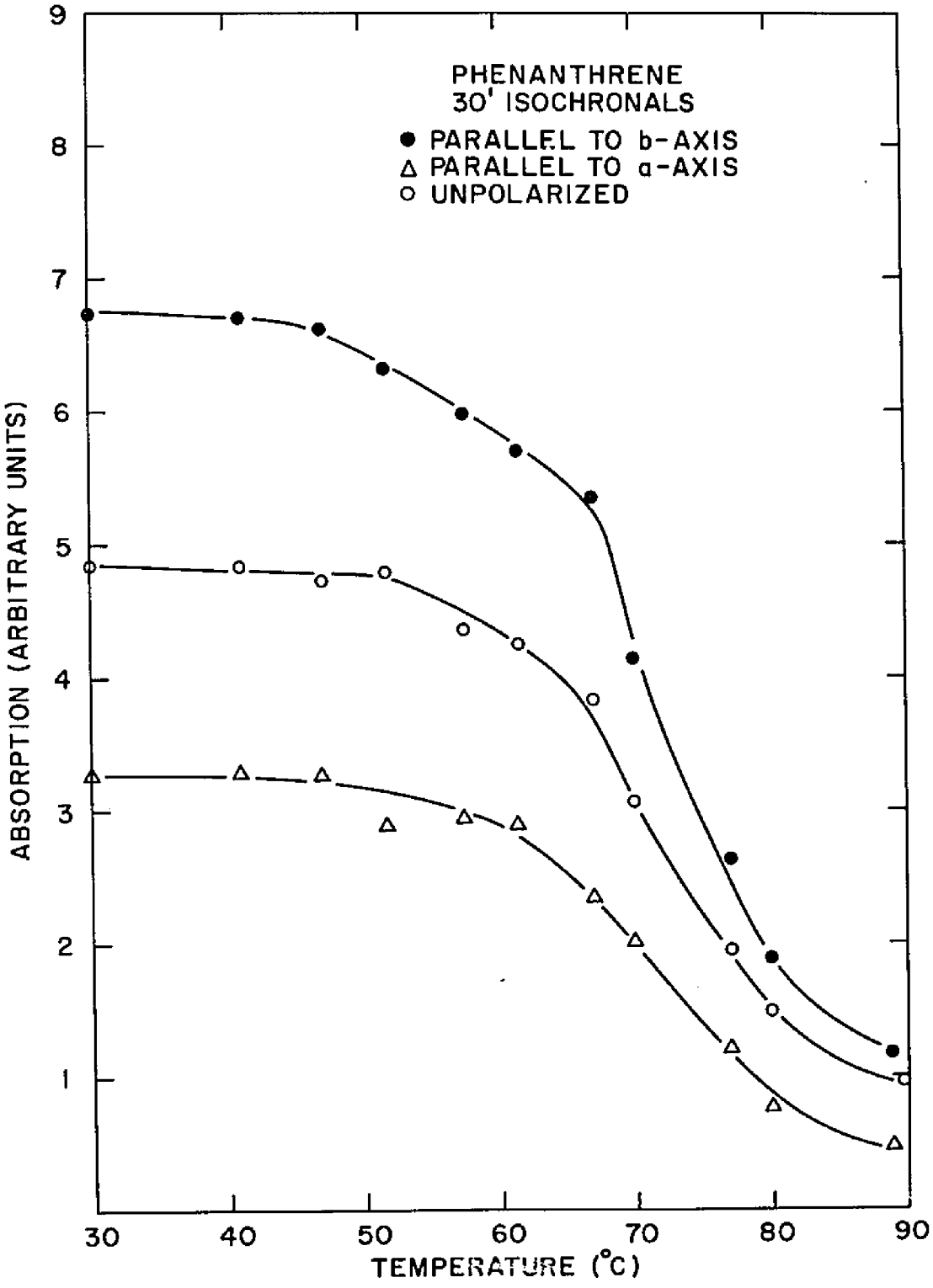

Figure 38. Phenanthrene: isochronal anneals.

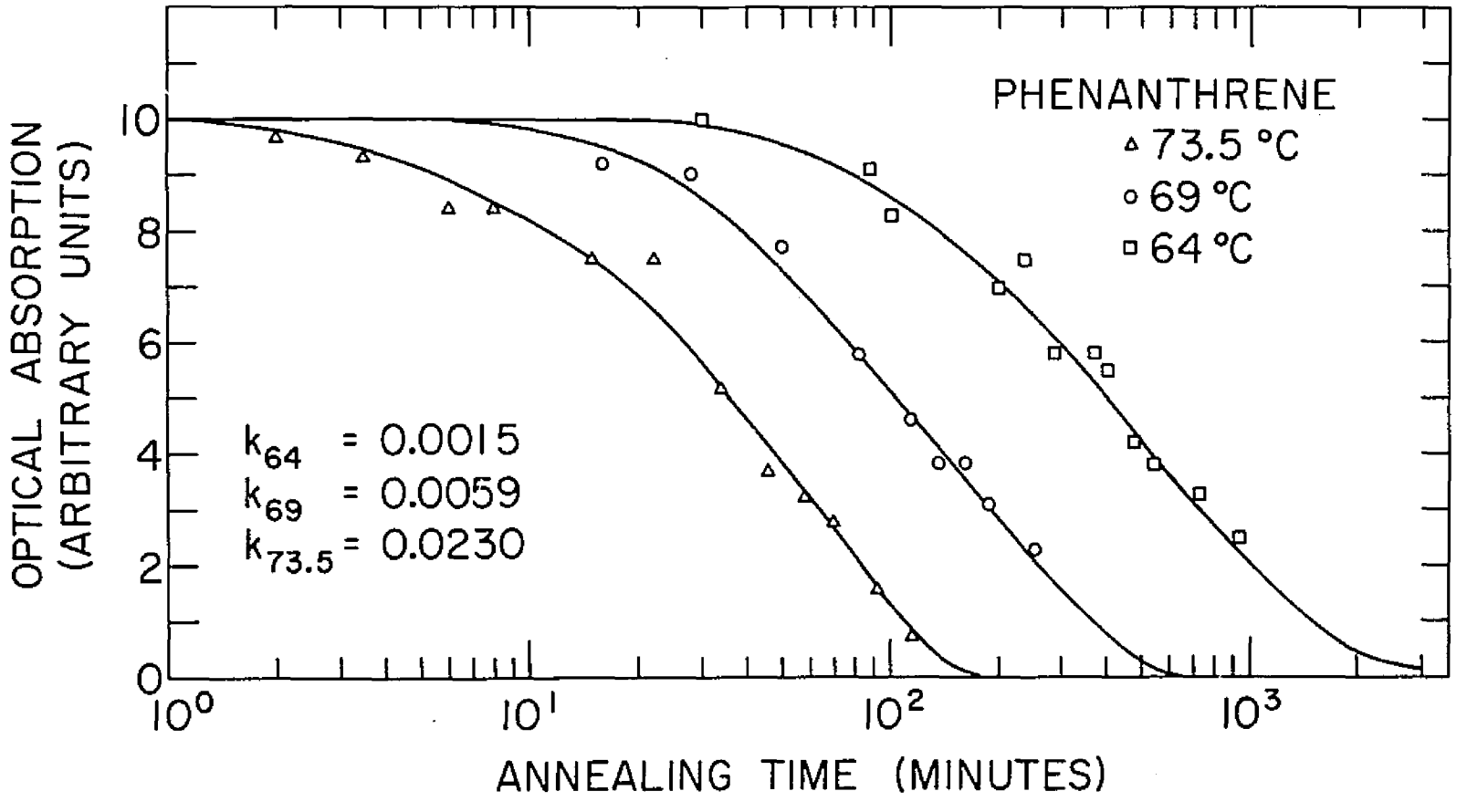

Figure 39. Phenanthrene: isothermal anneals.

F) Electron Spin Resonance

The analysis of the ESR spectra in irradiated aromatic systems can supply needed information for the identification of radiation induced defects.

The technique of electron spin resonance[17] is based on the absorption of energy by a system possessing an unpaired electron. When a unpaired electron is placed into a uniform DC magnetic field, two energy levels result from the alignment of the electron's magnetic moment either parallel or anti-parallel to the field. The splitting of these levels is given by $\Delta E = g\beta H$ where β is the Bohr magneton, $\frac{eh}{4\pi mc}$, g is the Lande factor, and H is the magnetic field intensity. If radiation of frequency is incident upon the sample, an absorption of energy will result if $h\nu = g\beta H$, a criterion known as the resonance condition.

If the orbit of the unpaired electron embraces an atom which has a nucleus with a magnetic moment and spin, the resulting interaction leads to a splitting of the energy levels (hyperfine interaction). The resulting hyperfine patterns are highly characteristic of the spatial distribution of the unpaired electron throughout the molecule. Consequently, interpretation of the hyperfine structure can often lead to identification of the paramagnetic species.

The basic ESR spectrometer consists of a source of

microwave radiation (3 cm wavelength), an absorption cell (resonant cavity) containing the sample and into which the microwave power is concentrated, a DC magnetic field ($\sim$ 3000 gauss), an alternating magnetic field at right angles to the DC field, and a detection system designed to detect power changes in the AC field. The spectrometer used in this survey is Varian Associates V-4500 system and the associated Varian components.

With respect to radiation induced defects the simplest of the aromatic hydrocarbons, benzene, has undergone the most extensive analysis. Chkeidze et al.[14] observed a main triplet, with quartet substructure ESR signal and attributed this to the formation of a phenyl radical whereby the benzene molecule loses a hydrogen atom and leaves the system with an unpaired electron (see Figure 40). Ohnishi et al.[15] found two types of signals present in irradiated benzene. Following irradiation at liquid nitrogen temperature the signal consisted of a triplet with quartet hyperfine structure, each quartet having further fine splitting. This signal was attributed to the cyclohexadienyl radical, $C_6H_7^{\bullet}$. After warming the sample above -50°C this spectrum decayed leaving a singlet spectrum of smaller intensity and narrower linewidth. The singlet spectrum was designated as due to the phenyl radical and disappeared at about 0°C. Ingalls and Kivelson[16] theoretically calculated the expected ESR spectrum of

A)

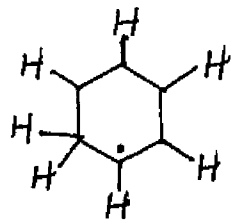

Cyclohexadienyl

C_6H_7

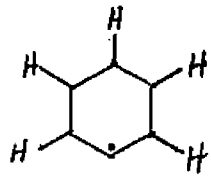

Phenyl

C_6H_5

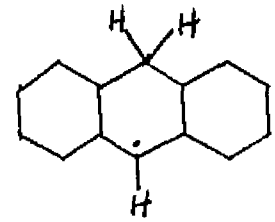

Dibenzocyclohexadienyl

$C_{14}H_{11}$

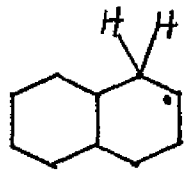

Naphthyl

$C_{10}H_9$

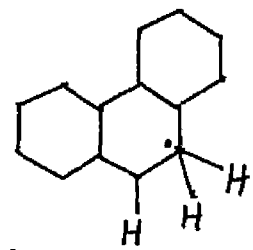

Phenanthrene radical

$C_{14}H_{11}$

B)

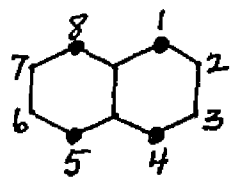

Naphthalene

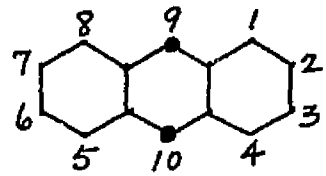

Anthracene

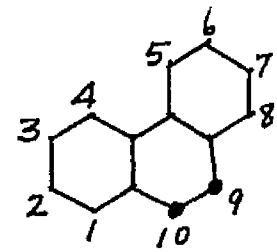

Phenanthrene

Figure 40. (A) Radicals produced by gamma radiation
(B) Positions of maximum spin density

cyclohexadienyl and found good agreement with the experimental observation.

Anthracene was the first of the aromatic hydrocarbons to be examined in high purity single crystal form.[3] The spectrum (Figure 41) can be described as four equally spaced lines with an intensity ratio of 1:3:3:1. By rotating the crystal, Blum et al. found that the magnitude of both the width and the spacings of the lines varied relative to the direction of the external magnetic field. The angular variation of the hyperfine splittings indicated that the defect was aligned with the c axis of the anthracene molecule. The spectrum is that expected from three equivalent spin 1/2 nuclei coupling with an unpaired electron and was attributed to the formation of a cross-linked structure (Figure 42). The spectrum arises from the interaction of the unpaired electron with the protons on the carbon atoms which form the linear cross-link. The width of the spectrum is attributed to the interaction of the unpaired electron with the remainder of the molecule.

The ESR signal, like the optical absorption, is stable at room temperature. However, unlike the color center, no growth in signal strength was found during isochronal annealing (Figure 25). The magnitude of the spectrum was constant at the lower temperatures but after 140°C it decreased in a manner similar to the optical absorption.

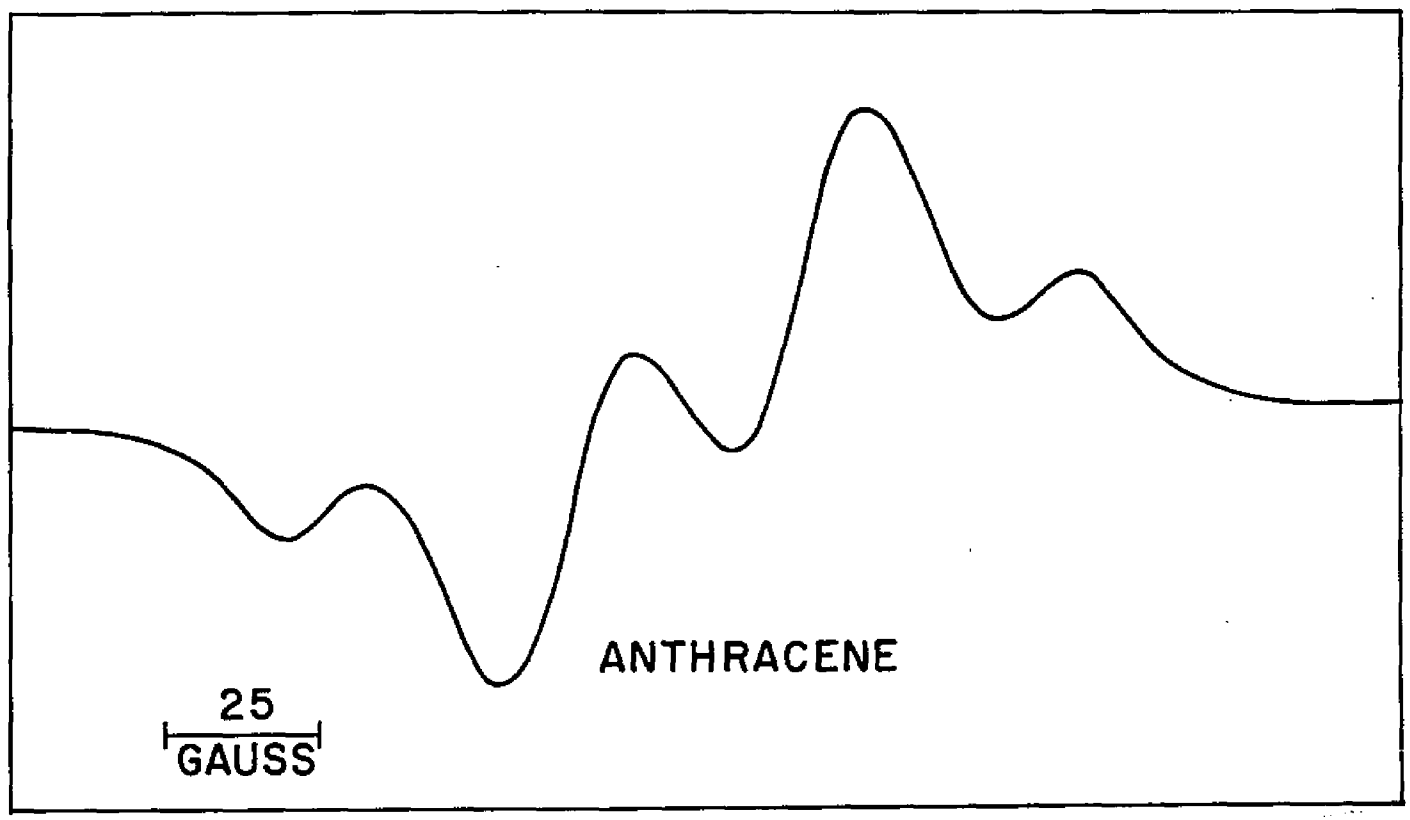

Figure 41. Typical ESR spectrum of irradiated anthracene as a function of external magnetic field. (from Blum et al.)

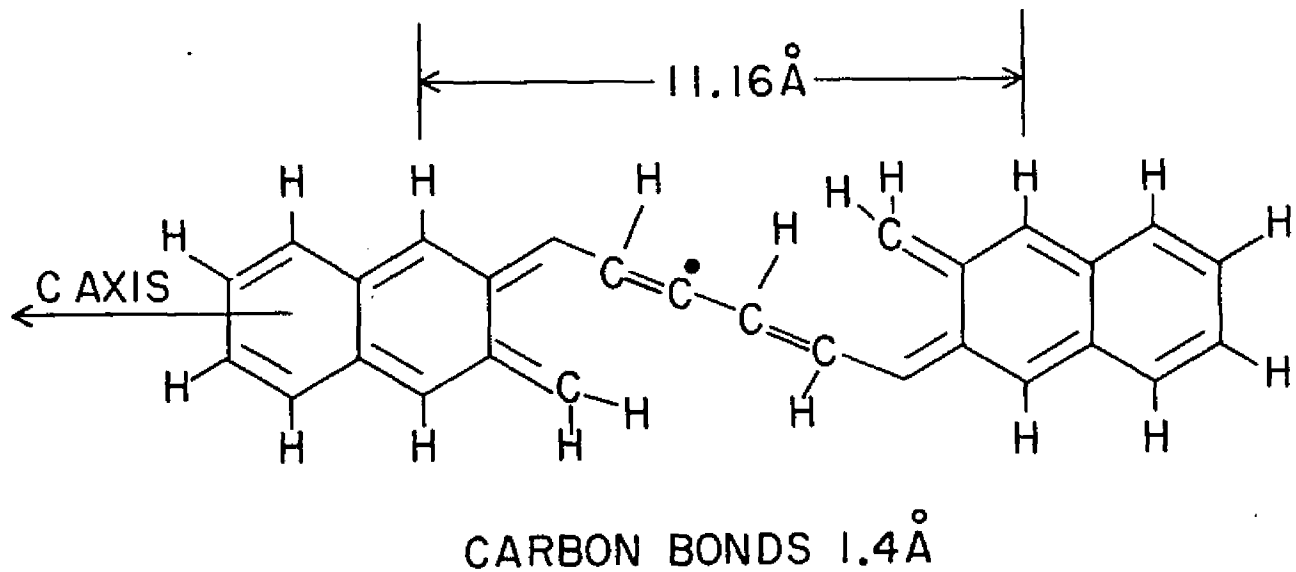

Figure 42. Proposed cross-linking of anthracene molecules, (from Blum et al.)

The magnitude of the signal strength is linear for doses of 10^6-10^9 R. It was estimated that for a dose of 10^7 R approximately 10^{17} spins/cm^3 contribute to the signal. A defect of this concentration should be detectable by other techniques and the results of a gas chromatographic study will be discussed in a later section.

Harrah and Hughes,[4] using the premise that radicals derived from aromatic systems by ionizing radiation are often assignable the cyclohexadienyl-type molecules, attribute the anthracene signal to the radical derived from anthracene by the addition of a hydrogen atom to the 9-position (Figure 40). They attribute the hyperfine splitting of this dibenzocyclohexadienyl radical to nearly equal interactions of the unpaired electron with the two protons on the carbon-9 position and the single proton on the carbon-10 site. The width of the line is thought to arise from the interaction with the remaining eight protons.

Leone and Koski[18] examined the effect of X-radiation on a binary mixture of naphthalene with methanol and ethanol at 77°K. The resulting ESR spectrum consists of a parent triplet containing further triplet substructure. The naphthyl radical (Figure 40), formed by the addition of a hydrogen atom to the α-position of the naphthalene molecule, was held responsible for this signal.

The ESR spectrum of irradiated single crystals of

phenanthrene is uncertain. Hankla and Bouldin[19] report a spectrum consisting of two sets of five lines, i.e. a doublet containing quintuplet hyperfine structure. The authors reject the model of the loss of a hydrogen atom as responsible for this signal and suggest that either a molecular distortion or a C-C-H interaction mechanism as responsible for the spectrum. One should note that no purification procedures were administered to the phenanthrene prior to crystal growth. Our experience with phenanthrene, obtained from several distributors, indicates an initial anthracene content of $\sim$ 1-2%.

Blum et al.[3] report the spectrum of irradiated phenanthrene as consisting of a triplet encompassing further hyperfine structure.

In the current investigation, the spectra of the EPR signals of irradiated single crystals of naphthalene and phenanthrene, purified in the previously mentioned method, were compared with the available data on these materials. In order to measure the signal strength during annealing, it was felt sufficient to anneal irradiated powders and thus preserve the crystals for future investigations.

The ESR signal of both a single crystal and a powder of naphthalene irradiated to a dose of 10^8 R is shown in Figure 43. The crystal spectrum is similar to the signal produced by naphthalene frozen in an alcohol matrix, i.e.

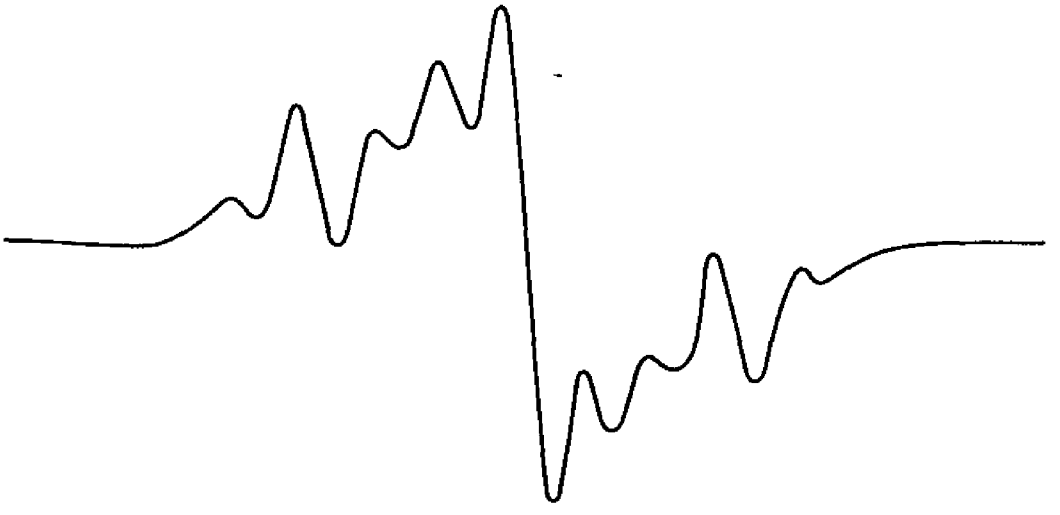

NAPHTHALENE CRYSTAL

NAPHTHALENE POWDER

Figure 43. ESR spectrum of irradiated naphthalene.

a triplet with triplet hyperfine structure. The annealing curve of the signal amplitude (Figure 44) shows a decrease of signal strength as the temperature is raised. Following annealing of the powder at a temperature above the melting point, a very small signal, singlet in nature was found. It is possible that the room temperature spectrum is, in effect, the superposition of the triplet due to the naphthyl radical and a singlet due to a naphthalene molecule which is lacking a hydrogen atom. Since the hydrogen atom added to naphthalene to form the naphthyl radical may result from the dissociation of other naphthalene molecules, a complementary defect lacking a hydrogen atom is expected to exist. Either of these defect structures or the presence of any other polymer radical, caused by cross-linking may also contribute to the EPR spectrum. Independent measurements by Okubo et al.,[20] published after the completion of the above investigation, substantiates the naphthalene signal.

The ESR signal of an irradiated single crystal of phenanthrene (Figure 45) consists of a parent triplet upon which is superimposed hyperfine coupling, possibly of a triplet nature. The amplitude of the signal decreases as the temperature is increased (Figure 44). As in naphthalene, the annealing was on an irradiated powder. After melting the irradiated powder, a residual ESR singlet of low intensity is retained which is similar to the pattern of

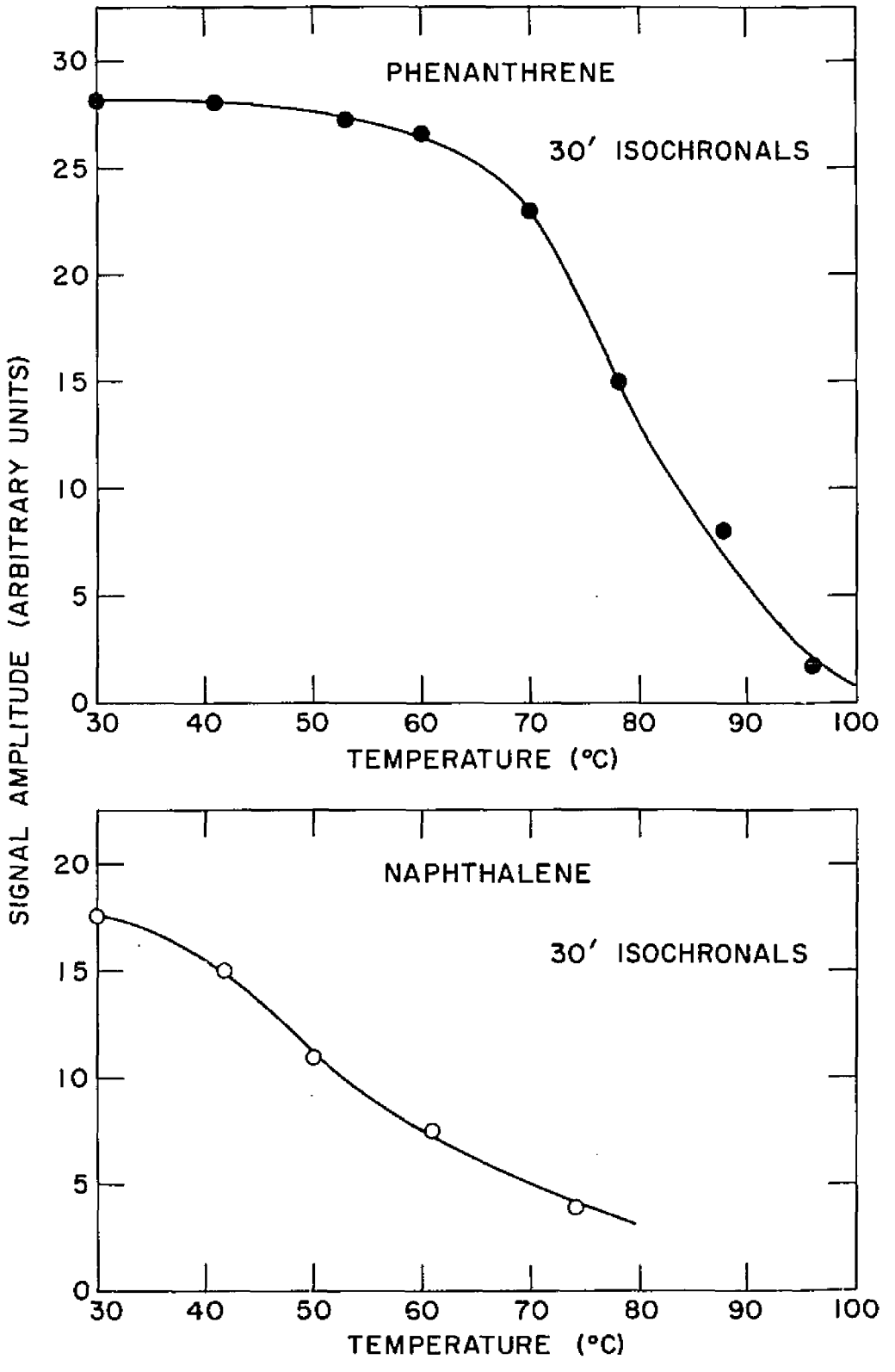

Figure 44. Isochronal annealing curves of ESR signals. (a) phenanthrene (b) naphthalene

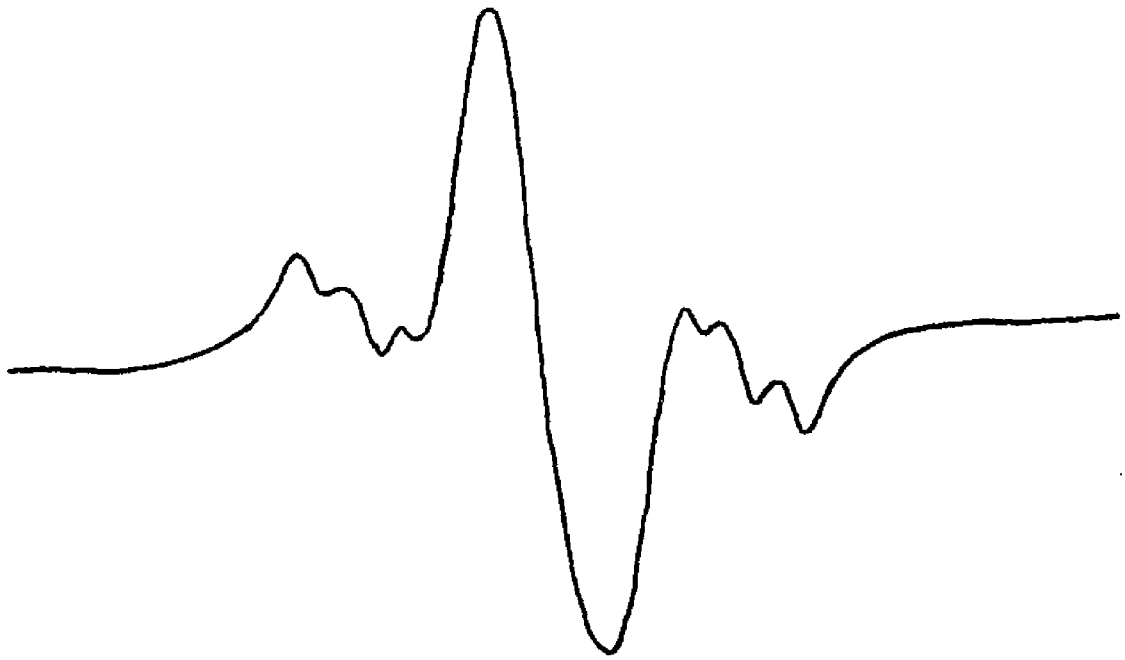

(a) Phenanthrene

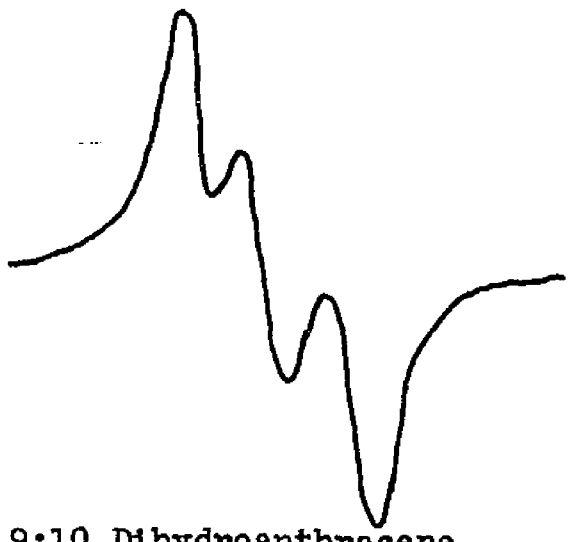

(b) 9:10 Dihydroanthracene

Figure 45. ESR spectra of irradiated phenanthrene and 9:10 dihydroanthracene.

melted irradiated naphthalene powder. The damage products responsible for these patterns may be similar in nature to those in anthracene and naphthalene, i.e. a signal due to the addition of a hydrogen atom to a molecule (Figure 40) superimposed upon a signal due to the loss of a hydrogen atom or a proton from one of the other molecules.

All sites on the organic molecule are equally susceptible to the incident gamma radiation. Some sites are more susceptible to substitution reactions or to radical formation with any free hydrogen atoms which were the result of a prior molecular dissociation. According to one hypothesis,[21] those positions which possess the largest portion of the charge density of the electrons in the highest filled molecular orbital have the highest degree of reactivity. In anthracene and phenanthrene these sites are the 9,10 positions and for naphthalene, the equivalent 1,4,5,8 positions (Figure 40). If the radiation induced ESR signals described herein are correctly identified they are consistent with this hypothesis.

G) Gas Chromatography

Gas chromatography was used in an attempt to identify the radiation induced products. For detection of radiation induced defects, the Varian Aerograph Model 204B gas chromatograph was used and the samples were injected as solids. The procedure was as follows: (1) a portion of the sample in an unirradiated condition was injected and the peak noted. (2) the irradiated material was injected andpositions of any new peaks noted. (3) the control sample was reinjected. The samples investigated, anthracene, naphthalene and phenanthrene, were irradiated to a dose of $\sim 10^9$R. The resulting chromatograms indicate a variety of new products, eluding both before and after the major peak. These products result either from the irradiation, and are thus stable at these high ($\sim 230^{\circ}$C) temperatures, or are formed in the chromatograph. Since reactions involving hydrogen abstraction sometimes occur in the apparatus as a result of the high temperatures[22] and irradiation of organic materials is known to produce hydrogen atoms,[23] some of the free radicals resulting from the irradiation may have combined with hydrogen to yield the observed new materials. Thus it is not certain that the observed products were in the crystal following irradiation.

The Autoprep A-700 gas chromatograph was utilized in an attempt to identify one of the major new constituents. Irradiated specimens were placed on the column, which was at room temperature, and the temperature of the apparatus was raised. The impurity eluding before the major peak was captured and identified by ultraviolet spectroscopy. These impurities were: 9:10 dihydroanthracene in irradiated anthracene and 9:10 dihydrophenanthrene in irradiated phenanthrene. Although the recovery of a product was unsuccessful in the case of naphthalene, injection of 1,4 dihydronaphthalene in the 204B gas chromatograph resulted in a peak with a retention time identical to one of the radiation products in naphthalene. However, a test of this type is not as definitive as is ultraviolet spectroscopy. If the dihydro- products result from hydrogen diffusion on the chromatograph column, the radical of the species, such as dibenzocyclohexadienyl in the case of anthracene, may be the result of the radiation.

H) Optical Absorption and ESR Measurement of 9:10 Dihydroanthracene.

To determine if either the optical absorption or the ESR signal in irradiated anthracene was due to dibenzocyclohexadienyl, i.e., dihydroanthracene less one hydrogen, a crystal of high dihydroanthracene content (> 99%) was studied. The crystal of 9:10 dihydroanthracene was grown from the melt by the Bridgeman technique. Following an irradiation of 10^8R, the transparent crystal became orange in color and exhibited an absorption at ~5300A, near one of the major absorption bands in irradiated anthracene. Annealing for 30 minute intervals from 30-100°C in ten degree temperature intervals, resulted in a decay of the absorption strength.

The ESR spectrum of this material consisted of a singlet absorption exhibiting triplet hyperfine structure (Figure 45) and a peak-to-peak width of about 50 gauss. This is in contrast to the four line structure of width ~100 gauss found in irradiated anthracene. If one of the hydrogen atoms at the 9 or 10 position in dihydroanthracene was removed by the irradiation, a four line spectrum similar to that found in anthracene might result. Therefore, either the resulting damage in 9:10 dihydroanthracene is different from that in anthracene of another species, such as the proposed cross-linked structure, may be responsible for the ESR signal in anthracene.

Summary

This investigation focused on the effects of gamma radiation on some of the electrical and optical properties of anthracene, naphthalene, and phenanthrene.

I) Low Dose Effects

Changes in charge carrier lifetime and space charge limited current measurements were used to examine the effects of low dose radiation ($< 10^5$R) on anthracene and naphthalene. In phenanthrene, the response of the polarization charge release was studied.

1. The lifetime of photoinjected holes and electrons in anthracene was found to decrease in the manner: $\frac{1}{\tau} = \text{Constant} + \alpha D$

where τ is the carrier lifetime, D the exposure dose, and α is a constant and is dependent upon the cross-section of the radiation induced traps.

From space charge limited current measurements, the density of the radiation induced electron traps was found to increase linearly with the exposure dose. Combining the results of the lifetime study with the density of the radiation induced electron traps, a value of 180×10^{-16} cm^2 was found for the cross-section of the electron traps in irradiated anthracene.

2. The lifetime of the charge carriers in naphthalene was found to decrease with increasing radiation in a manner similar to that of anthracene, However, the smaller photoresponse of naphthalene, compared to that of anthracene, prevented a quantitative study of the lifetimes.

3. The magnitude of the polarization charge release in phenanthrene was found to decrease due to radiation. The magnitude of the decrease suggested that the charge release is a cooperative effect and the damage of one molecule hinders the molecular alignment within a distance of 10^3 molecular centers from the damage site.

II) High Dose Effects

High dose radiation ($>10^5$R) was shown to produce color centers in anthracene, naphthalene and phenanthrene. By studying the annealing kinetics of the color centers, the reaction mechanisms and the associated activation energies were determined. Some of the radiation induced defects were identified using the techniques of gas chromatography and electron spin resonance.

1. Using unpolarized light, the annealing characteristics of the 6060Å absorption in irradiated anthracene was found to result from two consecutive first order reactions; one of growth, the other of decay. The activation energies for growth and decay were

1.0± 0.2 ev and 1.5± 0.1 ev respectively.

Using polarized light, the absorption was found to be anisotropic, with the major absorption along the c crystallographic axis of anthracene. The absorbing species exhibited a thermal reorientation in the ab plane as a consequence of annealing. Prior to annealing, light polarized along the b crystallographic axis was more highly absorbed than light polarized along the a axis. Following annealing, a reversal of the relative absorption magnitudes was found. The annealing of the absorptions was found to be consistent with a kinetic scheme of the form:

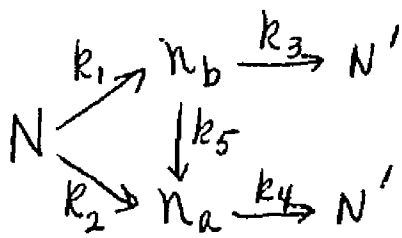

where N and N' are non-absorbers at 6060Å and n_b and n_a are the optical absorptions for the light incident parallel to the b and a axes respectively. The k's represent the rate constants for the reactions.

2. The 7070Å color center in irradiated naphthalene was found to decay as a first order process with an activation energy of 1.0± 0.2 ev. The relative magnitudes of the aniostropic absorptions indicate that a thermal reorientation, similar in nature to that observed in anthracene, has occurred during the irradiation.

3. The 6150A absorption in irradiated phenanthrene exhibited a first order decay with an activation energy of 2.7 ± 0.2 ev. No evidence for a thermal reorientation was noted.

4. Using gas chromatography, many radiation induced products were detected in anthracene, naphthalene, and phenanthrene. In anthracene, one of these products was identified as 9:10 dihydroanthracene. Dihydro-products were also found in naphthalene and phenanthrene. An irradiated single crystal of 9:10 dihydroanthracene exhibited a defect absorption at 5300Å, a wavelength close to one of the major absorptions in anthracene. The ESR spectrum of the 9:10 dihydroanthracene differed from the signal found in anthracene, indicating that the ESR signals are not due to the same defect.

References

1. J. B. Birks and F. A. Black, Proc. Phys. Soc. (London) 64A, 511 (1951), E. R. Hardwick and W. G. McMillan, J. Chem. Phys. 26, 1463 (1957), J. H. Schulman, H. Etzel, and J. Allard, J. Appl. Phys. 28, 792 (1957)

2. C. F. Sharn, J. Chem. Phys. 34, 240 (1961)

3. H. Blum, P. L. Mattern, R. A. Arndt, and A. C. Damask, Mol. Cryst. 3, 269 (1967)

4. L. A. Harrah and R. C. Hughes, Mol. Cryst. 5, 141 (1968)

5. T. Inoue, J. Phys. Soc. Japan 25, 914 (1968)

6. R. S. Alger, "Radiation Effects in Polymers," in Physics and Chemistry of the Organic Solid State, ed. D. Fox, M. M. Labes, and A. Weissberger, (Interscience Publishers, New York, 1965)

7. A. C. Damask and G. J. Dienes, Point Defects in Metals, (Gordon and Breach, New York, 1963)

8. R. P. Bauman, Absorption Spectroscopy, (J. Wiley, New York, 1962)

9. I. Nakada, J. Phys. Soc. Japan 17, 113 (1962)

10. K. J. Laidler, Reaction Kinetics, (Pergamon Press, New York, 1963)

11. S. Glasstone, The Elements of Physical Chemistry, (D. Van Nostrand, New York, 1946)

12. M. Born and E. Wolf, Principles of Optics, (Pergamon Press, New York, 1964)

13. J. W. Rohleder and T. Luty, Mol. Cryst. 5, 145 (1968)

14. I. I. Chkeidze, U. N. Molin, N. I. Buben, and V. V. Voevodskii, Dokl. Akad. Nauk S.S.S.R. 130, 1291 (1960)

15. S. Ohnishi, T. Tanei, and I. Nitta, J. Chem. Phys. 37, 2402 (1962)

16. R. B. Ingalls and D. Kivelson, J. Chem. Phys. 38, 1907 (1963)

17. D. J. E. Ingram, Free Radicals as Studied by Electron Spin Resonance, (Butterworths, London, 1958)

18. J. A. Leone and W. S. Koski, J. Amer. Chem. Soc. 88, 656 (1966)

19. R. H. Hankla and W. V. Bouldin, Bull. Am. Phys. Soc. 11, 514 (1966), R. H. Hankla, Thesis, Vanderbilt Univ. (1966)

20. T. Okubo, N. Itoh, and T. Suita, J. Phys. Soc. Japan 24, 1179 (1968)

21. K. Fukui, T. Yonezawa, and H. Shingu, J. Chem. Phys. 20, 722 (1952)

22. L. S. Ettre and A. Zlatkis, ed. The Practice of Gas Chromatography, (Interscience Publishers, New York, 1967)

23. R. O. Bolt and J. G. Carroll, ed. Radiation Effects on Organic Materials, (Academic Press, New York, 1963)